EUROPEAN ORGANISATION FOR NUCLEAR RESEARCH (CERN)

Submitted to: EPJC

CERN-EP-2017-048
12th May 2017

Measurement of multi-particle azimuthal correlations in *pp*, *p*+Pb and low-multiplicity Pb+Pb collisions with the ATLAS detector

The ATLAS Collaboration

Multi-particle cumulants and corresponding Fourier harmonics are measured for azimuthal angle distributions of charged particles in pp collisions at $\sqrt{s} = 5.02$ and 13 TeV and in p+Pb collisions at $\sqrt{s_{\mathrm{NN}}} = 5.02$ TeV, and compared to the results obtained for low-multiplicity Pb+Pb collisions at $\sqrt{s_{\mathrm{NN}}} = 2.76$ TeV. These measurements aim to assess the collective nature of particle production. The measurements of multi-particle cumulants confirm the evidence for collective phenomena in p+Pb and low-multiplicity Pb+Pb collisions. On the other hand, the pp results for four-particle cumulants do not demonstrate collective behaviour, indicating that they may be biased by contributions from non-flow correlations. A comparison of multi-particle cumulants and derived Fourier harmonics across different collision systems is presented as a function of the charged-particle multiplicity. For a given multiplicity, the measured Fourier harmonics are largest in Pb+Pb, smaller in p+Pb and smallest in pp collisions. The pp results show no dependence on the collision energy, nor on the multiplicity.

1 Introduction

One of the signatures of the collective behaviour of the hot, dense medium produced in heavy-ion collisions is the azimuthal anisotropy of produced particles. This anisotropy results from spatial asymmetry in the initial interaction region in off-centre ion–ion collisions. The initial asymmetry activates strong pressure gradients along the shorter axis of the overlap region, leading to increased production of particles within the reaction plane, defined by the impact parameter vector (the vector separation of the barycentres of the two nuclei) and the beam axis. The azimuthal anisotropy is commonly characterized by Fourier harmonics v_n, referred to as single-particle harmonic flow coefficients: $v_n = \langle \cos[n(\phi - \Phi_R)] \rangle$, where ϕ is the azimuthal angle of a produced particle and Φ_R is the azimuthal angle of the reaction plane [1]. This anisotropic, collective enhancement of particle production is a global long-range phenomenon extending over a wide pseudorapidity range.

The anisotropy of charged-particle azimuthal angle distributions in A+A collisions has been a subject of extensive experimental studies at RHIC [2–7] and at the LHC [8–22]. In non-central heavy-ion collisions, the large and dominating v_2 coefficient is mainly associated with the elliptic shape of the nuclear overlap. The v_2 coefficient in ultra-central collisions and other v_n coefficients in all collisions are related to various geometric configurations arising from fluctuations of the nucleon positions in the overlap region [23, 24]. The reported results are consistent with model calculations based on a hydrodynamic description of the system evolution and provide conclusive evidence that the hot and dense matter produced in A+A collisions behaves collectively in accordance with a hydrodynamic flow and has properties resembling those of a nearly perfect fluid [25–28].

The study of p+A collisions was thought to provide information on cold nuclear matter effects, relevant for understanding the hot and dense system produced in A+A collisions. In p+A collisions, the size of the produced system is small compared to the mean free path of its constituents. Therefore, it might be expected that the collective flow, if any, generated in p+A collisions is much weaker than in heavy-ion interactions. Contrary to these expectations, significant v_n coefficients, only about 40% smaller in magnitude than those obtained in Pb+Pb collisions, have been measured in p+Pb collisions at the LHC energy of $\sqrt{s_{\rm NN}} = 5.02$ TeV [29–38]. Observations of azimuthal anisotropies were also reported recently for d+Au [39, 40] and ^{3}He+Au [41] collisions at the RHIC energy.

Interestingly, long-range two-particle azimuthal correlations have also been observed in high-multiplicity pp collisions at the LHC energies [42–46]. It was found that the measured azimuthal correlations, which extend over a wide range in pseudorapidity, can be explained by the $\cos(n\phi)$ modulation of the single-particle azimuthal angle distribution. The extracted Fourier harmonics v_n for $n = 2$–4 [46] are generally much smaller than those measured in p+Pb and Pb+Pb collisions, and show no dependency on the charged-particle multiplicity. On the other hand, they display a similar dependence on particle transverse momenta, suggesting that the same underlying mechanism may be responsible for the long-range azimuthal correlations. These observations in pp collisions, together with the results from the p+A system described above, are among the most challenging and pressing problems in the domain of soft quantum chromodynamics. Various models have been proposed to explain the source of the observed long-range correlations in small collision systems [47–63], but the origin of the effect is still under intense debate. It is not yet known whether the mechanism responsible for the observed collective behaviour in A+A collisions is also relevant for the smaller systems. The main purpose of this paper is to contribute to this debate by providing new experimental results.

Several differing analysis methods are applied to measure Fourier harmonics in high-energy collisions. They differ principally in their sensitivity to correlations not related to the initial collision geometry (referred to as non-flow correlations), which can result from resonance decays, jet production, Bose–Einstein correlations or energy–momentum conservation. For small collision systems and low-multiplicity final states, the most common method uses two-particle correlation functions [29–31, 33, 35–38, 42–46, 64]. In this method, the non-flow correlations are suppressed by requiring a large pseudorapidity separation, $|\Delta\eta|$, between particles forming a pair. This requirement eliminates most of the short-range correlations including intra-jet correlations. The jet–jet correlations are subtracted from the two-particle correlation function using the correlations measured in low-multiplicity events (see e.g. [43, 46]).

The multi-particle cumulant method [65–67] was proposed to suppress the non-flow correlations. The method aims to measure correlations between a large number of particles, from which the correlations between a small number of particles are subtracted. Since non-flow correlations typically involve a low number of particles, they are suppressed in many-particle cumulants. The drawback of the method is the statistical limitation in calculating the cumulants of more than two particles. Furthermore, the multi-particle cumulants in small collision systems can be biased by non-flow jet and dijet correlations, which dominate the azimuthal correlation signal. The cumulant method has been applied to measure global correlations and Fourier harmonics in Pb+Pb and p+Pb collisions [18, 20, 32, 33, 36]. Recently, the four- and six-particle cumulants were also measured by the CMS Collaboration in pp collisions at 5, 7 and 13 TeV [45].

In this paper, the ATLAS measurements of multi-particle cumulants are presented for pp collisions at 5.02 and 13 TeV and for p+Pb collisions at $\sqrt{s_{\mathrm{NN}}} = 5.02$ TeV. For comparison, the results for low-multiplicity (peripheral) Pb+Pb collisions at $\sqrt{s_{\mathrm{NN}}} = 2.76$ TeV are also shown. The results are averaged over large ranges in p_{T} and pseudorapidity. Results obtained from different collision systems are compared as a function of the charged-particle multiplicity.

The paper is organized as follows. The analysis method is described in the next section, followed by the description of the detector (Section 3) and presentation of the analysed data samples and event and track selections in Sections 4 and 5. The analysis details are given in Section 6 while Section 7 contains a discussion of systematic uncertainties and cross-checks. The results for cumulants and the corresponding Fourier harmonics are shown in Section 8. A summary and concluding remarks are given in Section 9.

2 Multi-particle cumulants

The multi-particle cumulant method is useful in studying the global nature of correlations observed in azimuthal angles of particles produced in high-energy collisions. The cumulant method involves the calculation of $2k$-particle azimuthal correlations, $\mathrm{corr}_n\{2k\}$, and cumulants, $c_n\{2k\}$, for n^{th} Fourier harmonics, where $n = 2, 3, 4$ and $k = 1, 2, 3, 4$ for the analysis presented in this paper. The $\mathrm{corr}_n\{2k\}$ are defined as [65, 67]:

$$\begin{aligned}
\langle\langle \mathrm{corr}_n\{2\}\rangle\rangle &\equiv \langle\langle e^{in(\phi_1-\phi_2)}\rangle\rangle, \\
\langle\langle \mathrm{corr}_n\{4\}\rangle\rangle &\equiv \langle\langle e^{in(\phi_1+\phi_2-\phi_3-\phi_4)}\rangle\rangle, \\
\langle\langle \mathrm{corr}_n\{6\}\rangle\rangle &\equiv \langle\langle e^{in(\phi_1+\phi_2+\phi_3-\phi_4-\phi_5-\phi_6)}\rangle\rangle, \\
\langle\langle \mathrm{corr}_n\{8\}\rangle\rangle &\equiv \langle\langle e^{in(\phi_1+\phi_2+\phi_3+\phi_4-\phi_5-\phi_6-\phi_7-\phi_8)}\rangle\rangle,
\end{aligned}$$

where the brackets "$\langle\langle\rangle\rangle$" denote double averaging, performed first over particles in an event and then over all events within a given event class. For every event, the average is taken over all possible of the combinations of the azimuthal angles $\phi_i (i = 1, \ldots, 8)$ of the $2k$ particles.

With the calculated multi-particle azimuthal correlations, the cumulants $c_n\{2k\}$ are obtained after subtracting the correlations between $2(k-1)$ particles according to the following formulae [65, 67]:

$$
\begin{aligned}
c_n\{2\} &= \langle\langle \mathrm{corr}_n\{2\}\rangle\rangle, \\
c_n\{4\} &= \langle\langle \mathrm{corr}_n\{4\}\rangle\rangle - 2\langle\langle \mathrm{corr}_n\{2\}\rangle\rangle^2, \\
c_n\{6\} &= \langle\langle \mathrm{corr}_n\{6\}\rangle\rangle - 9\langle\langle \mathrm{corr}_n\{2\}\rangle\rangle\langle\langle \mathrm{corr}_n\{4\}\rangle\rangle + 12\langle\langle \mathrm{corr}_n\{2\}\rangle\rangle^3, \\
c_n\{8\} &= \langle\langle \mathrm{corr}_n\{8\}\rangle\rangle - 16\langle\langle \mathrm{corr}_n\{2\}\rangle\rangle\langle\langle \mathrm{corr}_n\{6\}\rangle\rangle - 18\langle\langle \mathrm{corr}_n\{4\}\rangle\rangle^2 \\
&\quad + 144\langle\langle \mathrm{corr}_n\{2\}\rangle\rangle^2\langle\langle \mathrm{corr}_n\{4\}\rangle\rangle - 144\langle\langle \mathrm{corr}_n\{2\}\rangle\rangle^4.
\end{aligned}
$$

The Q-cumulant method [67], used in this analysis, relies on the idea of expressing the multi-particle correlations in terms of powers of the flow vector Q_n. This approach allows multi-particle correlations and cumulants to be calculated in a single pass over data events. The flow vector is defined for each collision event with multiplicity M as:

$$
Q_{n,j} \equiv \sum_{i=1}^{M} w_i^j \mathrm{e}^{\mathrm{i}n\phi_i}, \tag{1}
$$

where the subscript n denotes the order of the flow harmonic, j is the power of the flow vector, and the sum runs over all particles in an event with w_i being the weight of the i^{th} particle. The weight accounts for detector effects including the tracking efficiency and is defined in Section 6.

If the measured $c_n\{2k\}$ cumulants are free of non-flow correlations, they can be used to estimate Fourier harmonics v_n. Furthermore, assuming that the event-by-event fluctuations of v_n are negligibly small, the Fourier harmonics denoted by $\mathrm{v}_n\{2k\}$ can be determined [65]:

$$
\mathrm{v}_n\{2\} = \sqrt{c_n\{2\}}, \tag{2}
$$

$$
\mathrm{v}_n\{4\} = \sqrt[4]{-c_n\{4\}}, \tag{3}
$$

$$
\mathrm{v}_n\{6\} = \sqrt[6]{c_n\{6\}/4}, \tag{4}
$$

$$
\mathrm{v}_n\{8\} = \sqrt[8]{-c_n\{8\}/33}. \tag{5}
$$

From the above definitions it is evident that determination of real values of Fourier harmonics requires negative (positive) $c_n\{4\}$ and $c_n\{8\}$ ($c_n\{2\}$ and $c_n\{6\}$) values.

3 ATLAS detector

The data were collected with the ATLAS detector [68].[1] The detector consists of three main systems: an inner tracking detector (ID) surrounded by a thin superconducting solenoid, electromagnetic and hadronic

[1] ATLAS uses a right-handed coordinate system with its origin at the nominal interaction point (IP) in the centre of the detector and the z-axis along the beam pipe. The x-axis points from the IP to the centre of the LHC ring, and the y-axis points upwards. Cylindrical coordinates (r, ϕ) are used in the transverse plane, ϕ being the azimuthal angle around the z-axis. The pseudorapidity is defined in terms of the polar angle θ as $\eta = -\ln\tan(\theta/2)$.

calorimeters, and a muon spectrometer. The ID is immersed in a 2 T axial magnetic field and provides charged-particle tracking in the range $|\eta| < 2.5$. It consists of silicon pixel, silicon microstrip (SCT), and straw-tube transition radiation tracking detectors. Since 2015 the pixel detector includes an additional layer at smaller radius, the "insertable B-layer" (IBL) [69]. The calorimeter system covers the pseudorapidity range up to $|\eta| = 4.9$. The muon spectrometer surrounds the calorimeters and is based on three large air-core toroid superconducting magnets with eight coils each. The field integral of the toroids ranges between 2 to 6 T m across most of the detector. Measurements presented in this document use signals from the ID while other components are used for triggering.

Events are selected with a trigger system [70]. The first-level (L1) trigger is implemented in hardware and uses a subset of the detector information. For this analysis the information from calorimeters, minimum bias trigger scintillator (MBTS) counters (covering the range $2.1 < |\eta| < 3.8$) and zero degree calorimeters (ZDCs) with the range $|\eta| > 8.3$ is used at L1. The L1 trigger is followed by two software-based trigger levels: level-2 (L2) and Event Filter (EF). In pp data-taking in 2015, the L2 and EF trigger levels are combined in a common high-level trigger (HLT) framework.

4 Data sets

The $\sqrt{s} = 5.02$ TeV pp data were recorded in November 2015 and correspond to an integrated luminosity of about 28 pb^{-1}. The average number of additional interactions in the same bunch crossing, μ, ranges from 0.4 to 1.3. For the low-multiplicity event selections, three minimum-bias triggers were used: the first required a hit in at least one MBTS counter, the second required a hit in at least one MBTS counter on each side, and the third required at least one reconstructed track at the HLT seeded by a random trigger at L1. In order to enhance the number of high-multiplicity events, dedicated high-multiplicity triggers (HMTs) were implemented. Three HMTs required at L1 more than 5 GeV, 10 GeV and 20 GeV in the total transverse energy ($\sum E_{\mathrm{T}}$) recorded in the calorimeters, and at the HLT more than 60, 90 and 90 reconstructed charged-particle tracks with $p_{\mathrm{T}} > 0.4$ GeV and $|\eta| < 2.5$, respectively.

The $\sqrt{s} = 13$ TeV pp data were taken over two running periods in June and August of 2015. For the first running period, μ varied between 0.002 and 0.03, while for the second μ ranged from 0.05 to 0.6. The total integrated luminosity collected over these two periods is approximately 0.075 pb $^{-1}$. In addition to the minimum-bias event trigger, HMTs were implemented seeded by a L1 requirement of $\sum E_{\mathrm{T}} > 10$ GeV. For the low-μ running period, the requirement of more than 60 reconstructed charged-particle tracks at the HLT was imposed. For the moderate-μ data (the second data-taking period), two requirements on the number of online reconstructed charged-particle tracks at the HLT, of more than 60 and 90, were employed.

The p+Pb data were collected during the LHC run at the beginning of 2013. The LHC operated in two configurations during this running period, by reversing the directions of the proton and lead beams. The proton beam with the energy of 4 TeV collided with a Pb beam of energy 1.57 TeV per nucleon. This leads to $\sqrt{s_{\mathrm{NN}}} = 5.02$ TeV in the nucleon–nucleon centre-of-mass frame, which is shifted by 0.465 in rapidity in the proton direction. The total integrated luminosity corresponds to approximately 0.028 pb^{-1}. The data were recorded with the minimum-bias trigger and several HMTs, seeded by L1 thresholds on the total transverse energy recorded in the forward calorimeters ($\sum E_{\mathrm{T}}^{\mathrm{FCal}}, 3.1 < |\eta| < 4.9$) and HLT thresholds on the number of online reconstructed charged-particle tracks, $N_{\mathrm{ch}}^{\mathrm{online}}$ [71]. Six different combinations of the L1 and HLT thresholds were implemented: ($\sum E_{\mathrm{T}}^{\mathrm{FCal}}$[GeV] $>, N_{\mathrm{ch}}^{\mathrm{online}} >$) = (10,100), (10,130), (50,150), (50,180), (65,200) and (65,225). More details can be found in Ref. [35]. For the p+Pb data, $\mu \approx 0.03$.

The $\sqrt{s_{\mathrm{NN}}}$ = 2.76 TeV Pb+Pb data set used in this analysis consists of the data collected in 2010 and then reprocessed in 2014 with the same reconstruction software as used for p+Pb data. The number of additional interactions per bunch crossing is negligibly small, of the order of 10^{-4}.

Monte Carlo (MC) simulated event samples are used to determine the track reconstruction efficiency (Section 5) and to perform closure tests, as described in Section 7. For the 13 TeV and 5.02 TeV pp data the baseline MC event generator used is Pythia 8 [72] with parameter values set according to the ATLAS A2 tune [73] and with MSTW2008LO parton distribution functions [74]. The Hijing event generator [75] is used to produce p+Pb and Pb+Pb collisions with the same energy as in the data. The detector response is simulated [76] with Geant 4 [77] and with detector conditions matching those during the data-taking. The simulated events are reconstructed with the same algorithms as data events, including track reconstruction.

5 Event and track selections

Additional event selections are implemented in the offline analysis. Events are required to have a reconstructed vertex. For the p+Pb and Pb+Pb data, only events with a reconstructed vertex for which $|z_{\mathrm{vtx}}| < 150$ mm are selected while for pp data sets this requirement is not applied.

In order to suppress additional interactions per bunch crossing (referred to as pile-up) in pp data sets, only tracks associated with the vertex for which the $\sum p_{\mathrm{T}}^2$ is the largest are used. In addition, all events with a second vertex reconstructed from at least four tracks are disregarded. For the p+Pb data, even though the average number of interactions per bunch crossing is small (~ 0.03), it can be significantly larger in events with a high multiplicity. Therefore, events containing more than one interaction per bunch crossing are rejected if they contain more than one good reconstructed vertex, where a good vertex is defined as that with the scalar sum of the tracks transverse momenta $\sum p_{\mathrm{T}} > 5$ GeV. The remaining pile-up events are further suppressed using the ZDC signal on the Pb-fragmentation side, calibrated to the number of recorded neutrons [35]. In order to suppress beam backgrounds in p+Pb and Pb+Pb data, a requirement on the time difference between signals from MBTS counters on opposite sides of the interaction region is imposed, $|\Delta t| < 10$ ns and < 3 ns, respectively.

For the pp data, charged-particle tracks are reconstructed in the ID with the tracking algorithm optimized for Run-2 data [78]. The tracks are required to have $|\eta| < 2.5$ and $p_{\mathrm{T}} > 0.1$ GeV. At least one pixel hit is required and a hit in the IBL is also required if the track passes through the active region of the IBL. If a track passes through an inactive area of the IBL, then a hit is required in the next pixel layer if one is expected. The requirement on the minimum number of SCT hits depends on p_{T}: ≥ 2 for $0.1 < p_{\mathrm{T}} < 0.3$ GeV, ≥ 4 for $0.3 < p_{\mathrm{T}} < 0.4$ GeV and ≥ 6 for $p_{\mathrm{T}} > 0.4$ GeV. Additional selection requirements are imposed on the transverse, $|d_0|$, and longitudinal, $|z_0 \sin\theta|$, impact parameters. The transverse impact parameter is measured with respect to the beam line, and z_0 is the difference between the longitudinal position (along the beam line) of the track at the point where d_0 is measured and the primary vertex. Both must be smaller than 1.5 mm. In order to reject tracks with incorrectly measured p_{T} due to interactions with the detector material, the track-fit probability must be larger than 0.01 for tracks with $p_{\mathrm{T}} > 10$ GeV.

For the reconstruction of p+Pb and Pb+Pb data, the same tracking algorithms are used. The track selection requirements are modified slightly from those applied in the pp reconstruction. Specifically, the same requirements are imposed on the impact parameters, although $|d_0|$ is determined with respect to

the primary vertex. To suppress falsely reconstructed charged-particle tracks, additional requirements are imposed on the significance of the transverse and longitudinal impact parameters: $|d_0|/\sigma_{d_0} < 3$ and $|z_0 \sin\theta|/\sigma_{z_0} < 3$, where σ_{d_0} and σ_{z_0} are the uncertainties in the transverse and longitudinal impact parameter values, respectively, as obtained from the covariance matrix of the track fit.

The tracking efficiencies are estimated using the MC samples reconstructed with the same tracking algorithms and the same track selection requirements. Efficiencies, $\epsilon(\eta, p_{\mathrm{T}})$, are evaluated as a function of track η, p_{T} and the number of reconstructed charged-particle tracks, but averaged over the full range in azimuth. For all collision systems, the efficiency increases by about 4% with p_{T} increasing from 0.3 GeV to 0.6 GeV. Above 0.6 GeV, the efficiency is independent of p_{T} and reaches 86% (72%) at $\eta \approx 0$ ($|\eta| > 2$), 83% (70%) and 83% (70%) for pp, p+Pb and peripheral Pb+Pb collisions, respectively. The efficiency is independent of the event multiplicity for $N_{\mathrm{ch}} > 40$. For lower-multiplicity events the efficiency is smaller by a few percent. The rate of falsely reconstructed charged-particle tracks, $f(p_{\mathrm{T}}, \eta)$, is also estimated and found to be small; even at the lowest transverse momenta it stays below 1% (3%) at $\eta \approx 0$ ($|\eta| > 2$).

Residual detector defects (not accounted for by tracking efficiencies), which may arise on a run-by-run basis and could lead to a non-uniformity of the azimuthal angle distribution, are corrected for by a data-driven approach, the so-called flattening procedure described in Section 6.

The analysis is performed as a function of the charged-particle multiplicity. Three measures of the event multiplicity are defined based on counting the number of particles observed in different transverse momentum ranges: $0.3 < p_{\mathrm{T}} < 3$ GeV, $0.5 < p_{\mathrm{T}} < 5$ GeV and $p_{\mathrm{T}} > 0.4$ GeV (see next section for details). For each multiplicity definition, only events with multiplicity ≥ 10 are used to allow a robust calculation of the multi-particle cumulants. Furthermore, in order to avoid potential biases due to HMT inefficiencies, events selected by the HMTs are accepted only if the trigger efficiency for each multiplicity definition exceeds 90%. The only exception is the pp 13 TeV data collected in August 2015 with the HMT requiring more than 90 particles reconstructed at the HLT, for which the 90% efficiency is not reached. It was carefully checked that inclusion of this data set does not generate any bias in the calculation of multi-particle cumulants.

6 Overview of the analysis

For each collision system, the multi-particle cumulants are calculated using the so-called reference particles. Two selections of reference particles are considered, for which the multiplicity M_{ref} in a given event is the number of reconstructed charged particles with $|\eta| < 2.5$ and with corresponding p_{T} ranges: $0.3 < p_{\mathrm{T}} < 3$ GeV or $0.5 < p_{\mathrm{T}} < 5$ GeV. Figure 1 shows the uncorrected M_{ref} multiplicity distributions for the reconstructed charged-particle tracks with $0.3 < p_{\mathrm{T}} < 3$ GeV for all collision systems. The observed discontinuities reflect the offline selection requirement of at least 90% efficiency for the HMT thresholds. Event weights are introduced to account for the trigger efficiency and the trigger prescale factors [35].

Particle weights (see Eq. (1)) are applied to account for detector effects via $w_\phi(\eta, \phi)$, the tracking efficiency $\epsilon(\eta, p_{\mathrm{T}})$ and the rate of fake tracks $f(\eta, p_{\mathrm{T}})$, and are defined as:

$$w_i(\eta, \phi, p_{\mathrm{T}}) = \frac{w_{\phi,i}(\eta, \phi)(1 - f_i(\eta, p_{\mathrm{T}}))}{\epsilon_i(\eta, p_{\mathrm{T}})}.$$

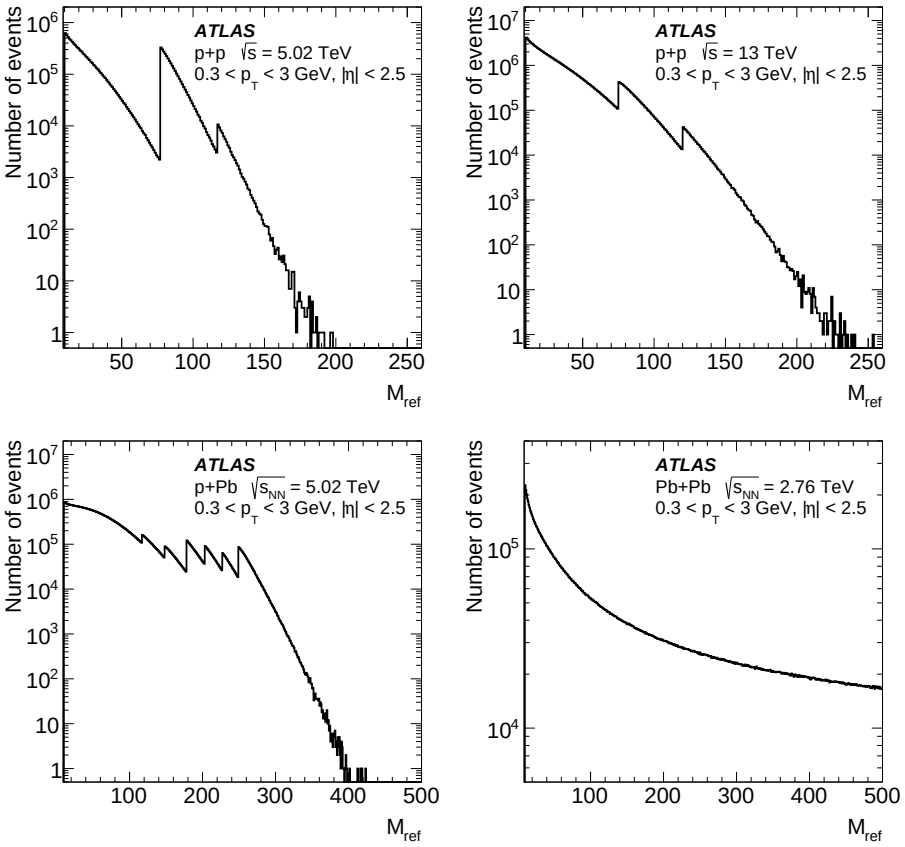

Figure 1: Distributions of the reference particle multiplicity, M_{ref}, for the selected reference particles with $0.3 < p_{\mathrm{T}} < 3$ GeV for pp collisions at $\sqrt{s} = 5.02$ and 13 TeV, p+Pb collisions at $\sqrt{s_{\mathrm{NN}}} = 5.02$ TeV and low-multiplicity Pb+Pb collisions at $\sqrt{s_{\mathrm{NN}}} = 2.76$ TeV. The discontinuities in the upper and lower-left distributions correspond to different high-multiplicity trigger thresholds.

The tracking efficiencies and fake rates are determined as described in Section 5. The weights $w_\phi(\eta, \phi)$ are determined from the data by the procedure of azimuthal-angle flattening in order to correct for non-uniformity of the azimuthal acceptance of the detector. The flattening procedure uses the η–ϕ map of all reconstructed charged-particle tracks. For each small interval $(\delta\eta, \delta\phi)$, a "flattening" weight is calculated as $w_\phi(\eta, \phi) = \langle N(\delta\eta)\rangle / N(\delta\eta, \delta\phi)$ where $\langle N(\delta\eta)\rangle$ is the event-averaged number of tracks in the $\delta\eta$ slice, averaged over the full range in ϕ, while $N(\delta\eta, \delta\phi)$ is the number of tracks within this interval.

The cumulants and corresponding Fourier harmonics are studied as a function of the charged-particle multiplicity. Two ways of selecting events according to the event multiplicity are considered. The first one is to select events with a given M_{ref}, which is referred to as EvSel_M_{ref}. An alternative way (EvSel_N_{ch}) is to apply the event-selection on the basis of the number of reconstructed charged particles with $p_{\mathrm{T}} > 0.4$ GeV, $N_{\mathrm{ch}}^{\mathrm{rec}}$, and then for such selected events calculate the cumulants using reference particles. For both event selections, the cumulants are calculated in unit-size bins in either M_{ref} or $N_{\mathrm{ch}}^{\mathrm{rec}}$, which are then combined into broader, statistically significant multiplicity intervals by averaging the cumulants, $c_n\{2k\}$.

For the purpose of a direct comparison of results obtained with different event selections, the standard

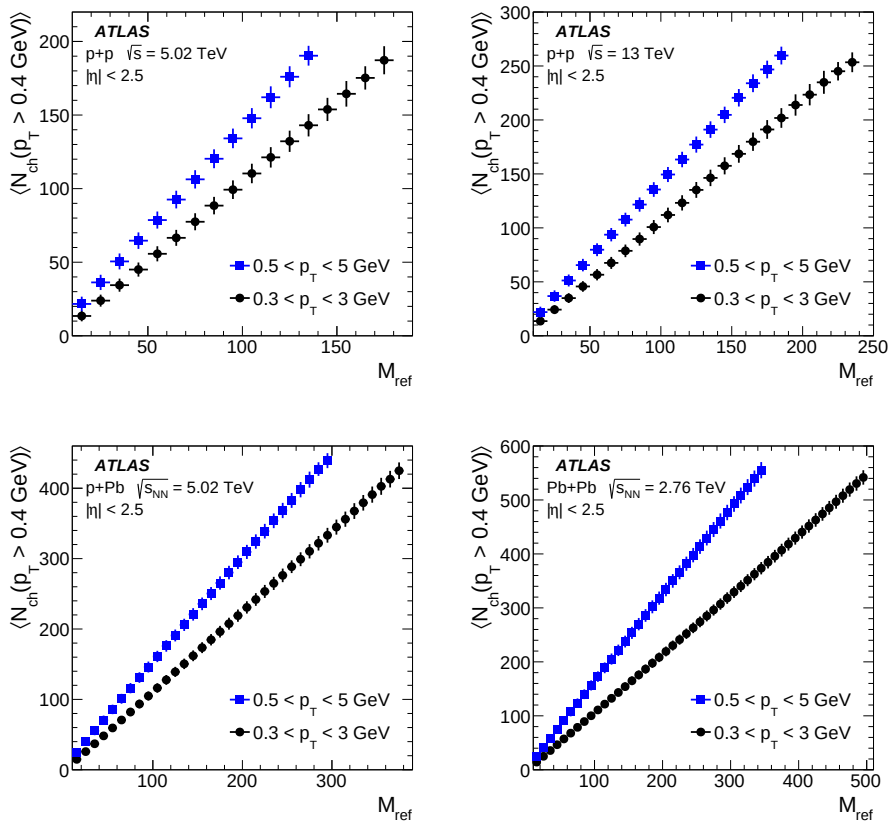

Figure 2: The average number of charged particles per event with $p_{\mathrm{T}} > 0.4$ GeV as a function of reference particle multiplicity for reference particles with $0.5 < p_{\mathrm{T}} < 5$ GeV and $0.3 < p_{\mathrm{T}} < 3$ GeV for pp collisions at $\sqrt{s} = 5.02$ and 13 TeV, p+Pb collisions at $\sqrt{s_{\mathrm{NN}}} = 5.02$ TeV and low-multiplicity Pb+Pb collisions at $\sqrt{s_{\mathrm{NN}}} = 2.76$ TeV. The error bars show one standard deviations on $\langle N_{\mathrm{ch}}(p_{\mathrm{T}} > 0.4\ \mathrm{GeV})\rangle$.

multiplicity variable measuring the event activity is used. The $N_{\mathrm{ch}}(p_{\mathrm{T}} > 0.4$ GeV) multiplicity, corrected for tracking efficiency and the rate of falsely reconstructed charged-particle tracks as well as for trigger efficiencies, is used to present the results. When selecting events according to M_{ref} multiplicity, the correlation between M_{ref} and the $N_{\mathrm{ch}}(p_{\mathrm{T}} > 0.4$ GeV) is employed. Figure 2 shows mean $N_{\mathrm{ch}}(p_{\mathrm{T}} > 0.4$ GeV) multiplicities calculated in M_{ref} intervals, which are used in the analysis. The correlation is shown for each collision system and for two p_{T} ranges of reference particles. In the case of EvSel_N_{ch}, a similar mapping of $N_{\mathrm{ch}}^{\mathrm{rec}}$ intervals into $\langle N_{\mathrm{ch}}(p_{\mathrm{T}} > 0.4$ GeV)$\rangle$ is made. The two event selections differ in their sensitivity to event-by-event multiplicity fluctuations and are biased in a different manner by contributions from non-flow correlations. In the selection based on M_{ref}, by construction, multiplicity fluctuations are eliminated. This is not the case for the selection using $N_{\mathrm{ch}}(p_{\mathrm{T}} > 0.4$ GeV): there are strong event-level fluctuations in $M_{\mathrm{ref}}(0.3 < p_{\mathrm{T}} < 3$ GeV) for events selected with fixed values of $N_{\mathrm{ch}}(p_{\mathrm{T}} > 0.4$ GeV). In order to illustrate how multiplicity fluctuations affect the determination of cumulants, the comparison of $c_2\{4\}$ cumulants obtained with two alternative ways of selecting events is shown in Figure 3 for reference particles with $0.3 < p_{\mathrm{T}} < 3$ GeV. In pp collisions, the cumulants obtained using events with fixed $N_{\mathrm{ch}}(p_{\mathrm{T}} > 0.4$ GeV), thus susceptible to fluctuations in M_{ref}, are systematically smaller than those obtained using events selected according to M_{ref}. This indicates that non-flow correlations associated

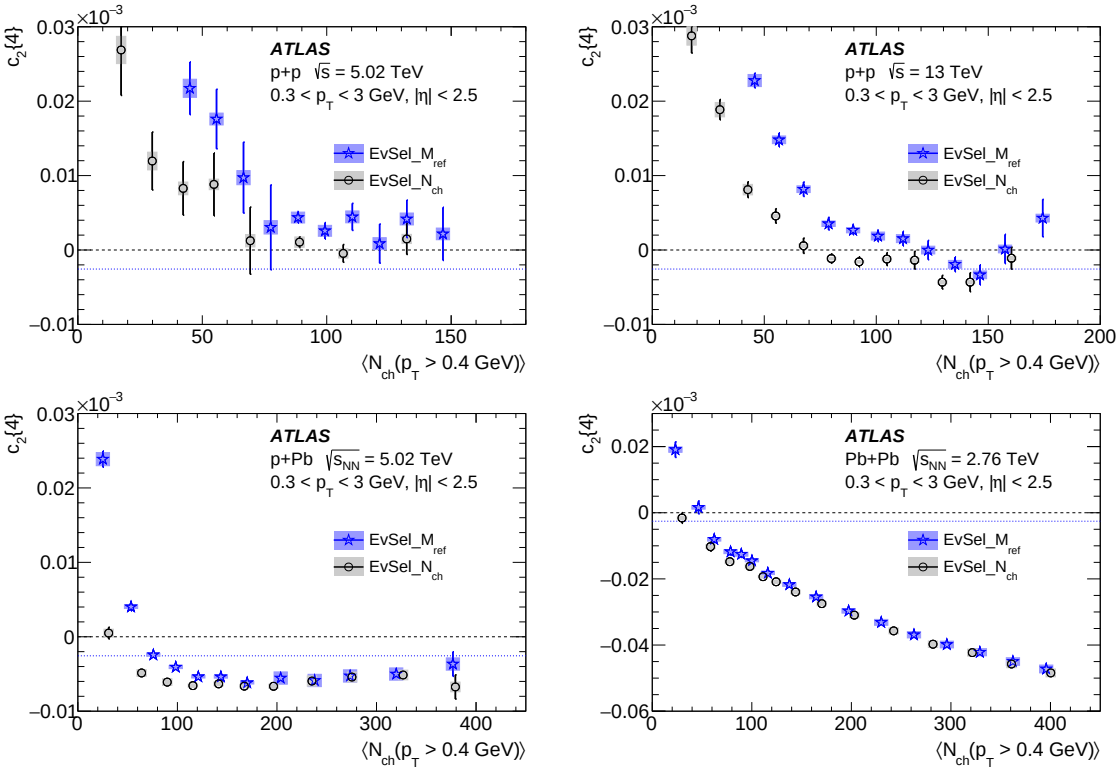

Figure 3: Comparison of $c_2\{4\}$ cumulants for reference particles with $0.3 < p_{\mathrm{T}} < 3.0$ GeV obtained with two different event selections: events selected according to M_{ref} (EvSel_M_{ref}) and according to $N_{\mathrm{ch}}(p_{\mathrm{T}} > 0.4$ GeV) (EvSel_N_{ch}) for pp collisions at $\sqrt{s} = 5.02$ and 13 TeV, p+Pb collisions at $\sqrt{s_{\mathrm{NN}}} = 5.02$ TeV and low-multiplicity Pb+Pb collisions at $\sqrt{s_{\mathrm{NN}}} = 2.76$ TeV. The vertical scale in the upper plots is cut off at 0.03×10^{-3} in order to clearly show differences in the region around $c_2\{4\} = 0$ .The error bars and shaded boxes denote statistical and systematic uncertainties, respectively. Dotted lines indicate the value of $c_2\{4\}$ corresponding to $\mathrm{v}_2\{4\} = 0.04$.

with multiplicity fluctuations give negative contributions to the measured $c_2\{4\}$ and, in the case of a small positive $c_2\{4\}$ signal, can mimic the collective effects. For p+Pb and Pb+Pb collisions, similar effects are seen at small event multiplicities, where biases from non-flow correlations are most significant. For large multiplicities, the non-flow correlations related to multiplicity fluctuations do not play a dominant role and the two event selections give consistent results. In this paper, the EvSel_M_{ref}, the event selection based on M_{ref} that is free of multiplicity fluctuations, is used as the default event selection.

Even when using an event selection free of multiplicity fluctuations, the cumulants calculated with a small number of particles can be contaminated by non-flow correlations. For two-particle cumulants, $c_n\{2\}$, the non-flow correlations can be reduced by requiring a large separation in pseudorapidity between particles forming a pair. As in the analysis of two-particle correlations [31, 35, 43, 46], the requirement of $|\Delta\eta| > 2$ is implemented in calculating the cumulants $c_n\{2, |\Delta\eta| > 2\}$. A comparison of $c_2\{2\}$ calculated without the $|\Delta\eta| > 2$ requirement and $c_2\{2, |\Delta\eta| > 2\}$ is shown in Figure 4 for all collision systems. A strong reduction of the cumulant values can be seen after requiring $|\Delta\eta| > 2$, which is the most significant at low multiplicities and for pp collisions, where the short-range two-particle non-flow correlations dominate. Unfortunately, such a requirement on $|\Delta\eta|$ cannot be applied in the calculation of cumulants of more than two particles in the standard cumulant approach applied in this analysis. This has to be taken into account

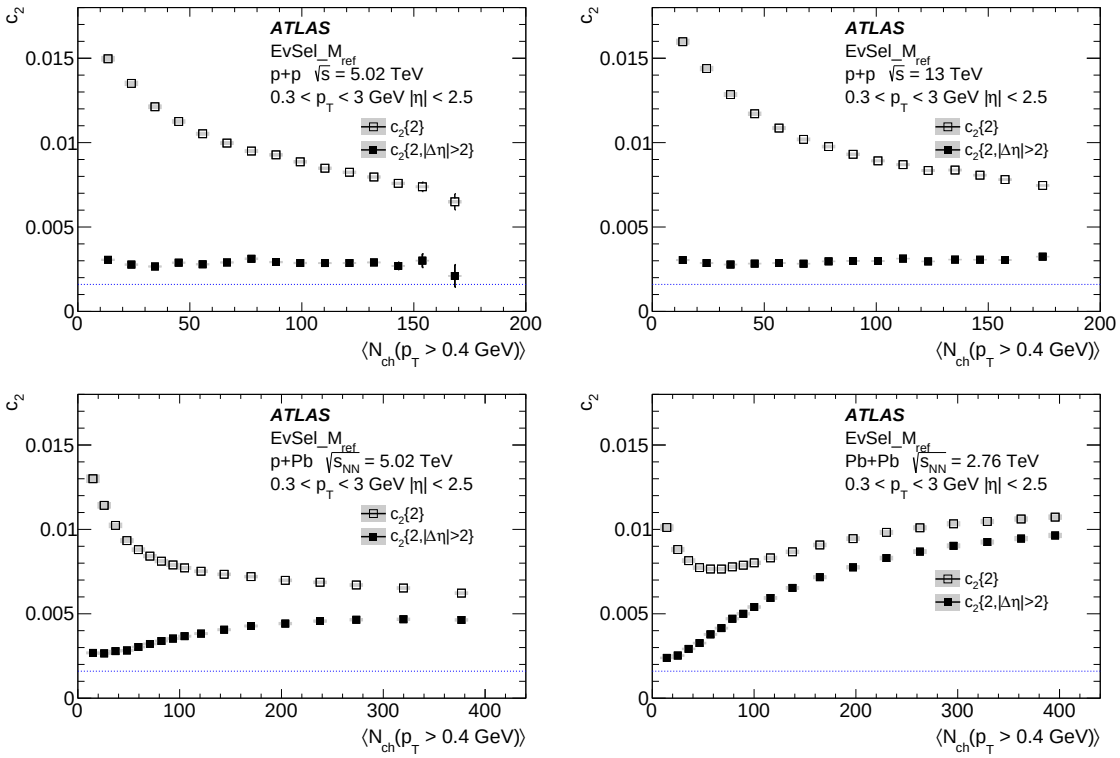

Figure 4: Comparison of $c_2\{2\}$ (open symbols) and $c_2\{2, |\Delta\eta| > 2\}$ (filled symbols) for reference particles with $0.3 < p_{\mathrm{T}} < 3.0$ GeV for pp collisions at $\sqrt{s} = 5.02$ and 13 TeV, p+Pb collisions at $\sqrt{s_{\mathrm{NN}}} = 5.02$ TeV and low-multiplicity Pb+Pb collisions at $\sqrt{s_{\mathrm{NN}}} = 2.76$ TeV. The error bars and shaded boxes denote statistical and systematic uncertainties, respectively. Dotted lines indicate the value of c_2 corresponding to $v_2\{2\} = 0.04$.

when interpreting the results obtained for $c_n\{4\}$. It is known (from PYTHIA [79] and HIJING simulations) that jet and dijet production can generate correlations between four particles, especially in collision systems (e.g. pp) where collective flow effects are expected to be small.

Measurements of multi-particle cumulants and the corresponding flow harmonics require very large event samples, especially when considering cumulants and correlations between more than two particles. This analysis uses the two-particle cumulants with a rapidity gap of $|\Delta\eta| > 2$ to determine $c_n\{2, |\Delta\eta| > 2\}$ for $n = 2$, 3 and 4 for all collision systems. Four-particle cumulants can be reliably determined for all collision systems only for $c_2\{4\}$. A statistically significant measurement of higher-order cumulants and harmonics, $n = 3, 4$, with more than two-particle correlations is not possible with the current data sets. Statistical limitations are particularly severe for six- and eight-particle cumulants measured in pp collisions. The statistical uncertainty of the pp data sets used in this analysis is significantly larger than the expected magnitude of the six- and eight-particle cumulants, preventing reliable measurements of these observables. Therefore, the measurements of $c_2\{6\}$ and $c_2\{8\}$ and the corresponding Fourier harmonics are reported only for p+Pb and Pb+Pb collisions.

7 Systematic uncertainties and cross-checks

The systematic uncertainties are estimated for $c_n\{2, |\Delta\eta| > 2\}$ (n= 2, 3 and 4) and $c_2\{4\}$, for all collision systems, and for $c_2\{6\}$ and $c_2\{8\}$ only for p+Pb and Pb+Pb data. The two ranges in p_{T} of reference particles are considered: $0.3 < p_{\mathrm{T}} < 3$ GeV and $0.5 < p_{\mathrm{T}} < 5$ GeV. The c_n uncertainties are then propagated to the corresponding v_n. Details on the contributions to systematic uncertainties from different sources are collected in tables included in the Appendix.

The following systematic uncertainties are considered:

Track-quality selections: The systematic uncertainties resulting from different track selection requirements are estimated as differences between the nominal results and the results obtained with modified track selection criteria. For pp data, the requirements on the impact parameters are varied from the nominal value of $|d_0| < 1.5$ mm and $|z_0 \sin\theta| < 1.5$ mm, to the tight selection, $|d_0| < 1$ mm and $|z_0 \sin\theta| < 1$ mm, and to the loose selection, $|d_0| < 2$ mm and $|z_0 \sin\theta| < 2$ mm. For p+Pb and Pb+Pb collisions the nominal selection requirements defined by the cuts on the impact parameters and the cuts on the significance of impact parameters ($|d_0| < 1.5$ mm, $|z_0 \sin\theta| < 1.5$ mm, $|d_0/\sigma_{d_0}| < 3$ and $|z_0 \sin(\theta)/\sigma_z| < 3$) are changed to the loose ones: $|d_0| < 2$ mm, $|z_0 \sin\theta| < 2$ mm, $|d_0/\sigma_{d_0}| < 4$ and $|z_0 \sin(\theta)/\sigma_z| < 4$. The tight selection requirements are: $|d_0| < 1$ mm, $|z_0 \sin\theta| < 1$ mm, $|d_0/\sigma_{d_0}| < 2$ and $|z_0 \sin(\theta)/\sigma_z| < 2$.

For each collision system, the track reconstruction efficiency is recalculated with the loose and tight track selections. The differences are obtained as averages over three ranges in $N_{\mathrm{ch}}(p_{\mathrm{T}} > 0.4$ GeV). The following ranges are defined: (<50), (50, 100) and (>100) for pp collisions at 5 and 13 TeV; (<100), (100, 200) and (>200) for p+Pb and Pb+Pb collisions. As a systematic uncertainty the largest difference, $c_n\{2k\}^{\mathrm{base}} - c_n\{2k\}^{\mathrm{loose}}$ or $c_n\{2k\}^{\mathrm{base}} - c_n\{2k\}^{\mathrm{tight}}$, is taken.

Tracking efficiency: Systematic uncertainty in the track reconstruction efficiency results from an imperfect detector geometry description in the simulations. It affects the particle weights determined using the MC-derived tracking efficiency, $\epsilon(\eta, p_{\mathrm{T}})$. For pp collisions, the efficiency uncertainty depends on η and p_{T}, as derived from the studies with the varied detector material budget [80]. It is found to vary between 1% and 4%, depending on η and p_{T}. For p+Pb and Pb+Pb collisions, the efficiency uncertainty is assumed to vary with p_{T} up to 4%, independently of η. The systematic uncertainty of the multi-particle cumulants is estimated by repeating the analysis with the tracking efficiency varied up and down by its corresponding uncertainty. The systematic uncertainty is taken as the largest deviation of the nominal result from the result obtained assuming a higher or lower efficiency. It is estimated for each bin in the charged-particle multiplicity.

Pile-up: The pile-up effects may be important for the analysis of pp data. The pile-up is significantly reduced by removing events with a second vertex reconstructed from at least four tracks. Furthermore, in the analysis the M_{ref} and cumulants are always calculated using the tracks associated with the primary vertex. As a result the pile-up effects should not play a significant role. The exception might be due to events where the pile-up vertex is so close to the primary vertex that the two are merged. To assess the pile-up effect on the cumulants calculated for 13 TeV pp data, the results for the low-μ June data ($\mu < 0.03$) and the moderate-μ August data ($\mu \sim 0.6$) are compared and the differences are found to be negligible.

However, such pile-up studies for pp collisions are strongly affected by statistical fluctuations, which arise due to the small number of data events with low or high pile-up as well as to the smallness of the measured signal. This is particularly true for four-particle cumulants as well as higher-order cumulants

$c_3\{2, |\Delta\eta| > 2\}$ and $c_4\{2, |\Delta\eta| > 2\}$, for pp collisions. Therefore, an alternative approach is also considered, where different criteria are used to reduce the pile-up. In the nominal approach, all events with a second vertex containing at least four tracks are removed. Here, the removal of events with a second vertex reconstructed from at least two or six tracks is also considered and the results for these two selections of events are compared to the nominal results. The maximum difference between the nominal measurement and the cumulants obtained from the data set with higher pile-up or lower pile-up is taken as a systematic uncertainty.

For p+Pb results, the pile-up effects are studied by comparing the nominal results, for which events with the second vertex with $\sum p_{\mathrm{T}} > 5$ GeV are removed, to the results obtained without removing the pile-up events. The maximum difference between the nominal measurement and the cumulants obtained without removing the pile-up events is taken as a systematic uncertainty.

For low-multiplicity Pb+Pb collisions the pile-up is negligibly small ($\mu \approx 10^{-4}$) and not considered to contribute to the systematic uncertainty.

Comparison of results for *p*+Pb and Pb+*p*: For p+Pb data the comparison is made between the results obtained during two running configurations with reversed beams directions, p+Pb and Pb+p. The results obtained from two running periods are consistent and give a negligible contribution to the systematic uncertainty.

The systematic uncertainty of the measured cumulants across all systems and the two p_{T} ranges of reference particles is not dominated by a single source. However, in most cases the largest contribution is from the track selection uncertainty, which mostly dominates uncertainties for higher-order harmonic cumulants. A sizeable contribution to the total uncertainty is also due to the tracking efficiency uncertainty, and this uncertainty is the largest for low multiplicities. The pile-up effects also give sizeable contributions to uncertainties in 5.02 TeV pp cumulants. The total systematic uncertainty is obtained by adding all individual contributions in quadrature. Table 1 lists the total systematic uncertainties of the measured cumulants in different collision systems for reference particles with $0.3 < p_{\mathrm{T}} < 3$ GeV. The listed systematic uncertainties are averaged over the N_{ch} range. For reference particles in the higher transverse momentum range, $0.5 < p_{\mathrm{T}} < 5$ GeV, the total systematic uncertainties are included in Table 2. The total systematic uncertainty of the cumulants is then propagated to the systematic uncertainties of the Fourier harmonics according to Eqs. (2) - (5).

Several cross-checks are also performed to validate the analysis method, but are not included in the systematic uncertainty. To account for the detector imperfections and to make the analysed azimuthal angle distribution uniform, data-determined weights $w_\phi(\eta, \phi)$ are used, as described in Section 6. To verify the robustness of the weighting procedure, the nominal results for cumulants are compared with those obtained with all weights $w_\phi(\eta, \phi)$ set to 1. The difference between the two measurements relative to the nominal results is found to be negligibly small.

Changing the trigger efficiency from 90% to 95% is also found to have negligible impact on the measured cumulants.

The global correlation effects should be independent of the charge sign of the produced particles. However, in reality the non-flow contributions may differ for same-sign and opposite-sign charged particles. To verify whether the results reported here depend on the charge of particles, the analysis is performed separately for same-sign charged particles only and compared to the results for all charged particles. In all cases, no systematic difference is observed when comparing the cumulants for all charged particles with those obtained using only same-sign charged particles.

Table 1: Total systematic uncertainties of the measured multi-particle cumulants for pp collisions at $\sqrt{s}$ = 5.02 and 13 TeV, p+Pb collisions at $\sqrt{s_{\rm NN}}$ = 5.02 TeV and low-multiplicity Pb+Pb collisions at $\sqrt{s_{\rm NN}}$ = 2.76 TeV, for $M_{\rm ref}$ with $0.3 < p_{\rm T} < 3$ GeV as estimated in a given $N_{\rm ch}$ interval.

Total systematic uncertainties				
System	Systematic uncertainty	$N_{\rm ch}$	$N_{\rm ch}$	$N_{\rm ch}$
		<50	50–100	>100
pp 5 TeV	$\delta c_2\{2, \lvert\Delta\eta\rvert > 2\} \times 10^4$	0.40	0.47	0.30
	$\delta c_2\{4\} \times 10^6$	4.25	0.95	0.80
	$\delta c_3\{2, \lvert\Delta\eta\rvert > 2\} \times 10^4$	0.26	0.33	0.15
	$\delta c_4\{2, \lvert\Delta\eta\rvert > 2\} \times 10^4$	0.12	0.12	-
		<50	50–100	>100
pp 13 TeV	$\delta c_2\{2, \lvert\Delta\eta\rvert > 2\} \times 10^4$	0.32	0.22	0.20
	$\delta c_2\{4\} \times 10^6$	3.76	0.52	0.54
	$\delta c_3\{2, \lvert\Delta\eta\rvert > 2\} \times 10^4$	0.05	0.03	0.07
	$\delta c_4\{2, \lvert\Delta\eta\rvert > 2\} \times 10^4$	0.02	0.05	-
		<100	100–200	>200
p+Pb	$\delta c_2\{2, \lvert\Delta\eta\rvert > 2\} \times 10^4$	0.59	0.59	0.70
	$\delta c_2\{4\} \times 10^6$	0.88	0.17	0.83
	$\delta c_2\{6\} \times 10^7$	0.62	0.22	0.09
	$\delta c_2\{8\} \times 10^8$	3.20	0.11	0.02
	$\delta c_3\{2, \lvert\Delta\eta\rvert > 2\} \times 10^4$	0.24	0.24	0.19
	$\delta c_4\{2, \lvert\Delta\eta\rvert > 2\} \times 10^4$	0.22	0.22	0.11
		<100	100–200	>200
Pb+Pb	$\delta c_2\{2, \lvert\Delta\eta\rvert > 2\} \times 10^4$	0.66	1.00	1.27
	$\delta c_2\{4\} \times 10^6$	0.82	0.67	1.19
	$\delta c_2\{6\} \times 10^7$	0.35	0.23	0.44
	$\delta c_2\{8\} \times 10^8$	1.23	0.13	0.31
	$\delta c_3\{2, \lvert\Delta\eta\rvert > 2\} \times 10^4$	0.10	0.09	0.13
	$\delta c_4\{2, \lvert\Delta\eta\rvert > 2\} \times 10^4$	0.03	0.04	0.05

Table 2: Total systematic uncertainties of the measured multi-particle cumulants for pp collisions at $\sqrt{s}$ = 5.02 and 13 TeV, p+Pb collisions at $\sqrt{s_{\rm NN}}$ = 5.02 TeV and low-multiplicity Pb+Pb collisions at $\sqrt{s_{\rm NN}}$ = 2.76 TeV, for $M_{\rm ref}$ with $0.5 < p_{\rm T} < 5$ GeV as estimated in a given $N_{\rm ch}$ interval.

Total systematic uncertainties				
System	Systematic uncertainty	$N_{\rm ch}$	$N_{\rm ch}$	$N_{\rm ch}$
		<50	50–100	>100
pp 5 TeV	$\delta c_2\{2, \lvert\Delta\eta\rvert > 2\} \times 10^4$	0.56	0.31	0.41
	$\delta c_2\{4\} \times 10^6$	7.20	1.85	2.45
	$\delta c_3\{2, \lvert\Delta\eta\rvert > 2\} \times 10^4$	0.35	0.34	0.23
	$\delta c_4\{2, \lvert\Delta\eta\rvert > 2\} \times 10^4$	0.29	0.45	-
		<50	50–100	>100
pp 13 TeV	$\delta c_2\{2, \lvert\Delta\eta\rvert > 2\} \times 10^4$	0.41	0.27	0.25
	$\delta c_2\{4\} \times 10^6$	6.40	1.77	0.59
	$\delta c_3\{2, \lvert\Delta\eta\rvert > 2\} \times 10^4$	0.07	0.07	0.08
	$\delta c_4\{2, \lvert\Delta\eta\rvert > 2\} \times 10^4$	0.03	0.05	0.06
		<100	100–200	>200
p+Pb	$\delta c_2\{2, \lvert\Delta\eta\rvert > 2\} \times 10^4$	0.31	0.32	0.38
	$\delta c_2\{4\} \times 10^6$	0.66	0.91	1.31
	$\delta c_2\{6\} \times 10^7$	1.43	0.65	0.40
	$\delta c_2\{8\} \times 10^8$	3.91	0.40	0.20
	$\delta c_3\{2, \lvert\Delta\eta\rvert > 2\} \times 10^4$	0.18	0.25	0.14
	$\delta c_4\{2, \lvert\Delta\eta\rvert > 2\} \times 10^4$	0.12	0.08	0.12
		<100	100–200	>200
Pb+Pb	$\delta c_2\{2, \lvert\Delta\eta\rvert > 2\} \times 10^4$	0.56	0.63	0.56
	$\delta c_2\{4\} \times 10^6$	1.84	0.82	0.72
	$\delta c_2\{6\} \times 10^7$	0.93	0.44	0.40
	$\delta c_2\{8\} \times 10^8$	0.86	0.54	0.51
	$\delta c_3\{2, \lvert\Delta\eta\rvert > 2\} \times 10^4$	0.06	0.09	0.07
	$\delta c_4\{2, \lvert\Delta\eta\rvert > 2\} \times 10^4$	0.13	0.02	0.05

8 Results

8.1 Second-order multi-particle cumulants and Fourier harmonics

The comparison between different collision systems is made for the cumulants calculated in M_{ref}-bins, where the p_{T} range of reference particles is $0.3 < p_{\mathrm{T}} < 3.0$ GeV and $0.5 < p_{\mathrm{T}} < 5.0$ GeV. A direct comparison of $c_2\{2, |\Delta\eta| > 2\}$ for different collision systems is shown in Figure 5 as a function of $\langle N_{\mathrm{ch}}(p_{\mathrm{T}} > 0.4\ \mathrm{GeV})\rangle$. An ordering in the magnitude of cumulants, with the largest for Pb+Pb, and then decreasing for smaller collision systems, is observed. Interestingly, for the three systems the N_{ch}-dependence changes from a clear increase for Pb+Pb, to a weaker increase in p+Pb and to no increase or even a decreasing trend in pp collisions. There is no dependence on the collision energy for pp data.

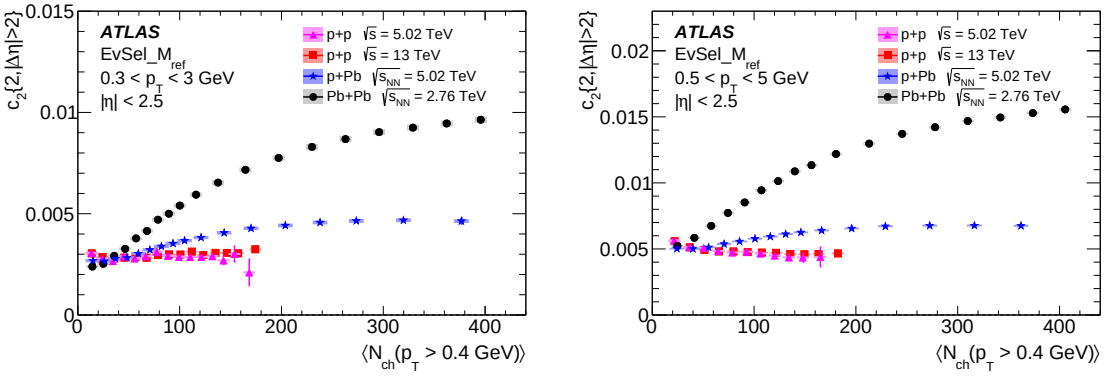

Figure 5: The two-particle cumulant $c_2\{2, |\Delta\eta| > 2\}$ as a function of $\langle N_{\mathrm{ch}}(p_{\mathrm{T}} > 0.4\ \mathrm{GeV})\rangle$ for pp collisions at $\sqrt{s}$ = 5.02 and 13 TeV, p+Pb collisions at $\sqrt{s_{\mathrm{NN}}}$ = 5.02 TeV and low-multiplicity Pb+Pb collisions at $\sqrt{s_{\mathrm{NN}}}$ = 2.76 TeV. The left panel shows the results obtained for M_{ref} with $0.3 < p_{\mathrm{T}} < 3.0$ GeV while the right panel is for M_{ref} with $0.5 < p_{\mathrm{T}} < 5.0$ GeV. The error bars and shaded boxes denote statistical and systematic uncertainties, respectively.

Four-particle cumulants, as shown in Figure 6, follow the ordering $|c_2\{4\}|_{\mathrm{p+Pb}} < |c_2\{4\}|_{\mathrm{Pb+Pb}}$ for $N_{\mathrm{ch}}(p_{\mathrm{T}} > 0.4\ \mathrm{GeV}) > 100$. The magnitude of $v_2\{4\}$ derived from $c_2\{4\}$ is larger for Pb+Pb collisions than for p+Pb events with the same $N_{\mathrm{ch}}(p_{\mathrm{T}} > 0.4\ \mathrm{GeV})$. For pp collisions, the cumulants depend weakly on the collision energy, although systematically larger cumulant values are measured at 13 TeV than at 5.02 TeV at low $N_{\mathrm{ch}}(p_{\mathrm{T}} > 0.4\ \mathrm{GeV})$. At higher multiplicities, this systematic dependence is reversed. Over the full range of particle multiplicities, the cumulants are positive or consistent with zero at 5.02 TeV for both p_{T} ranges and at 13 TeV for $0.5 < p_{\mathrm{T}} < 5.0$ GeV. For the 13 TeV pp data, the cumulants for $0.3 < p_{\mathrm{T}} < 3.0$ GeV also have positive values over the large range of multiplicities, with the exception of N_{ch} from 130 to 150, where $c_2\{4\}$ is negative but less than 1–2 standard deviations from zero. Therefore, these measurements of $c_2\{4\}$ cumulants in pp collisions, based on the event selection that suppresses the event-by-event fluctuations in the number of reference particles, do not allow determination of the Fourier harmonics. This indicates that the $c_2\{4\}$ obtained with the standard cumulant method used in this paper, even though free of multiplicity fluctuations, may still be biased by non-flow correlations.

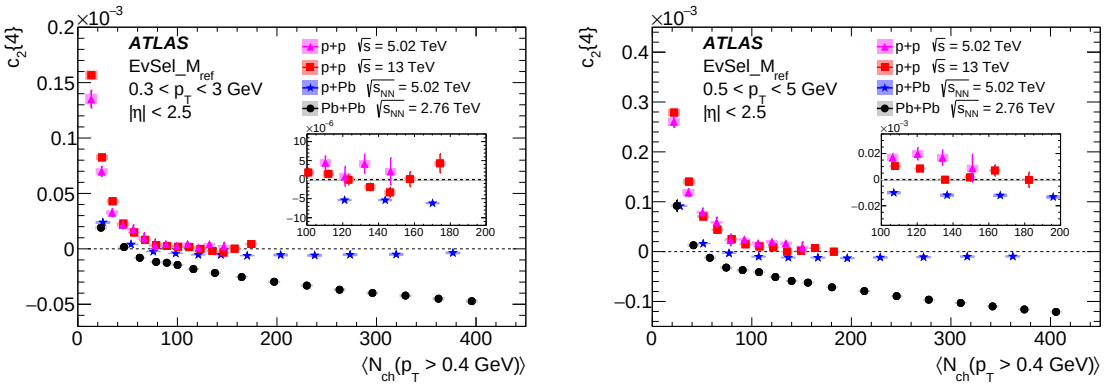

Figure 6: The second-order cumulant $c_2\{4\}$ obtained from four-particle correlations as a function of $\langle N_{\mathrm{ch}}(p_{\mathrm{T}} > 0.4\ \mathrm{GeV})\rangle$ for pp collisions at $\sqrt{s} = 5.02$ and 13 TeV, p+Pb collisions at $\sqrt{s_{\mathrm{NN}}} = 5.02$ TeV and low-multiplicity Pb+Pb collisions at $\sqrt{s_{\mathrm{NN}}} = 2.76$ TeV. The left panel shows the results obtained for M_{ref} with $0.3 < p_{\mathrm{T}} < 3.0$ GeV while the right panel is for M_{ref} with $0.5 < p_{\mathrm{T}} < 5.0$ GeV. The insets zoom in on the region around $c_2\{4\} = 0$. The error bars and shaded boxes denote statistical and systematic uncertainties, respectively.

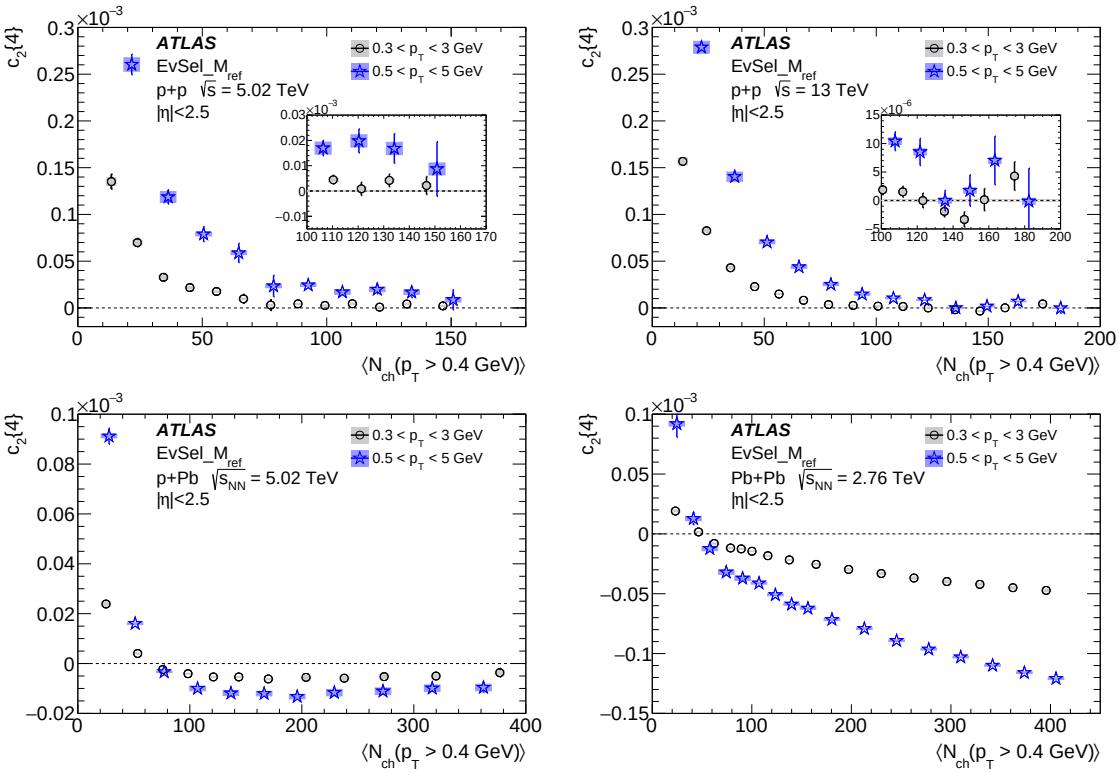

Figure 7: Comparison of $c_2\{4\}$ obtained for two p_{T} ranges of reference tracks as a function of $\langle N_{\mathrm{ch}}(p_{\mathrm{T}} > 0.4\ \mathrm{GeV})\rangle$ for 5.02 TeV and 13 TeV pp collisions, and 5.02 TeV p+Pb collisions, and 2.76 TeV Pb+Pb collisions. The insets in the upper panels zoom in on the high-multiplicity data. The error bars and shaded boxes denote statistical and systematic uncertainties, respectively.

A comparison of results for $c_2\{4\}$ obtained with two p_{T} ranges for reference tracks is shown in Figure 7. For p+Pb and Pb+Pb collisions, in the region where $c_2\{4\} < 0$, the $|c_2\{4\}|$ is larger for higher-p_{T} reference particles, as expected due to the rise of v_2 with p_{T}. For all collision systems, it is observed that for $c_2\{4\} > 0$, $c_2\{4\}$ is larger for higher-p_{T} reference particles. This indicates the influence of non-flow, jet-like correlations.

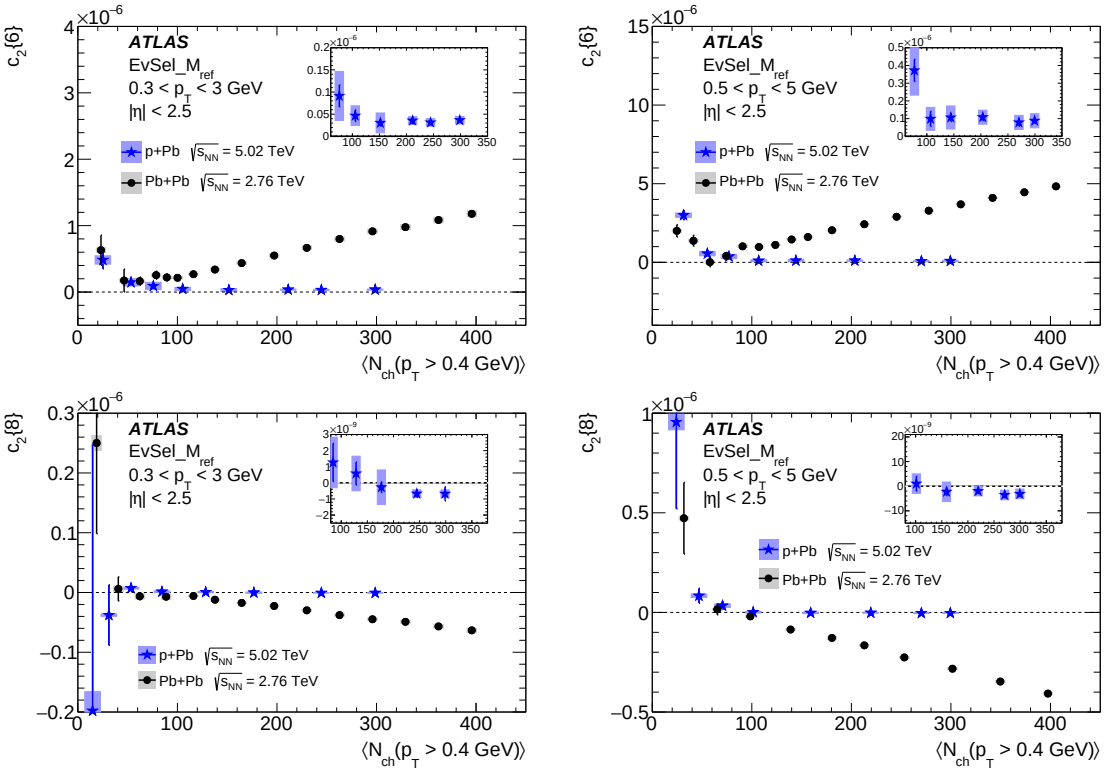

Figure 8: Comparison of $c_2\{6\}$ (top) and $c_2\{8\}$ (bottom) obtained for two p_{T} ranges of reference tracks as a function of $\langle N_{\mathrm{ch}}(p_{\mathrm{T}} > 0.4\ \mathrm{GeV})\rangle$ for p+Pb collisions at $\sqrt{s_{\mathrm{NN}}} = 5.02$ TeV and low-multiplicity Pb+Pb collisions at $\sqrt{s_{\mathrm{NN}}} = 2.76$ TeV. The left (right) panels show cumulants calculated for reference particles with $0.3 < p_{\mathrm{T}} < 3$ GeV ($0.5 < p_{\mathrm{T}} < 5$ GeV). The insets zoom in on the regions around $c_2\{6\} = 0$ and $c_2\{8\} = 0$. The error bars and shaded boxes denote statistical and systematic uncertainties, respectively.

The six- and eight-particle c_2 cumulants are compared for p+Pb and Pb+Pb collision systems in Figure 8. The measured $c_2\{6\}$ values are positive for both p_{T} ranges of reference particles. Positive values of $c_2\{6\}$ allow $\mathrm{v}_2\{6\}$ to be determined (see Eq. (4)). For Pb+Pb data, the $c_2\{8\}$, obtained for both p_{T} ranges of reference particles have negative values, and as such permit the evaluation of $\mathrm{v}_2\{8\}$; however, for p+Pb this requirement is only satisfied for a limited range of very high multiplicities.

The second-order Fourier harmonics, v_2, is obtained from c_2, following Eqs. (2) - (5). Real values of v_2 can only be obtained when the values of $c_2\{4\}$ and $c_2\{8\}$ ($c_2\{2, |\Delta\eta| > 2\}$ and $c_2\{6\}$) are negative (positive). Results for the v_2 harmonic can only be compared for four analysed collision systems for $\mathrm{v}_2\{2, |\Delta\eta| > 2\}$, derived from $c_2\{2, |\Delta\eta| > 2\}$. Such a comparison is shown in Figure 9. A number of distinct differences can be observed: (i) for the same $N_{\mathrm{ch}}(p_{\mathrm{T}} > 0.4\ \mathrm{GeV})$, the largest values of the second-order Fourier harmonic are observed for Pb+Pb collisions and at the highest multiplicities $\mathrm{v}_2\{2, |\Delta\eta| > 2\}$ for Pb+Pb is almost twice as large as for p+Pb collisions; (ii) the smallest v_2 values are observed for pp data, which

show no dependence on collision energy. For pp collisions, the $v_2\{2, |\Delta\eta| > 2\}$ is weakly dependent on multiplicity, showing a slight decrease for reference particles with higher transverse momenta. For p+Pb and Pb+Pb collisions, $v_2\{2, |\Delta\eta| > 2\}$ increases with increasing multiplicity up to $N_{\rm ch}(p_{\rm T} > 0.4$ GeV) $\simeq 250$. At higher multiplicities the increase gets weaker for Pb+Pb collisions, while for p+Pb data the second-order flow harmonics are observed to be independent of the multiplicity. Larger $v_2\{2, |\Delta\eta| > 2\}$ values are observed for reference particles with higher transverse momenta.

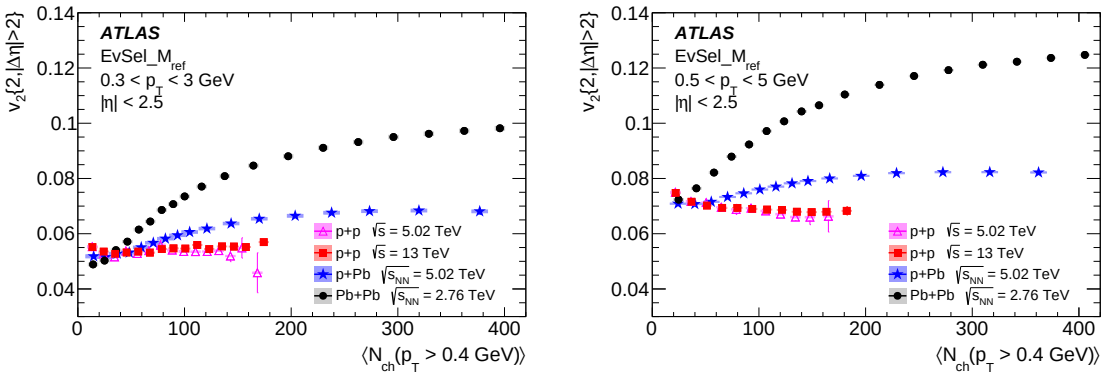

Figure 9: Comparison of $v_2\{2, |\Delta\eta| > 2\}$ as a function of $\langle N_{\rm ch}(p_{\rm T} > 0.4$ GeV)$\rangle$ for pp collisions at $\sqrt{s} = 5.02$ and 13 TeV, p+Pb collisions at $\sqrt{s_{\rm NN}} = 5.02$ TeV and low-multiplicity Pb+Pb collisions at $\sqrt{s_{\rm NN}} = 2.76$ TeV, and for two $p_{\rm T}$ ranges of reference particles. The error bars and shaded boxes denote statistical and systematic uncertainties, respectively.

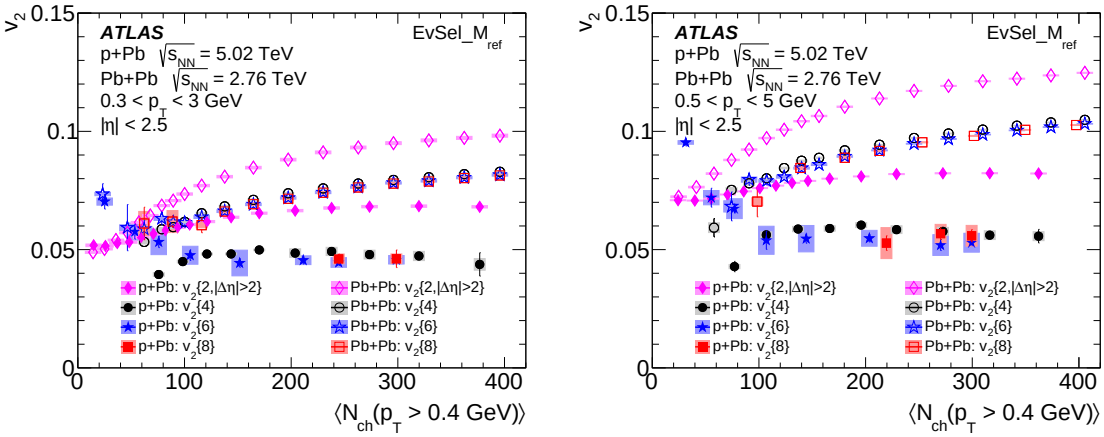

Figure 10: Comparison of $v_2\{2, |\Delta\eta| > 2\}$, $v_2\{4\}$, $v_2\{6\}$ and $v_2\{8\}$ as a function of $\langle N_{\rm ch}(p_{\rm T} > 0.4$ GeV)$\rangle$ for p+Pb collisions at $\sqrt{s_{\rm NN}} = 5.02$ TeV and low-multiplicity Pb+Pb collisions at $\sqrt{s_{\rm NN}} = 2.76$ TeV. The results are presented for two $p_{\rm T}$ ranges of the reference particles as indicated in the legend. The error bars and shaded boxes denote statistical and systematic uncertainties, respectively.

A comparison of the v_2 harmonic obtained with different cumulants, $v_2\{2, |\Delta\eta| > 2\}$, $v_2\{4\}$, $v_2\{6\}$ and $v_2\{8\}$, is shown in Figure 10 for p+Pb and low-multiplicity Pb+Pb collisions for the two $p_{\rm T}$ ranges of reference particles. All derived v_2 harmonics in Pb+Pb collisions have magnitudes larger than those

in p+Pb collisions with the same multiplicity. For both systems, $v_2\{2k\}$ are similar for $k = 2, 3$ and 4 while $v_2\{2, |\Delta\eta| > 2\}$ are systematically larger. However, compared to almost degenerate values of $v_2\{2k\}, k > 1$, a larger v_2 derived from two-particle cumulants is also predicted by models assuming fluctuation-driven initial-state anisotropies in small collision systems, either in the context of hydrodynamics as in Ref. [59] or in the effective theory of quantum chromodynamics in the regime of weak coupling [81, 82]. Figure 11 shows the ratio $v_2\{2k\}/v_2\{2k-2\}$ for p+Pb and low-multiplicity Pb+Pb collisions as a function of charged-particle multiplicity. Interestingly, for Pb+Pb collisions all three ratios are independent of $N_{\rm ch}(p_{\rm T} > 0.4$ GeV) beyond 120, independent of the $p_{\rm T}$ range of reference particles. The $v_2\{4\}/v_2\{2, |\Delta\eta| > 2\}$ ratios stay constant at the value of 0.85, while $v_2\{6\}/v_2\{4\}$ and $v_2\{8\}/v_2\{6\}$ ratios are almost degenerate at a value close to one, yet systematically $v_2\{8\}/v_2\{6\} > v_2\{6\}/v_2\{4\}$. For p+Pb collisions, similar universal behaviour of $v_2\{2k\}/v_2\{2k-2\}$ ratios is seen, although within much larger uncertainties. The $v_2\{4\}/v_2\{2, |\Delta\eta| > 2\}$ ratio has a value of about 0.7, thus smaller than in Pb+Pb collisions, and shows a tendency to decrease weakly with increasing multiplicity. These observations are qualitatively consistent with the predictions of the model of fluctuating initial geometry from Ref. [59], and provide further constraints on the initial state.

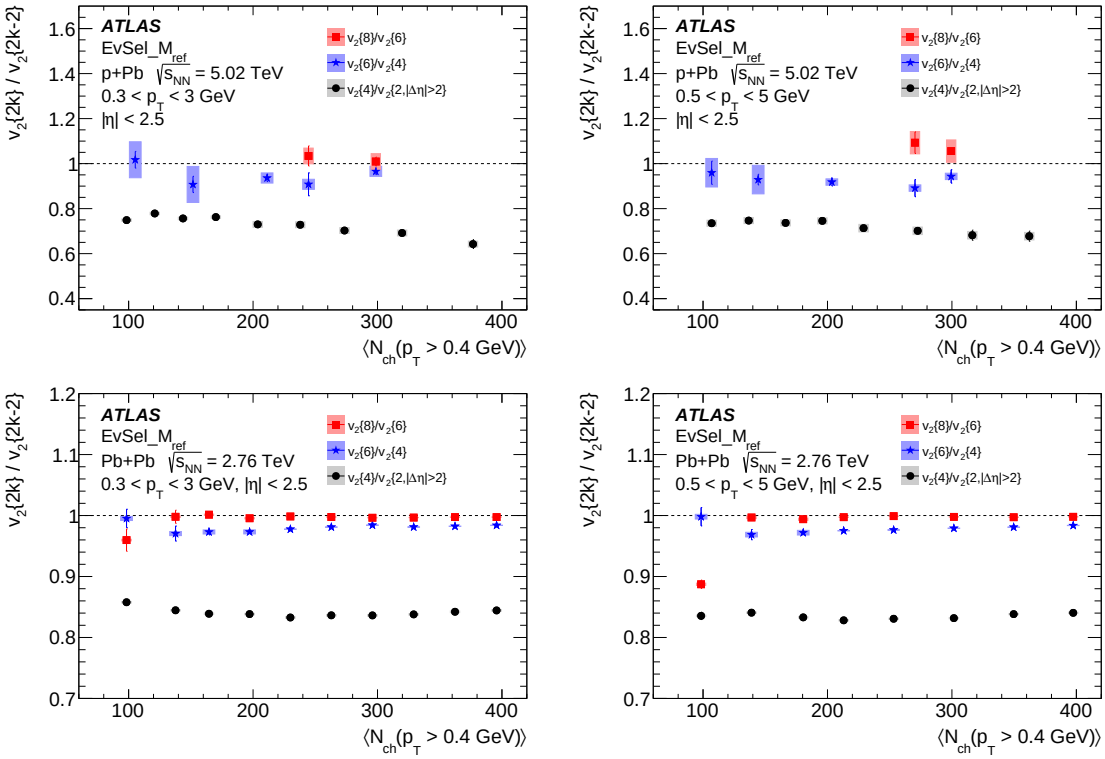

Figure 11: The ratios $v_2\{4\}/v_2\{2, |\Delta\eta| > 2\}$, $v_2\{6\}/v_2\{4\}$ and $v_2\{8\}/v_2\{6\}$ as a function of $\langle N_{\rm ch}(p_{\rm T} > 0.4$ GeV)$\rangle$ for p+Pb collisions at $\sqrt{s_{\rm NN}} = 5.02$ TeV (top) and low-multiplicity Pb+Pb collisions at $\sqrt{s_{\rm NN}} = 2.76$ TeV (bottom). Left (right) panels show cumulants calculated for reference particles with $0.3 < p_{\rm T} < 3$ GeV ($0.5 < p_{\rm T} < 5$ GeV). The error bars and shaded boxes denote statistical and systematic uncertainties, respectively.

8.2 Higher-order multi-particle cumulants and Fourier harmonics

Calculations of c_3 and c_4 multi-particle cumulants are statistics-limited and statistically significant results can only be obtained using two-particle cumulants with the superimposed $|\Delta\eta| > 2$ gap. Figure 12 shows a comparison between different collision systems for $c_3\{2, |\Delta\eta| > 2\}$ and $c_4\{2, |\Delta\eta| > 2\}$ cumulants calculated for M_{ref}, where the p_{T} range of reference particles is either $0.3 < p_{\text{T}} < 3.0$ GeV or $0.5 < p_{\text{T}} < 5.0$ GeV.

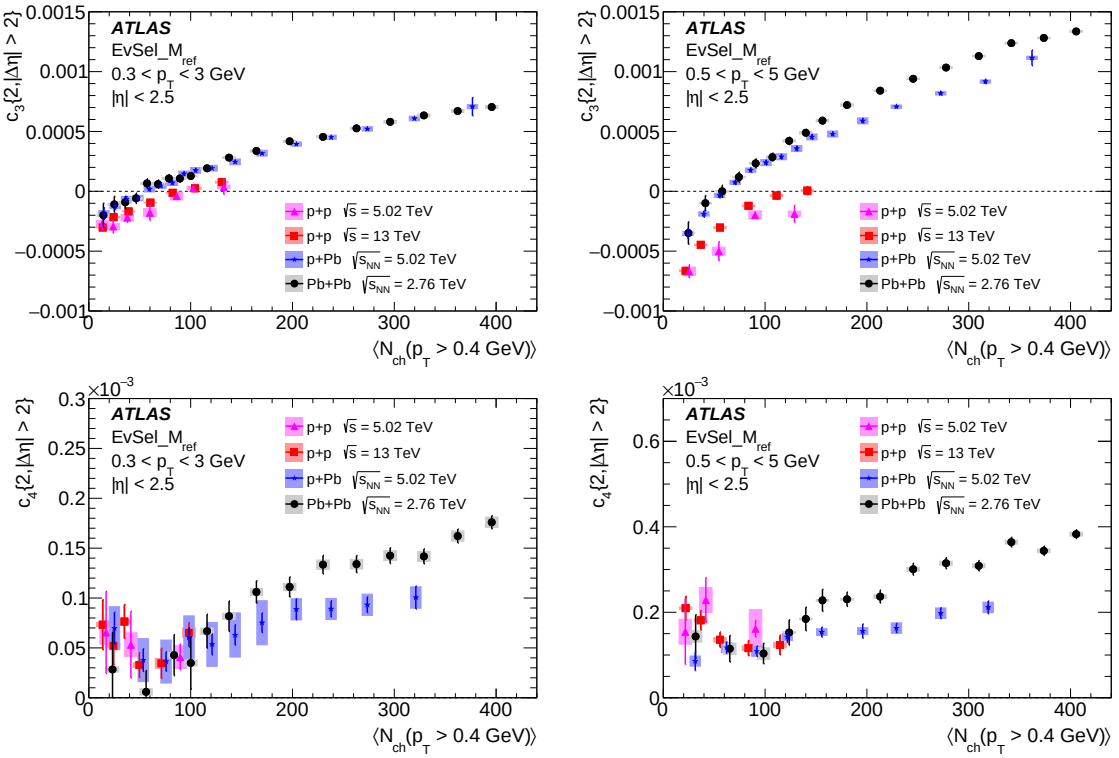

Figure 12: The two-particle cumulant c_3 (top) and c_4 (bottom) calculated with the $|\Delta\eta| > 2$ requirement as a function of $\langle N_{\text{ch}}(p_{\text{T}} > 0.4 \text{ GeV})\rangle$ for pp collisions at $\sqrt{s} = 5.02$ and 13 TeV, p+Pb collisions at $\sqrt{s_{\text{NN}}} = 5.02$ TeV and low-multiplicity Pb+Pb collisions at $\sqrt{s_{\text{NN}}} = 2.76$ TeV for two p_{T} ranges of reference particles. The error bars and shaded boxes denote statistical and systematic uncertainties, respectively.

For pp data, the $c_3\{2, |\Delta\eta| > 2\}$ values are either negative or consistent with zero over the whole range of $N_{\text{ch}}(p_{\text{T}} > 0.4 \text{ GeV})$, except for the two highest multiplicities measured for pp collisions at 13 TeV. Therefore, for $N_{\text{ch}}(p_{\text{T}} > 0.4 \text{ GeV}) < 100$, the v_3 signal in pp collisions is undefined or zero within the errors. A positive c_3 signal is obtained from p+Pb and Pb+Pb data, except for the charged-particle multiplicities below about 50. The magnitude of c_3 is comparable for Pb+Pb and p+Pb collisions when reference particles with $0.3 < p_{\text{T}} < 3.0$ GeV are selected, and systematically slightly larger for Pb+Pb than for p+Pb for reference particles with $0.5 < p_{\text{T}} < 5.0$ GeV. The fourth-order cumulants, c_4, have positive values of $c_4\{2, |\Delta\eta| > 2\}$ even for the pp data, and their magnitude is comparable to that for p+Pb and Pb+Pb collisions in the overlapping range of N_{ch}. For $N_{\text{ch}}(p_{\text{T}} > 0.4 \text{ GeV}) > 120$, where only the measurements for p+Pb and Pb+Pb are accessible, the c_4 cumulants measured at the same charged-particle multiplicity are larger for Pb+Pb than for p+Pb.

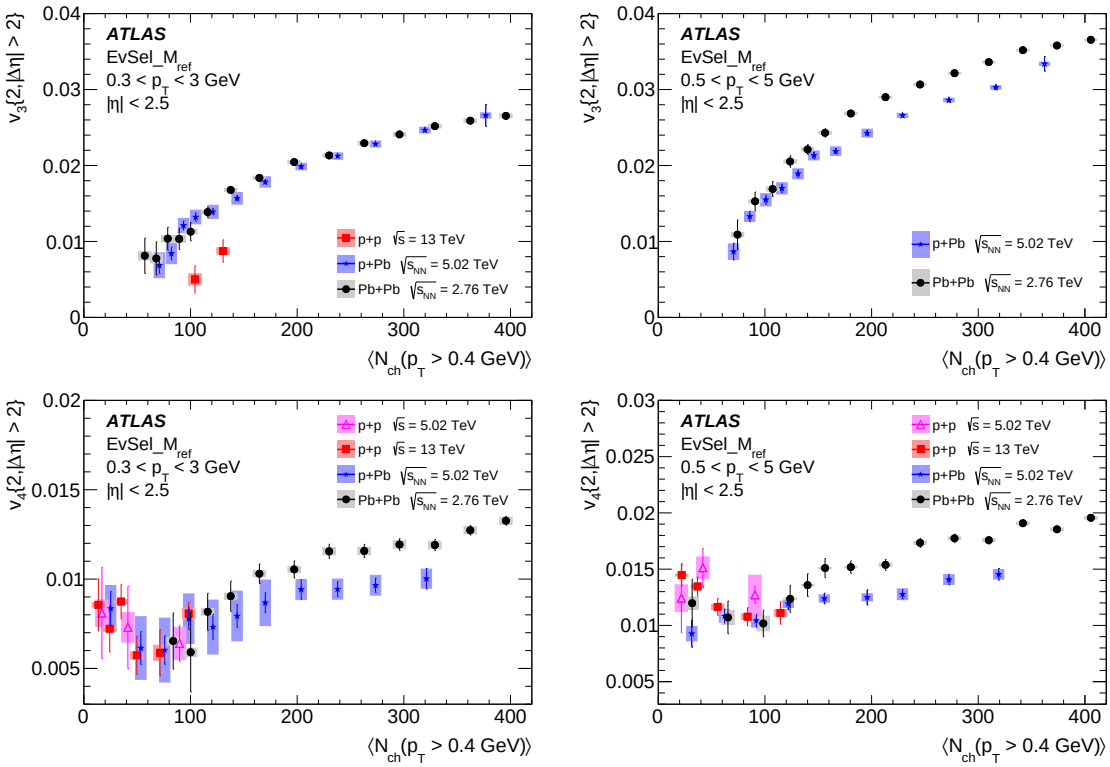

Figure 13: The $v_3\{2, |\Delta\eta| > 2\}$ (top) and $v_4\{2, |\Delta\eta| > 2\}$ (bottom) as a function of $\langle N_{\rm ch}(p_{\rm T} > 0.4\ {\rm GeV})\rangle$ for pp collisions at $\sqrt{s} = 5.02$ and 13 TeV, p+Pb collisions at $\sqrt{s_{\rm NN}} = 5.02$ TeV and low-multiplicity Pb+Pb collisions at $\sqrt{s_{\rm NN}} = 2.76$ TeV, and for two $p_{\rm T}$ ranges of the reference particles. The error bars and shaded boxes denote statistical and systematic uncertainties, respectively.

The third- and fourth-order flow harmonics, v_3 and v_4, calculated with two-particle cumulants with the $|\Delta\eta| > 2$ requirement are shown in Figure 13. For p+Pb and Pb+Pb collisions the $v_3\{2, |\Delta\eta| > 2\}$ values are similar for reference particles with $0.3 < p_{\rm T} < 3.0$ GeV, and much larger than for the 13 TeV pp data. For higher-$p_{\rm T}$ reference particles, the Pb+Pb v_3 is systematically larger than v_3 in p+Pb collisions with the same multiplicity. The v_3 increases with increasing multiplicity. A weaker increase is seen for $v_4\{2, |\Delta\eta| > 2\}$, but at high multiplicities the values observed in Pb+Pb collisions are systematically larger than in p+Pb, for two $p_{\rm T}$ ranges of reference particles. For multiplicities below 100, where the $v_4\{2, |\Delta\eta| > 2\}$ can also be obtained from pp collisions, no system dependence is seen.

8.3 Comparison to other results

ATLAS results for $c_2\{4\}$ cumulants measured for pp data at 5.02 TeV and 13 TeV are compared to similar results obtained by CMS [45] in Figure 14. The ATLAS results are shown for two event selections: EvSel_$M_{\rm ref}$ and EvSel_$N_{\rm ch}$ (see Section 6). For the nominal event selection (EvSel_$M_{\rm ref}$), the $c_2\{4\}$ cumulants at 5.02 TeV agree with the CMS measurement at high multiplicities, while at low multiplicities the CMS cumulants are systematically smaller in magnitude than those measured by ATLAS. This discrepancy is more pronounced at 13 TeV, and extends over the full range of collision multiplicities. At high multiplicities, CMS reported a clear signal of negative $c_2\{4\}$ in contrast to our default method based

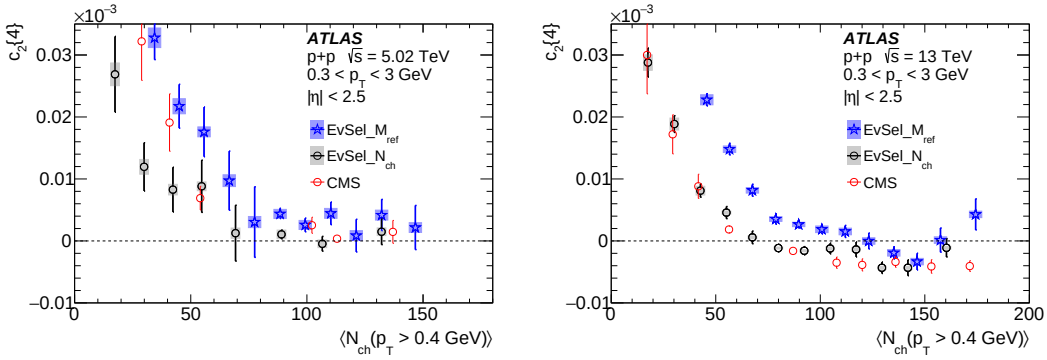

Figure 14: Comparison of the ATLAS and CMS [45] results for $c_2\{4\}$ cumulants in pp collisions at 5.02 TeV (left) and 13 TeV (right) shown as a function of $\langle N_{\mathrm{ch}}(p_{\mathrm{T}} > 0.4\ \mathrm{GeV})\rangle$. The ATLAS results are shown for two event selections: EvSel_M_{ref} and EvSel_N_{ch} with the error bars and shaded boxes denoting statistical and systematic uncertainties, respectively. For the CMS results, the error bars indicate statistical and systematic uncertainties added in quadrature.

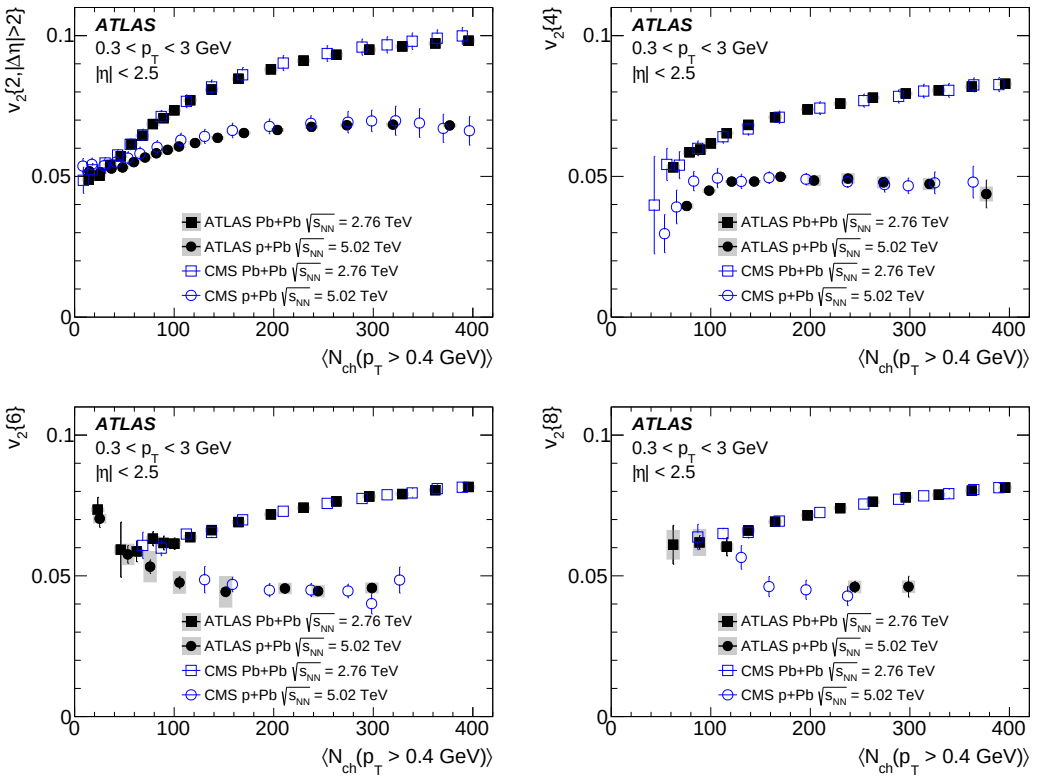

Figure 15: Comparison of the ATLAS (EvSel_M_{ref}) and CMS [36] results for v_2 harmonics obtained with multi-particle cumulants in p+Pb collisions at 5.02 TeV and Pb+Pb collisions at 2.76 TeV shown as a function of $\langle N_{\mathrm{ch}}(p_{\mathrm{T}} > 0.4\ \mathrm{GeV})\rangle$. The ATLAS results are shown with the error bars and shaded boxes denoting statistical and systematic uncertainties, respectively. For the CMS results, the error bars indicate statistical and systematic uncertainties added in quadrature.

on EvSel_M_{ref}, but is roughly consistent with our measurements based on selecting events according to EvSel_N_{ch}.

For p+Pb and Pb+Pb collisions, the results for v_2 harmonics obtained with multi-particle cumulants agree very well with the CMS data [36], as shown in Figure 15. Figure 16 shows a similar compability of ATLAS and ALICE [18] measurements of $v_2\{4\}$ in p+Pb collisions. For Pb+Pb collisions, the ALICE results on $v_2\{4\}$ are slightly above those measured by ATLAS.

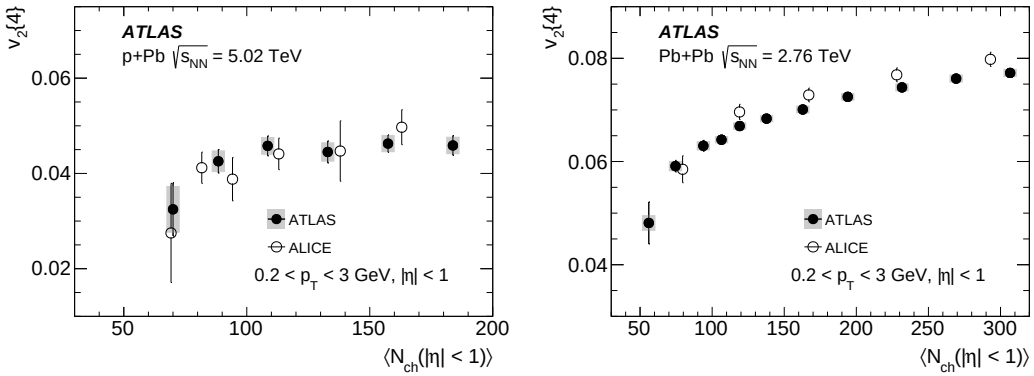

Figure 16: Comparison of the ATLAS (EvSel_M_{ref}) and ALICE [18] results for $v_2\{4\}$ harmonics obtained with four-particle cumulants in p+Pb collisions at 5.02 TeV (left) and Pb+Pb collisions at 2.76 TeV (right) shown as a function of $\langle N_{\mathrm{ch}}(|\eta| < 1)\rangle$. The ATLAS results are shown with the error bars and shaded boxes denoting statistical and systematic uncertainties, respectively. For the ALICE results, the error bars indicate statistical and systematic uncertainties added in quadrature.

A comparison of flow harmonics measured with distinct analysis methods, which primarily differ in their sensitivity to non-flow correlations, is also of interest. The method, commonly used to measure flow harmonics in small collision systems, is the two-particle correlation function method (2PC). This method was used by ATLAS to measure v_n harmonics in pp and p+Pb collisions [46]. In that measurement, the non-flow correlations were suppressed by requiring the $|\Delta\eta| > 2$ gap, as in this analysis. However, additional procedures were undertaken in Ref. [46] to also suppress the jet–jet correlations. The ATLAS results for flow harmonics obtained using the two-particle correlation function method, $v_n\{2\mathrm{PC}\}$, are compared with the results reported here, obtained with two-particle cumulants, in Figure 17. For the v_2 harmonic the two measurements give consistent results for p+Pb collisions. For pp collisions the cumulant method gives v_2 values larger than those obtained with the 2PC method, suggesting that the former are contaminated by the non-flow correlations not removed by the $|\Delta\eta| > 2$ requirement. The fact that in contrast to $v_2\{2\mathrm{PC}\}$ the v_2 harmonic cannot be determined from the measurement of the $c_2\{4\}$ cumulant reported here for pp collisions clearly indicates that this cumulant is biased by non-flow correlations. In the case of the third-order flow harmonic, v_3, the comparison can be made only for p+Pb collisions, and here it can be seen that $v_3\{2, |\Delta\eta| > 2\} < v_3\{2\mathrm{PC}\}$. This difference results from elimination of the jet–jet non-flow correlations by the additional procedure supplementing the $|\Delta\eta| > 2$ gap in the 2PC method. The two methods give consistent results for the v_4 harmonic measured in p+Pb collisions at 5.02 TeV as well as in pp collisions at 13 TeV, indicating that the aforementioned differences between the two analysis methods have a negligible impact on v_4.

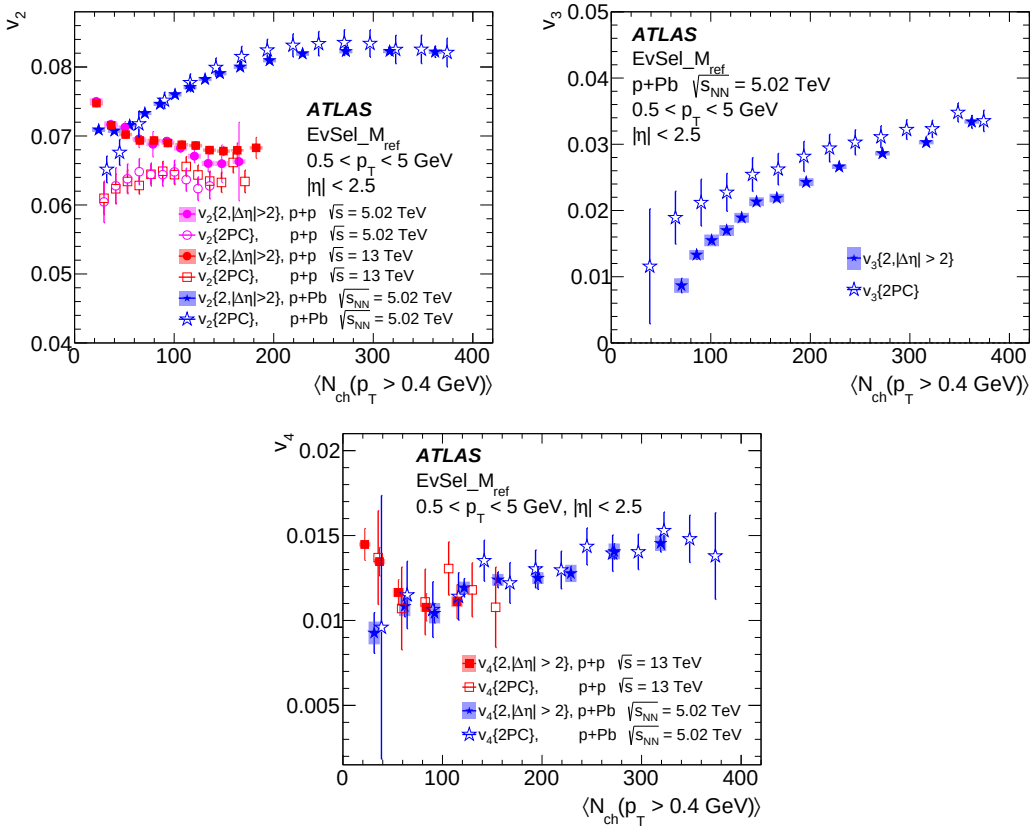

Figure 17: Comparison of the ATLAS (EvSel_M_{ref}) measurements of v_2 (top left), v_3 (top right) and v_4 (bottom) harmonics obtained with two-particle cumulants (filled symbols) and two-particle correlation function method (open symbols) for pp collisions at $\sqrt{s}$ = 5.02 and 13 TeV, p+Pb collisions at $\sqrt{s_{\text{NN}}}$ = 5.02 TeV. The error bars and shaded boxes for the cumulant measurements denote statistical and systematic uncertainties, respectively. For the two-particle correlation function results, the error bars indicate statistical and systematic uncertainties added in quadrature.

9 Summary and conclusions

Multi-particle cumulants and corresponding Fourier harmonics are measured by the ATLAS experiment at the LHC for azimuthal angle distributions of charged particles in pp collisions at $\sqrt{s}$ = 5.02 and 13 TeV and in p+Pb collisions at $\sqrt{s_{\text{NN}}}$ = 5.02 TeV, and compared to the results obtained from low-multiplicity Pb+Pb collisions at $\sqrt{s_{\text{NN}}}$ = 2.76 TeV. The results are presented as a function of charged-particle multiplicity for two ranges of the particles' transverse momenta: $0.3 < p_{\text{T}} < 3$ GeV and $0.5 < p_{\text{T}} < 5$ GeV. For the same charged-particle multiplicity the second-order cumulants and harmonics ($c_2\{2, |\Delta\eta| > 2\}$ and $v_2\{2, |\Delta\eta| > 2\}$), derived from two-particle correlations with the $|\Delta\eta| > 2$ gap, have larger magnitudes in Pb+Pb collisions than in p+Pb collisions. The smallest signal is observed in pp collisions. The latter show no energy or multiplicity dependence while the cumulants and the second-order harmonic increase with increasing multiplicity in p+Pb and Pb+Pb collisions.

Four-particle cumulants, $c_2\{4\}$, show that $|c_2\{4\}|$ in p+Pb collisions is less than $|c_2\{4\}|$ measured for Pb+Pb data. For charged-particle multiplicities above 100, the $c_2\{4\}$ cumulants have negative values in p+Pb and

Pb+Pb collisions, confirming the collective nature of multi-particle correlations in these collision systems. The derived magnitude of the $v_2\{4\}$ harmonic is larger in Pb+Pb collisions than in p+Pb collisions with the same multiplicity. In pp collisions, over the full range of particle multiplicities, the cumulants are positive or consistent with zero at 5.02 TeV for both p_T ranges. In the 13 TeV pp data, the cumulants measured for charged particles with lower p_T ($0.3 < p_T < 3$ GeV) also have positive values over the large range of multiplicities. Therefore, these measurements of four-particle cumulants in pp collisions, based on a method that suppresses the non-flow correlations associated with event-by-event fluctuations in the number of reference particles, generally do not satisfy the requirement of being negative. This indicates that $c_2\{4\}$ cumulants obtained from the standard procedure used in this paper may still be biased by residual non-flow correlations. The $c_2\{4\}$ cumulant in 13 TeV pp collisions measured by CMS is smaller over the full range of collision multiplicities than the $c_2\{4\}$ cumulant obtained by ATLAS with the nominal event selection (EvSel_M_{ref}) while it is consistent with the ATLAS measurement obtained with the EvSel_N_{ch} event selection.

Six- and eight-particle c_2 cumulants can be obtained with sufficient statistical precision only for p+Pb and Pb+Pb collisions. All derived v_2 harmonics have larger magnitudes for Pb+Pb collisions than for p+Pb collisions with the same multiplicity. For both systems, $v_2\{2k\}$ are similar for $k = 2$, 3 and 4 while $v_2\{2, |\Delta\eta| > 2\}$ is systematically larger than the second-order Fourier component calculated with cumulants of more than two-particles. Compared to the almost degenerate values of $v_2\{2k\}, k > 1$, a larger v_2 derived from two-particle cumulants is also predicted by models assuming fluctuation-driven initial-state anisotropies in small collision systems. Interestingly, the ratios $v_2\{2k\}/v_2\{2k-2\}$ for p+Pb and low-multiplicity Pb+Pb collisions are independent of the charged-particle multiplicity for $N_{\mathrm{ch}} > 120$, regardless of the p_T range of particles used to calculate the cumulants and Fourier harmonics.

Higher-order cumulants, c_3 and c_4, are measured only using two-particle cumulants with an imposed $|\Delta\eta| > 2$ gap. For pp data $c_3\{2, |\Delta\eta| > 2\}$ values are either negative or consistent with zero over almost the full range of N_{ch} multiplicities, except at the highest multiplicities measured in pp collisions at 13 TeV. Therefore, the v_3 signal for pp collisions is undefined or zero within the errors. A positive c_3 signal is obtained for p+Pb and Pb+Pb data, except for the charged-particle multiplicities below ~120. The magnitude of c_3 and the corresponding $v_3\{2, |\Delta\eta| > 2\}$ harmonic are comparable for Pb+Pb and p+Pb collisions when particles with $0.3 < p_T < 3.0$ GeV are considered, and systematically slightly larger for Pb+Pb than for p+Pb for particles with $0.5 < p_T < 5.0$ GeV. The fourth-order cumulants, c_4, have positive values of $c_4\{2, |\Delta\eta| > 2\}$ even for the pp data, and their magnitude is comparable to that for p+Pb and Pb+Pb collisions in the overlapping range of N_{ch}. For $N_{\mathrm{ch}} > 120$, where only the measurements for p+Pb and Pb+Pb are accessible, the c_4 cumulants measured at the same charged-particle multiplicity are larger for Pb+Pb than for p+Pb.

The ATLAS results are compared to measurements reported by CMS and ALICE. An agreement across the experiments is observed for p+Pb and Pb+Pb collisions. The comparison with the ATLAS results obtained for pp and p+Pb collisions with the two-particle correlation method shows some differences, which can be explained by the additional requirements applied in the two-particle correlation method in order to reduce the jet–jet correlations.

The comprehensive data on multi-particle cumulants presented in this paper provide insights into the origin of azimuthal angle anisotropies in small collision systems, and as such can be used to constrain the theoretical modelling of the underlying mechanism.

Acknowledgements

We thank CERN for the very successful operation of the LHC, as well as the support staff from our institutions without whom ATLAS could not be operated efficiently.

We acknowledge the support of ANPCyT, Argentina; YerPhI, Armenia; ARC, Australia; BMWFW and FWF, Austria; ANAS, Azerbaijan; SSTC, Belarus; CNPq and FAPESP, Brazil; NSERC, NRC and CFI, Canada; CERN; CONICYT, Chile; CAS, MOST and NSFC, China; COLCIENCIAS, Colombia; MSMT CR, MPO CR and VSC CR, Czech Republic; DNRF and DNSRC, Denmark; IN2P3-CNRS, CEA-DSM/IRFU, France; SRNSF, Georgia; BMBF, HGF, and MPG, Germany; GSRT, Greece; RGC, Hong Kong SAR, China; ISF, I-CORE and Benoziyo Center, Israel; INFN, Italy; MEXT and JSPS, Japan; CNRST, Morocco; NWO, Netherlands; RCN, Norway; MNiSW and NCN, Poland; FCT, Portugal; MNE/IFA, Romania; MES of Russia and NRC KI, Russian Federation; JINR; MESTD, Serbia; MSSR, Slovakia; ARRS and MIZŠ, Slovenia; DST/NRF, South Africa; MINECO, Spain; SRC and Wallenberg Foundation, Sweden; SERI, SNSF and Cantons of Bern and Geneva, Switzerland; MOST, Taiwan; TAEK, Turkey; STFC, United Kingdom; DOE and NSF, United States of America. In addition, individual groups and members have received support from BCKDF, the Canada Council, CANARIE, CRC, Compute Canada, FQRNT, and the Ontario Innovation Trust, Canada; EPLANET, ERC, ERDF, FP7, Horizon 2020 and Marie Skłodowska-Curie Actions, European Union; Investissements d'Avenir Labex and Idex, ANR, Région Auvergne and Fondation Partager le Savoir, France; DFG and AvH Foundation, Germany; Herakleitos, Thales and Aristeia programmes co-financed by EU-ESF and the Greek NSRF; BSF, GIF and Minerva, Israel; BRF, Norway; CERCA Programme Generalitat de Catalunya, Generalitat Valenciana, Spain; the Royal Society and Leverhulme Trust, United Kingdom.

The crucial computing support from all WLCG partners is acknowledged gratefully, in particular from CERN, the ATLAS Tier-1 facilities at TRIUMF (Canada), NDGF (Denmark, Norway, Sweden), CC-IN2P3 (France), KIT/GridKA (Germany), INFN-CNAF (Italy), NL-T1 (Netherlands), PIC (Spain), ASGC (Taiwan), RAL (UK) and BNL (USA), the Tier-2 facilities worldwide and large non-WLCG resource providers. Major contributors of computing resources are listed in Ref. [83].

Appendix

The following tables list individual contributions to the systematic uncertainty for the following collision systems: pp at 5.02 TeV, pp at 13 TeV, p+Pb at 5.02 TeV and Pb+Pb at 2.76 TeV. Table 3 lists contributions to the systematic uncertainty from the track selection requirements, taken as the maximum difference between the base measurement and the results obtained with loose or tight track selections in a given range of N_{ch}, for reference particles with $0.3 < p_{\mathrm{T}} < 3$ GeV. Table 4 includes systematic uncertainties for reference particles with $0.5 < p_{\mathrm{T}} < 5$ GeV.

Table 3: Systematic uncertainties related to the track selection requirements for multi-particle cumulants measured in different collision systems for M_{ref} with $0.3 < p_{\mathrm{T}} < 3$ GeV.

Systematic uncertainties due to track selection requirements				
System	Systematic uncertainty	N_{ch}	N_{ch}	N_{ch}
		<50	50–100	>100
pp 5 TeV	$\delta c_2\{2, \lvert\Delta\eta\rvert > 2\} \times 10^4$	–0.05	0.33	0.13
	$\delta c_2\{4\} \times 10^6$	–0.87	0.50	–0.48
	$\delta c_3\{2, \lvert\Delta\eta\rvert > 2\} \times 10^4$	–0.26	0.32	0.11
	$\delta c_4\{2, \lvert\Delta\eta\rvert > 2\} \times 10^4$	0.01	0.11	-
		<50	50–100	>100
pp 13 TeV	$\delta c_2\{2, \lvert\Delta\eta\rvert > 2\} \times 10^4$	–0.07	–0.09	–0.02
	$\delta c_2\{4\} \times 10^6$	–0.54	–0.33	0.50
	$\delta c_3\{2, \lvert\Delta\eta\rvert > 2\} \times 10^4$	–0.03	0.02	–0.07
	$\delta c_4\{2, \lvert\Delta\eta\rvert > 2\} \times 10^4$	0.02	–0.04	-
		<100	100–200	>200
p+Pb	$\delta c_2\{2, \lvert\Delta\eta\rvert > 2\} \times 10^4$	0.26	0.26	0.41
	$\delta c_2\{4\} \times 10^6$	0.18	–0.06	0.68
	$\delta c_2\{6\} \times 10^7$	–0.45	–0.05	0.04
	$\delta c_2\{8\} \times 10^8$	0.15	0.01	–0.02
	$\delta c_3\{2, \lvert\Delta\eta\rvert > 2\} \times 10^4$	–0.19	–0.23	–0.16
	$\delta c_4\{2, \lvert\Delta\eta\rvert > 2\} \times 10^4$	–0.21	–0.17	–0.10
		<100	100–200	>200
Pb+Pb	$\delta c_2\{2, \lvert\Delta\eta\rvert > 2\} \times 10^4$	0.12	0.23	0.35
	$\delta c_2\{4\} \times 10^6$	–0.52	–0.12	–0.48
	$\delta c_2\{6\} \times 10^7$	0.19	–0.13	0.16
	$\delta c_2\{8\} \times 10^8$	–0.43	0.08	–0.11
	$\delta c_3\{2, \lvert\Delta\eta\rvert > 2\} \times 10^4$	–0.09	–0.06	0.04
	$\delta c_4\{2, \lvert\Delta\eta\rvert > 2\} \times 10^4$	0.03	0.03	0.04

Table 5 lists contributions to the systematic uncertainty due to the uncertainty in the tracking efficiency, taken as the largest difference between the base measurement and the results obtained with the efficiency

Table 4: Systematic uncertainties related to the track selection requirements for multi-particle cumulants measured in different collision systems for M_{ref} with $0.5 < p_{\mathrm{T}} < 5$ GeV.

Systematic uncertainties due to track selection requirements				
System	Systematic uncertainty	N_{ch}	N_{ch}	N_{ch}
		<50	50–100	>100
pp 5 TeV	$\delta c_2\{2, \lvert\Delta\eta\rvert > 2\} \times 10^4$	–0.08	0.10	0.19
	$\delta c_2\{4\} \times 10^6$	–3.73	–1.09	0.88
	$\delta c_3\{2, \lvert\Delta\eta\rvert > 2\} \times 10^4$	0.01	–0.20	0.21
	$\delta c_4\{2, \lvert\Delta\eta\rvert > 2\} \times 10^4$	–0.12	–0.15	-
		<50	50–100	>100
pp 13 TeV	$\delta c_2\{2, \lvert\Delta\eta\rvert > 2\} \times 10^4$	–0.19	–0.12	0.01
	$\delta c_2\{4\} \times 10^6$	–4.02	–1.11	–0.34
	$\delta c_3\{2, \lvert\Delta\eta\rvert > 2\} \times 10^4$	–0.03	–0.06	0.08
	$\delta c_4\{2, \lvert\Delta\eta\rvert > 2\} \times 10^4$	–0.02	–0.05	–0.05
		<100	100–200	>200
p+Pb	$\delta c_2\{2, \lvert\Delta\eta\rvert > 2\} \times 10^4$	0.26	0.29	0.35
	$\delta c_2\{4\} \times 10^6$	0.16	0.09	–0.59
	$\delta c_2\{6\} \times 10^7$	0.13	–0.19	0.31
	$\delta c_2\{8\} \times 10^8$	0.89	–0.01	–0.19
	$\delta c_3\{2, \lvert\Delta\eta\rvert > 2\} \times 10^4$	–0.06	–0.15	–0.08
	$\delta c_4\{2, \lvert\Delta\eta\rvert > 2\} \times 10^4$	–0.08	–0.06	0.04
		<100	100–200	>200
Pb+Pb	$\delta c_2\{2, \lvert\Delta\eta\rvert > 2\} \times 10^4$	0.53	0.58	0.46
	$\delta c_2\{4\} \times 10^6$	–1.72	–0.79	–0.62
	$\delta c_2\{6\} \times 10^7$	0.85	–0.43	0.33
	$\delta c_2\{8\} \times 10^8$	–0.37	0.54	–0.45
	$\delta c_3\{2, \lvert\Delta\eta\rvert > 2\} \times 10^4$	0.06	0.09	0.06
	$\delta c_4\{2, \lvert\Delta\eta\rvert > 2\} \times 10^4$	–0.13	–0.02	0.04

varied up or down for reference particles with $0.3 < p_{\mathrm{T}} < 3$ GeV. The maximum deviations in a given range of N_{ch} are listed. Table 6 includes systematic uncertainties for reference particles with $0.5 < p_{\mathrm{T}} < 5$ GeV.

Table 5: Systematic uncertainties related to the tracking efficiency uncertainty for multi-particle cumulants measured in different collision systems for M_{ref} with $0.3 < p_{\mathrm{T}} < 3$ GeV. The maximum deviations in a given range of N_{ch} are listed.

Systematic uncertainties due to the tracking efficiency uncertainty				
System	Systematic uncertainty	N_{ch}	N_{ch}	N_{ch}
		<50	50–100	>100
pp 5 TeV	$\delta c_2\{2, \lvert\Delta\eta\rvert > 2\} \times 10^4$	0.27	0.33	0.24
	$\delta c_2\{4\} \times 10^6$	4.10	0.64	0.17
	$\delta c_3\{2, \lvert\Delta\eta\rvert > 2\} \times 10^4$	–0.02	–0.03	0.01
	$\delta c_4\{2, \lvert\Delta\eta\rvert > 2\} \times 10^4$	0.01	0.01	-
		<50	50–100	>100
pp 13 TeV	$\delta c_2\{2, \lvert\Delta\eta\rvert > 2\} \times 10^4$	0.31	0.20	0.19
	$\delta c_2\{4\} \times 10^6$	3.72	0.39	0.13
	$\delta c_3\{2, \lvert\Delta\eta\rvert > 2\} \times 10^4$	–0.04	–0.01	0.01
	$\delta c_4\{2, \lvert\Delta\eta\rvert > 2\} \times 10^4$	0.01	0.02	-
		<100	100–200	>200
p+Pb	$\delta c_2\{2, \lvert\Delta\eta\rvert > 2\} \times 10^4$	–0.53	–0.51	–0.56
	$\delta c_2\{4\} \times 10^6$	–0.86	0.13	0.14
	$\delta c_2\{6\} \times 10^7$	–0.29	–0.01	–0.02
	$\delta c_2\{8\} \times 10^8$	–3.20	0.01	0.01
	$\delta c_3\{2, \lvert\Delta\eta\rvert > 2\} \times 10^4$	0.09	–0.05	–0.10
	$\delta c_4\{2, \lvert\Delta\eta\rvert > 2\} \times 10^4$	–0.01	–0.02	–0.02
		<100	100–200	>200
Pb+Pb	$\delta c_2\{2, \lvert\Delta\eta\rvert > 2\} \times 10^4$	–0.65	–0.97	–1.22
	$\delta c_2\{4\} \times 10^6$	–0.64	0.66	1.09
	$\delta c_2\{6\} \times 10^7$	–0.30	–0.19	–0.41
	$\delta c_2\{8\} \times 10^8$	–1.15	0.10	0.29
	$\delta c_3\{2, \lvert\Delta\eta\rvert > 2\} \times 10^4$	0.04	–0.07	–0.12
	$\delta c_4\{2, \lvert\Delta\eta\rvert > 2\} \times 10^4$	–0.02	–0.03	–0.04

Table 6: Systematic uncertainties related to the tracking efficiency uncertainty for multi-particle cumulants measured in different collision systems for M_{ref} with $0.5 < p_{\mathrm{T}} < 5$ GeV. The maximum deviations in a given range of N_{ch} are listed.

Systematic uncertainties due to the tracking efficiency uncertainty				
System	Systematic uncertainty	N_{ch}	N_{ch}	N_{ch}
		<50	50–100	>100
pp 5 TeV	$\delta c_2\{2, \lvert\Delta\eta\rvert > 2\} \times 10^4$	0.35	0.27	0.27
	$\delta c_2\{4\} \times 10^6$	5.11	1.38	0.70
	$\delta c_3\{2, \lvert\Delta\eta\rvert > 2\} \times 10^4$	–0.05	–0.04	–0.02
	$\delta c_4\{2, \lvert\Delta\eta\rvert > 2\} \times 10^4$	0.02	0.02	-
		<50	50–100	>100
pp 13 TeV	$\delta c_2\{2, \lvert\Delta\eta\rvert > 2\} \times 10^4$	0.36	0.24	0.21
	$\delta c_2\{4\} \times 10^6$	4.97	1.37	0.43
	$\delta c_3\{2, \lvert\Delta\eta\rvert > 2\} \times 10^4$	–0.06	–0.03	–0.01
	$\delta c_4\{2, \lvert\Delta\eta\rvert > 2\} \times 10^4$	0.02	0.02	0.01
		<100	100–200	>200
p+Pb	$\delta c_2\{2, \lvert\Delta\eta\rvert > 2\} \times 10^4$	–0.15	–0.13	–0.14
	$\delta c_2\{4\} \times 10^6$	–0.60	0.04	0.06
	$\delta c_2\{6\} \times 10^7$	–0.30	–0.01	–0.01
	$\delta c_2\{8\} \times 10^8$	–3.81	–0.01	0.01
	$\delta c_3\{2, \lvert\Delta\eta\rvert > 2\} \times 10^4$	0.02	–0.01	–0.03
	$\delta c_4\{2, \lvert\Delta\eta\rvert > 2\} \times 10^4$	–0.01	–0.01	–0.01
		<100	100–200	>200
Pb+Pb	$\delta c_2\{2, \lvert\Delta\eta\rvert > 2\} \times 10^4$	–0.18	–0.24	–0.32
	$\delta c_2\{4\} \times 10^6$	–0.66	0.19	0.38
	$\delta c_2\{6\} \times 10^7$	–0.39	–0.09	–0.22
	$\delta c_2\{8\} \times 10^8$	–0.77	0.09	0.25
	$\delta c_3\{2, \lvert\Delta\eta\rvert > 2\} \times 10^4$	0.02	–0.02	–0.04
	$\delta c_4\{2, \lvert\Delta\eta\rvert > 2\} \times 10^4$	–0.01	–0.01	–0.02

Table 7 lists contributions to the systematic uncertainty from the pile-up effects, taken as the maximum difference between the base measurement and the results obtained with the higher or lower pile-up in pp collisions and with the higher pile-up in the case of p+Pb collisions in a given range of N_{ch}, for reference particles with $0.3 < p_{\mathrm{T}} < 3$ GeV. Table 8 includes systematic uncertainties for reference particles with $0.5 < p_{\mathrm{T}} < 5$ GeV.

Table 7: Systematic uncertainties related to the pile-up for multi-particle cumulants measured in different collision systems for M_{ref} with $0.3 < p_{\mathrm{T}} < 3$ GeV.

Systematic uncertainties due to the pile-up				
System	Systematic uncertainty	N_{ch}	N_{ch}	N_{ch}
		<50	50–100	>100
pp 5 TeV	$\delta c_2\{2, \lvert\Delta\eta\rvert > 2\} \times 10^4$	0.29	0.03	–0.12
	$\delta c_2\{4\} \times 10^6$	–0.66	0.50	–0.62
	$\delta c_3\{2, \lvert\Delta\eta\rvert > 2\} \times 10^4$	–0.03	–0.07	–0.10
	$\delta c_4\{2, \lvert\Delta\eta\rvert > 2\} \times 10^4$	0.12	–0.05	-
		<50	50–100	>100
pp 13 TeV	$\delta c_2\{2, \lvert\Delta\eta\rvert > 2\} \times 10^4$	–0.02	–0.02	0.06
	$\delta c_2\{4\} \times 10^6$	–0.05	–0.05	–0.14
	$\delta c_3\{2, \lvert\Delta\eta\rvert > 2\} \times 10^4$	–0.01	0.02	0.02
	$\delta c_4\{2, \lvert\Delta\eta\rvert > 2\} \times 10^4$	–0.01	0.02	-
		<100	100–200	>200
p+Pb	$\delta c_2\{2, \lvert\Delta\eta\rvert > 2\} \times 10^4$	–0.01	0.01	0.03
	$\delta c_2\{4\} \times 10^6$	–0.01	–0.02	–0.01
	$\delta c_2\{6\} \times 10^7$	0.01	–0.01	0.01
	$\delta c_2\{8\} \times 10^8$	–0.01	0.01	0.01
	$\delta c_3\{2, \lvert\Delta\eta\rvert > 2\} \times 10^4$	–0.01	–0.01	–0.01
	$\delta c_4\{2, \lvert\Delta\eta\rvert > 2\} \times 10^4$	–0.01	–0.01	0.01

Table 8: Systematic uncertainties related to the pile-up for multi-particle cumulants measured in different collision systems for M_{ref} with $0.5 < p_{\mathrm{T}} < 5$ GeV.

Systematic uncertainties due to the pile-up				
System	Systematic uncertainty	N_{ch}	N_{ch}	N_{ch}
		<50	50–100	>100
pp 5 TeV	$\delta c_2\{2, \lvert\Delta\eta\rvert > 2\} \times 10^4$	0.43	0.12	0.25
	$\delta c_2\{4\} \times 10^6$	–3.43	–0.58	–2.17
	$\delta c_3\{2, \lvert\Delta\eta\rvert > 2\} \times 10^4$	0.35	0.28	–0.09
	$\delta c_4\{2, \lvert\Delta\eta\rvert > 2\} \times 10^4$	0.27	–0.42	-
		<50	50–100	>100
pp 13 TeV	$\delta c_2\{2, \lvert\Delta\eta\rvert > 2\} \times 10^4$	–0.03	0.01	–0.13
	$\delta c_2\{4\} \times 10^6$	–0.35	–0.16	–0.23
	$\delta c_3\{2, \lvert\Delta\eta\rvert > 2\} \times 10^4$	–0.01	–0.02	0.03
	$\delta c_4\{2, \lvert\Delta\eta\rvert > 2\} \times 10^4$	0.02	0.01	–0.04
		<100	100–200	>200
p+Pb	$\delta c_2\{2, \lvert\Delta\eta\rvert > 2\} \times 10^4$	–0.03	0.02	0.01
	$\delta c_2\{4\} \times 10^6$	–0.08	–0.04	–0.03
	$\delta c_2\{6\} \times 10^7$	0.03	–0.02	0.01
	$\delta c_2\{8\} \times 10^8$	–0.11	0.05	0.01
	$\delta c_3\{2, \lvert\Delta\eta\rvert > 2\} \times 10^4$	–0.01	–0.01	–0.01
	$\delta c_4\{2, \lvert\Delta\eta\rvert > 2\} \times 10^4$	0.01	–0.01	–0.01

Tables 9 and 10 list contributions to the systematic uncertainty related to the two running periods for p+Pb collisions at 5.02 TeV, taken as the maximum difference between the base measurement and the results obtained for the two running periods in a given range of N_{ch}, for reference particles with $0.3 < p_{\mathrm{T}} < 3$ GeV and $0.5 < p_{\mathrm{T}} < 5$ GeV, respectively.

Table 9: Systematic uncertainties related to the two running periods (p+Pb vs. Pb+p) for p+Pb collisions for M_{ref} with $0.3 < p_{\mathrm{T}} < 3$ GeV.

Systematic uncertainties in p+Pb results due to the two running periods				
System	Systematic uncertainty	N_{ch}	N_{ch}	N_{ch}
		<100	100–200	>200
p+Pb	$\delta c_2\{2, \lvert\Delta\eta\rvert > 2\} \times 10^4$	–0.02	–0.15	–0.08
	$\delta c_2\{4\} \times 10^6$	0.02	0.10	0.45
	$\delta c_2\{6\} \times 10^7$	–0.31	–0.22	–0.08
	$\delta c_2\{8\} \times 10^8$	0.05	0.11	0.02
	$\delta c_3\{2, \lvert\Delta\eta\rvert > 2\} \times 10^4$	–0.12	0.05	–0.03
	$\delta c_4\{2, \lvert\Delta\eta\rvert > 2\} \times 10^4$	0.03	–0.13	0.02

Table 10: Systematic uncertainties related to the two running periods (p+Pb vs. Pb+p) for p+Pb collisions for M_{ref} with $0.5 < p_{\mathrm{T}} < 5$ GeV.

Systematic uncertainties in p+Pb results due to two running periods				
System	Systematic uncertainty	N_{ch}	N_{ch}	N_{ch}
		<100	100–200	>200
p+Pb	$\delta c_2\{2, \lvert\Delta\eta\rvert > 2\} \times 10^4$	–0.06	–0.03	–0.03
	$\delta c_2\{4\} \times 10^6$	0.21	0.91	1.17
	$\delta c_2\{6\} \times 10^7$	–1.39	–0.62	–0.24
	$\delta c_2\{8\} \times 10^8$	0.07	0.39	0.06
	$\delta c_3\{2, \lvert\Delta\eta\rvert > 2\} \times 10^4$	–0.16	0.20	0.11
	$\delta c_4\{2, \lvert\Delta\eta\rvert > 2\} \times 10^4$	–0.09	–0.05	0.12

References

[1] A. M. Poskanzer and S. A. Voloshin, Phys. Rev. C **58** (1998) 1671, arXiv: nucl-ex/9805001.

[2] S. A. Voloshin, A. M. Poskanzer and R. Snellings, (2008), arXiv: 0809.2949 [nucl-ex].

[3] P. Sorensen, (2009), arXiv: 0905.0174 [nucl-ex].

[4] BRAHMS Collaboration, I. Arsene et al., Nucl. Phys. A **757** (2005) 1, arXiv: nucl-ex/0410020.

[5] PHOBOS Collaboration, B. B. Back et al., Nucl. Phys. A **757** (2005) 28, arXiv: nucl-ex/0410022.

[6] STAR Collaboration, J. Adams et al., Nucl. Phys. A **757** (2005) 102, arXiv: nucl-ex/0501009.

[7] PHENIX Collaboration, K. Adcox et al., Nucl. Phys. A **757** (2005) 184, arXiv: nucl-ex/0410003.

[8] ALICE Collaboration, K. Aamodt et al., Phys. Rev. Lett. **105** (2010) 252302, arXiv: 1011.3914 [nucl-ex].

[9] ALICE Collaboration, K. Aamodt et al., Phys. Rev. Lett. **107** (2011) 032301, arXiv: 1105.3865 [nucl-ex].

[10] ATLAS Collaboration, Phys. Lett. B **707** (2012) 330, arXiv: 1108.6018 [nucl-ex].

[11] ALICE Collaboration, K. Aamodt et al., Phys. Lett. B **708** (2012) 249, arXiv: 1109.2501 [nucl-ex].

[12] ATLAS Collaboration, Phys. Rev. C **86** (2012) 014907, arXiv: 1203.3087 [hep-ex].

[13] CMS Collaboration, Phys. Rev. C **87** (2013) 014902, arXiv: 1204.1409 [nucl-ex].

[14] CMS Collaboration, Phys. Rev. Lett. **109** (2012) 022301, arXiv: 1204.1850 [nucl-ex].

[15] ATLAS Collaboration, JHEP **11** (2013) 183, arXiv: 1305.2942 [hep-ex].

[16] CMS Collaboration, Phys. Rev. C **89** (2014) 044906, arXiv: 1310.8651 [nucl-ex].

[17] CMS Collaboration, JHEP **02** (2014) 088, arXiv: 1312.1845 [nucl-ex].

[18] ALICE Collaboration, B. Abelev et al., Phys. Rev. C **90** (2014) 054901, arXiv: 1406.2474 [nucl-ex].

[19] ATLAS Collaboration, Eur. Phys. J. C **74** (2014) 2982, arXiv: 1405.3936 [hep-ex].

[20] ATLAS Collaboration, Eur. Phys. J. C **74** (2014) 3157, arXiv: 1408.4342 [hep-ex].

[21] ALICE Collaboration, J. Adam et al., Phys. Rev. Lett. **116** (2016) 132302, arXiv: 1602.01119 [nucl-ex].

[22] ALICE Collaboration, J. Adam et al., Phys. Lett. B **762** (2016) 376, arXiv: 1605.02035 [nucl-ex].

[23] B. Alver and G. Roland, Phys. Rev. C **81** (2010) 054905, [Erratum: Phys. Rev. C 82 (2010) 039903], arXiv: 1003.0194 [nucl-ex].

[24] B. Schenke, P. Tribedy and R. Venugopalan, Phys. Rev. Lett. **108** (2012) 252301, arXiv: 1202.6646 [nucl-th].

[25] J.-Y Ollitrault, Phys. Rev. D **46** (1992) 229.

[26] U. Heinz and R. Snellings, Annu. Rev. Nucl. Part. Sci. **63** (2013) 123, arXiv: 1301.2826 [nucl-th].

[27] C. Gale, S. Jeon and B. Schenke, Int. J. Mod. Phys. A **28** (2013) 1340011, arXiv: 1301.5893 [nucl-th].

[28] P. Kovtun, D. T. Son and A. O. Starinets, Phys. Rev. Lett. **94** (2005) 111601, arXiv: hep-th/0405231.

[29] CMS Collaboration, Phys. Lett. B **718** (2013) 795, arXiv: 1210.5482 [nucl-ex].

[30] ALICE Collaboration, B. Abelev et al., Phys. Lett. B **719** (2013) 29, arXiv: 1212.2001 [nucl-ex].

[31] ATLAS Collaboration, Phys. Rev. Lett. **110** (2013) 182302, arXiv: 1212.5198 [hep-ex].

[32] ATLAS Collaboration, Phys. Lett. B **725** (2013) 60, arXiv: 1303.2084 [hep-ex].

[33] CMS Collaboration, Phys. Lett. B **724** (2013) 213, arXiv: 1305.0609 [nucl-ex].

[34] ALICE Collaboration, B. Abelev et al., Phys. Lett. B **726** (2013) 164, arXiv: 1307.3237 [nucl-ex].

[35] ATLAS Collaboration, Phys. Rev. C **90** (2014) 044906, arXiv: 1409.1792 [hep-ex].

[36] CMS Collaboration, Phys. Rev. Lett. **115** (2015) 012301, arXiv: 1502.05382 [nucl-ex].

[37] LHCb Collaboration, R. Aaij et al., Phys. Lett. B **762** (2016) 473, arXiv: 1512.00439 [hep-ex].

[38] CMS Collaboration, (2016), arXiv: 1604.05347 [hep-ex].

[39] PHENIX Collaboration, A. Adare et al., Phys. Rev. Lett. **114** (2015) 192301, arXiv: 1404.7461 [nucl-ex].

[40] STAR Collaboration, L. Adamczyk et al., Phys. Lett. B **747** (2015) 265, arXiv: 1502.07652 [nucl-ex].

[41] PHENIX Collaboration, A. Adare et al., Phys. Rev. Lett. **115** (2015) 142301, arXiv: 1507.06273 [nucl-ex].

[42] CMS Collaboration, JHEP **09** (2010) 091, arXiv: 1009.4122 [hep-ex].

[43] ATLAS Collaboration, Phys. Rev. Lett. **116** (2016) 172301, arXiv: 1509.04776 [nucl-ex].

[44] CMS Collaboration, Phys. Rev. Lett. **116** (2016) 172302, arXiv: 1510.03068 [nucl-ex].

[45] CMS Collaboration, Phys. Lett. B **765** (2017) 193, arXiv: 1606.06198 [nucl-ex].

[46] ATLAS Collaboration, (2016), arXiv: 1609.06213 [nucl-ex].

[47] K. Werner, I. Karpenko and T. Pierog, Phys. Rev. Lett. **106** (2011) 122004, arXiv: 1011.0375 [hep-ph].

[48] M. Ryskin, A. Martin and V. Khoze, J. Phys. G **38** (2011) 085006, arXiv: 1105.4987 [hep-ph].

[49] C. Y. Wong, Phys. Rev. C **84** (2011) 024901, arXiv: 1105.5871 [hep-ph].

[50] E. Avsar et al., J. Phys. G **38** (2011) 124053, arXiv: 1106.4356 [hep-ph].

[51] T. W. Deng, Z. Xu and C. Greiner, Phys. Lett. B **711** (2012) 301, arXiv: 1112.0470 [hep-ph].

[52] P. Bozek, Phys. Rev. C **85** (2012) 014911, arXiv: 1112.0915 [hep-ph].

[53] M. Strikman, Acta Phys. Pol. B **42** (2011) 2607, arXiv: 1112.3834 [hep-ph].

[54] P. Bozek and W. Broniowski, Phys. Lett. B **718** (2013) 1557, arXiv: 1211.0845 [hep-ph].

[55] K. Dusling and R. Venugopalan, Phys. Rev. D **87** (2013) 054014, arXiv: 1211.3701 [hep-ph].

[56] Y. V. Kovchegov and D. E. Wertepny, Nucl. Phys. A **906** (2013) 50, arXiv: 1212.1195 [hep-ph].

[57] K. Dusling and R. Venugopalan, Phys. Rev. D **87** (2013) 094034, arXiv: 1302.7018 [hep-ph].

[58] A. Bzdak, B. Schenke, P. Tribedy and R. Venugopalan, Phys. Rev. C **87** (2013) 064906, arXiv: 1304.3403 [nucl-th].

[59] L. Yan and J.-Y. Ollitrault, Phys. Rev. Lett. **112** (2014) 082301, arXiv: 1312.6555 [nucl-th].

[60] G. L. Ma and A. Bzdak, Phys. Lett. B **739** (2014) 209, arXiv: 1404.4129 [hep-ph].

[61] B. Schenke and R. Venugopalan, Phys. Rev. Lett. **113** (2014) 102301, arXiv: 1405.3605 [nucl-th].

[62] P. M. Chesler, Phys. Rev. Lett. **115** (2015) 241602, arXiv: 1506.02209 [hep-th].

[63] P. M. Chesler, JHEP **03** (2016) 146, arXiv: 1601.01583 [hep-th].

[64] PHENIX Collaboration, K. Adcox et al., Phys. Rev. Lett. **89** (2002) 212301, arXiv: nucl-ex/0204005.

[65] N. Borghini, P. M. Dinh and J. Y. Ollitrault, Phys. Rev. C **63** (2001) 054906, arXiv: nucl-th/0007063.

[66] N. Borghini, P. M. Dinh and J. Y. Ollitrault, Phys. Rev. C **64** (2001) 054901, arXiv: nucl-th/0105040.

[67] A. Bilandzic, R. Snellings and S. Voloshin, Phys. Rev. C **83** (2011) 044913, arXiv: 1010.0233 [nucl-ex].

[68] ATLAS Collaboration, JINST **3** (2008) S08003.

[69] ATLAS Collaboration, ATLAS-TDR-19, 2010, URL: https://cds.cern.ch/record/1291633, ATLAS-TDR-19-ADD-1, 2012, URL: https://cds.cern.ch/record/1451888.

[70] ATLAS Collaboration, Eur. Phys. J. C **72** (2012) 1849, arXiv: 1110.1530 [hep-ex].

[71] ATLAS Collaboration, ATLAS-CONF-2013-104, 2013, URL: https://cdsweb.cern.ch/record/1624013.

[72] T. Sjöstrand, S. Mrenna and P. Skands, Comp. Phys. Comm. **178** (2008) 852, arXiv: 0710.3820 [hep-ph].

[73] ATLAS Collaboration, ATL-PHYS-PUB-2011-009, 2011, URL: https://cds.cern.ch/record/1363300.

[74] A.D. Martin, W.J. Stirling, R.S.Thorne and G. Watt, Eur. Phys. J. C **63** (2009) 189, arXiv: 0901.0002 [hep-ph].

[75] X. N. Wang and M. Gyulassy, Comp. Phys. Comm. **83** (1995) 307, arXiv: nucl-th/9502021.

[76] ATLAS Collaboration, Eur. Phys. J. C **70** (2010) 823, arXiv: 1005.4568 [hep-ex].

[77] S. Agostinelli et al., Nucl. Instrum. Meth. A **506** (2003) 250.

[78] ATLAS Collaboration, ATL-PHYS-PUB-2015-006, 2015, URL: https://cds.cern.ch/record/2002609.

[79] J. Jia, M. Zhou and A. Trzupek, (2017), arXiv: 1701.03830 [nucl-th].

[80] ATLAS Collaboration, Phys. Lett. B **758** (2016) 67, arXiv: 1602.01633 [hep-ex].

[81] A. Bzdak, P. Bozek and L. McLerran, Nucl. Phys. A **927** (2014) 15, arXiv: 1311.7325 [hep-ph].

[82] A. Bzdak and V. Skokov, Nucl. Phys. A **943** (2015) 1, arXiv: 1312.7349 [hep-ph].

[83] ATLAS Collaboration, ATL-GEN-PUB-2016-002, 2016, URL: https://cds.cern.ch/record/2202407.

The ATLAS Collaboration

M. Aaboud[137d], G. Aad[88], B. Abbott[115], J. Abdallah[8], O. Abdinov[12,*], B. Abeloos[119], S.H. Abidi[161], O.S. AbouZeid[139], N.L. Abraham[151], H. Abramowicz[155], H. Abreu[154], R. Abreu[118], Y. Abulaiti[148a,148b], B.S. Acharya[167a,167b,a], S. Adachi[157], L. Adamczyk[41a], J. Adelman[110], M. Adersberger[102], T. Adye[133], A.A. Affolder[139], T. Agatonovic-Jovin[14], C. Agheorghiesei[28c], J.A. Aguilar-Saavedra[128a,128f], S.P. Ahlen[24], F. Ahmadov[68,b], G. Aielli[135a,135b], S. Akatsuka[71], H. Akerstedt[148a,148b], T.P.A. Åkesson[84], A.V. Akimov[98], G.L. Alberghi[22a,22b], J. Albert[172], P. Albicocco[50], M.J. Alconada Verzini[74], M. Aleksa[32], I.N. Aleksandrov[68], C. Alexa[28b], G. Alexander[155], T. Alexopoulos[10], M. Alhroob[115], B. Ali[130], M. Aliev[76a,76b], G. Alimonti[94a], J. Alison[33], S.P. Alkire[38], B.M.M. Allbrooke[151], B.W. Allen[118], P.P. Allport[19], A. Aloisio[106a,106b], A. Alonso[39], F. Alonso[74], C. Alpigiani[140], A.A. Alshehri[56], M. Alstaty[88], B. Alvarez Gonzalez[32], D. Álvarez Piqueras[170], M.G. Alviggi[106a,106b], B.T. Amadio[16], Y. Amaral Coutinho[26a], C. Amelung[25], D. Amidei[92], S.P. Amor Dos Santos[128a,128c], A. Amorim[128a,128b], S. Amoroso[32], G. Amundsen[25], C. Anastopoulos[141], L.S. Ancu[52], N. Andari[19], T. Andeen[11], C.F. Anders[60b], J.K. Anders[77], K.J. Anderson[33], A. Andreazza[94a,94b], V. Andrei[60a], S. Angelidakis[9], I. Angelozzi[109], A. Angerami[38], A.V. Anisenkov[111,c], N. Anjos[13], A. Annovi[126a,126b], C. Antel[60a], M. Antonelli[50], A. Antonov[100,*], D.J. Antrim[166], F. Anulli[134a], M. Aoki[69], L. Aperio Bella[32], G. Arabidze[93], Y. Arai[69], J.P. Araque[128a], V. Araujo Ferraz[26a], A.T.H. Arce[48], R.E. Ardell[80], F.A. Arduh[74], J-F. Arguin[97], S. Argyropoulos[66], M. Arik[20a], A.J. Armbruster[145], L.J. Armitage[79], O. Arnaez[161], H. Arnold[51], M. Arratia[30], O. Arslan[23], A. Artamonov[99], G. Artoni[122], S. Artz[86], S. Asai[157], N. Asbah[45], A. Ashkenazi[155], L. Asquith[151], K. Assamagan[27], R. Astalos[146a], M. Atkinson[169], N.B. Atlay[143], K. Augsten[130], G. Avolio[32], B. Axen[16], M.K. Ayoub[119], G. Azuelos[97,d], A.E. Baas[60a], M.J. Baca[19], H. Bachacou[138], K. Bachas[76a,76b], M. Backes[122], M. Backhaus[32], P. Bagnaia[134a,134b], H. Bahrasemani[144], J.T. Baines[133], M. Bajic[39], O.K. Baker[179], E.M. Baldin[111,c], P. Balek[175], F. Balli[138], W.K. Balunas[124], E. Banas[42], Sw. Banerjee[176,e], A.A.E. Bannoura[178], L. Barak[32], E.L. Barberio[91], D. Barberis[53a,53b], M. Barbero[88], T. Barillari[103], M-S Barisits[32], T. Barklow[145], N. Barlow[30], S.L. Barnes[36c], B.M. Barnett[133], R.M. Barnett[16], Z. Barnovska-Blenessy[36a], A. Baroncelli[136a], G. Barone[25], A.J. Barr[122], L. Barranco Navarro[170], F. Barreiro[85], J. Barreiro Guimarães da Costa[35a], R. Bartoldus[145], A.E. Barton[75], P. Bartos[146a], A. Basalaev[125], A. Bassalat[119,f], R.L. Bates[56], S.J. Batista[161], J.R. Batley[30], M. Battaglia[139], M. Bauce[134a,134b], F. Bauer[138], H.S. Bawa[145,g], J.B. Beacham[113], M.D. Beattie[75], T. Beau[83], P.H. Beauchemin[165], P. Bechtle[23], H.P. Beck[18,h], K. Becker[122], M. Becker[86], M. Beckingham[173], C. Becot[112], A.J. Beddall[20e], A. Beddall[20b], V.A. Bednyakov[68], M. Bedognetti[109], C.P. Bee[150], T.A. Beermann[32], M. Begalli[26a], M. Begel[27], J.K. Behr[45], A.S. Bell[81], G. Bella[155], L. Bellagamba[22a], A. Bellerive[31], M. Bellomo[154], K. Belotskiy[100], O. Beltramello[32], N.L. Belyaev[100], O. Benary[155,*], D. Benchekroun[137a], M. Bender[102], K. Bendtz[148a,148b], N. Benekos[10], Y. Benhammou[155], E. Benhar Noccioli[179], J. Benitez[66], D.P. Benjamin[48], M. Benoit[52], J.R. Bensinger[25], S. Bentvelsen[109], L. Beresford[122], M. Beretta[50], D. Berge[109], E. Bergeaas Kuutmann[168], N. Berger[5], J. Beringer[16], S. Berlendis[58], N.R. Bernard[89], G. Bernardi[83], C. Bernius[145], F.U. Bernlochner[23], T. Berry[80], P. Berta[131], C. Bertella[35a], G. Bertoli[148a,148b], F. Bertolucci[126a,126b], I.A. Bertram[75], C. Bertsche[45], D. Bertsche[115], G.J. Besjes[39], O. Bessidskaia Bylund[148a,148b], M. Bessner[45], N. Besson[138], C. Betancourt[51], A. Bethani[87], S. Bethke[103], A.J. Bevan[79], R.M. Bianchi[127], O. Biebel[102], D. Biedermann[17], R. Bielski[87], N.V. Biesuz[126a,126b], M. Biglietti[136a], J. Bilbao De Mendizabal[52], T.R.V. Billoud[97], H. Bilokon[50], M. Bindi[57], A. Bingul[20b], C. Bini[134a,134b], S. Biondi[22a,22b], T. Bisanz[57], C. Bittrich[47], D.M. Bjergaard[48], C.W. Black[152], J.E. Black[145], K.M. Black[24], D. Blackburn[140], R.E. Blair[6], T. Blazek[146a], I. Bloch[45], C. Blocker[25], A. Blue[56], W. Blum[86,*], U. Blumenschein[79], S. Blunier[34a], G.J. Bobbink[109],

V.S. Bobrovnikov[111,c], S.S. Bocchetta[84], A. Bocci[48], C. Bock[102], M. Boehler[51], D. Boerner[178], D. Bogavac[102], A.G. Bogdanchikov[111], C. Bohm[148a], V. Boisvert[80], P. Bokan[168,i], T. Bold[41a], A.S. Boldyrev[101], A.E. Bolz[60b], M. Bomben[83], M. Bona[79], M. Boonekamp[138], A. Borisov[132], G. Borissov[75], J. Bortfeldt[32], D. Bortoletto[122], V. Bortolotto[62a,62b,62c], D. Boscherini[22a], M. Bosman[13], J.D. Bossio Sola[29], J. Boudreau[127], J. Bouffard[2], E.V. Bouhova-Thacker[75], D. Boumediene[37], C. Bourdarios[119], S.K. Boutle[56], A. Boveia[113], J. Boyd[32], I.R. Boyko[68], J. Bracinik[19], A. Brandt[8], G. Brandt[57], O. Brandt[60a], U. Bratzler[158], B. Brau[89], J.E. Brau[118], W.D. Breaden Madden[56], K. Brendlinger[45], A.J. Brennan[91], L. Brenner[109], R. Brenner[168], S. Bressler[175], D.L. Briglin[19], T.M. Bristow[49], D. Britton[56], D. Britzger[45], F.M. Brochu[30], I. Brock[23], R. Brock[93], G. Brooijmans[38], T. Brooks[80], W.K. Brooks[34b], J. Brosamer[16], E. Brost[110], J.H Broughton[19], P.A. Bruckman de Renstrom[42], D. Bruncko[146b], A. Bruni[22a], G. Bruni[22a], L.S. Bruni[109], BH Brunt[30], M. Bruschi[22a], N. Bruscino[23], P. Bryant[33], L. Bryngemark[45], T. Buanes[15], Q. Buat[144], P. Buchholz[143], A.G. Buckley[56], I.A. Budagov[68], F. Buehrer[51], M.K. Bugge[121], O. Bulekov[100], D. Bullock[8], T.J. Burch[110], H. Burckhart[32], S. Burdin[77], C.D. Burgard[51], A.M. Burger[5], B. Burghgrave[110], K. Burka[42], S. Burke[133], I. Burmeister[46], J.T.P. Burr[122], E. Busato[37], D. Büscher[51], V. Büscher[86], P. Bussey[56], J.M. Butler[24], C.M. Buttar[56], J.M. Butterworth[81], P. Butti[32], W. Buttinger[27], A. Buzatu[35c], A.R. Buzykaev[111,c], S. Cabrera Urbán[170], D. Caforio[130], V.M. Cairo[40a,40b], O. Cakir[4a], N. Calace[52], P. Calafiura[16], A. Calandri[88], G. Calderini[83], P. Calfayan[64], G. Callea[40a,40b], L.P. Caloba[26a], S. Calvente Lopez[85], D. Calvet[37], S. Calvet[37], T.P. Calvet[88], R. Camacho Toro[33], S. Camarda[32], P. Camarri[135a,135b], D. Cameron[121], R. Caminal Armadans[169], C. Camincher[58], S. Campana[32], M. Campanelli[81], A. Camplani[94a,94b], A. Campoverde[143], V. Canale[106a,106b], M. Cano Bret[36c], J. Cantero[116], T. Cao[155], M.D.M. Capeans Garrido[32], I. Caprini[28b], M. Caprini[28b], M. Capua[40a,40b], R.M. Carbone[38], R. Cardarelli[135a], F. Cardillo[51], I. Carli[131], T. Carli[32], G. Carlino[106a], B.T. Carlson[127], L. Carminati[94a,94b], R.M.D. Carney[148a,148b], S. Caron[108], E. Carquin[34b], S. Carrá[94a,94b], G.D. Carrillo-Montoya[32], J. Carvalho[128a,128c], D. Casadei[19], M.P. Casado[13,j], M. Casolino[13], D.W. Casper[166], R. Castelijn[109], V. Castillo Gimenez[170], N.F. Castro[128a,k], A. Catinaccio[32], J.R. Catmore[121], A. Cattai[32], J. Caudron[23], V. Cavaliere[169], E. Cavallaro[13], D. Cavalli[94a], M. Cavalli-Sforza[13], V. Cavasinni[126a,126b], E. Celebi[20a], F. Ceradini[136a,136b], L. Cerda Alberich[170], A.S. Cerqueira[26b], A. Cerri[151], L. Cerrito[135a,135b], F. Cerutti[16], A. Cervelli[18], S.A. Cetin[20d], A. Chafaq[137a], D. Chakraborty[110], S.K. Chan[59], W.S. Chan[109], Y.L. Chan[62a], P. Chang[169], J.D. Chapman[30], D.G. Charlton[19], C.C. Chau[161], C.A. Chavez Barajas[151], S. Che[113], S. Cheatham[167a,167c], A. Chegwidden[93], S. Chekanov[6], S.V. Chekulaev[163a], G.A. Chelkov[68,l], M.A. Chelstowska[32], C. Chen[67], H. Chen[27], S. Chen[35b], S. Chen[157], X. Chen[35c,m], Y. Chen[70], H.C. Cheng[92], H.J. Cheng[35a], A. Cheplakov[68], E. Cheremushkina[132], R. Cherkaoui El Moursli[137e], V. Chernyatin[27,*], E. Cheu[7], L. Chevalier[138], V. Chiarella[50], G. Chiarelli[126a,126b], G. Chiodini[76a], A.S. Chisholm[32], A. Chitan[28b], Y.H. Chiu[172], M.V. Chizhov[68], K. Choi[64], A.R. Chomont[37], S. Chouridou[156], V. Christodoulou[81], D. Chromek-Burckhart[32], M.C. Chu[62a], J. Chudoba[129], A.J. Chuinard[90], J.J. Chwastowski[42], L. Chytka[117], A.K. Ciftci[4a], D. Cinca[46], V. Cindro[78], I.A. Cioara[23], C. Ciocca[22a,22b], A. Ciocio[16], F. Cirotto[106a,106b], Z.H. Citron[175], M. Citterio[94a], M. Ciubancan[28b], A. Clark[52], B.L. Clark[59], M.R. Clark[38], P.J. Clark[49], R.N. Clarke[16], C. Clement[148a,148b], Y. Coadou[88], M. Cobal[167a,167c], A. Coccaro[52], J. Cochran[67], L. Colasurdo[108], B. Cole[38], A.P. Colijn[109], J. Collot[58], T. Colombo[166], P. Conde Muiño[128a,128b], E. Coniavitis[51], S.H. Connell[147b], I.A. Connelly[87], S. Constantinescu[28b], G. Conti[32], F. Conventi[106a,n], M. Cooke[16], A.M. Cooper-Sarkar[122], F. Cormier[171], K.J.R. Cormier[161], M. Corradi[134a,134b], F. Corriveau[90,o], A. Cortes-Gonzalez[32], G. Cortiana[103], G. Costa[94a], M.J. Costa[170], D. Costanzo[141], G. Cottin[30], G. Cowan[80], B.E. Cox[87], K. Cranmer[112], S.J. Crawley[56], R.A. Creager[124], G. Cree[31], S. Crépé-Renaudin[58], F. Crescioli[83], W.A. Cribbs[148a,148b], M. Cristinziani[23], V. Croft[108], G. Crosetti[40a,40b], A. Cueto[85], T. Cuhadar Donszelmann[141],

A.R. Cukierman[145], J. Cummings[179], M. Curatolo[50], J. Cúth[86], H. Czirr[143], P. Czodrowski[32], G. D'amen[22a,22b], S. D'Auria[56], M. D'Onofrio[77], M.J. Da Cunha Sargedas De Sousa[128a,128b], C. Da Via[87], W. Dabrowski[41a], T. Dado[146a], T. Dai[92], O. Dale[15], F. Dallaire[97], C. Dallapiccola[89], M. Dam[39], J.R. Dandoy[124], N.P. Dang[176], A.C. Daniells[19], N.S. Dann[87], M. Danninger[171], M. Dano Hoffmann[138], V. Dao[150], G. Darbo[53a], S. Darmora[8], J. Dassoulas[3], A. Dattagupta[118], T. Daubney[45], W. Davey[23], C. David[45], T. Davidek[131], M. Davies[155], P. Davison[81], E. Dawe[91], I. Dawson[141], K. De[8], R. de Asmundis[106a], A. De Benedetti[115], S. De Castro[22a,22b], S. De Cecco[83], N. De Groot[108], P. de Jong[109], H. De la Torre[93], F. De Lorenzi[67], A. De Maria[57], D. De Pedis[134a], A. De Salvo[134a], U. De Sanctis[135a,135b], A. De Santo[151], K. De Vasconcelos Corga[88], J.B. De Vivie De Regie[119], W.J. Dearnaley[75], R. Debbe[27], C. Debenedetti[139], D.V. Dedovich[68], N. Dehghanian[3], I. Deigaard[109], M. Del Gaudio[40a,40b], J. Del Peso[85], T. Del Prete[126a,126b], D. Delgove[119], F. Deliot[138], C.M. Delitzsch[52], A. Dell'Acqua[32], L. Dell'Asta[24], M. Dell'Orso[126a,126b], M. Della Pietra[106a,106b], D. della Volpe[52], M. Delmastro[5], C. Delporte[119], P.A. Delsart[58], D.A. DeMarco[161], S. Demers[179], M. Demichev[68], A. Demilly[83], S.P. Denisov[132], D. Denysiuk[138], D. Derendarz[42], J.E. Derkaoui[137d], F. Derue[83], P. Dervan[77], K. Desch[23], C. Deterre[45], K. Dette[46], M.R. Devesa[29], P.O. Deviveiros[32], A. Dewhurst[133], S. Dhaliwal[25], F.A. Di Bello[52], A. Di Ciaccio[135a,135b], L. Di Ciaccio[5], W.K. Di Clemente[124], C. Di Donato[106a,106b], A. Di Girolamo[32], B. Di Girolamo[32], B. Di Micco[136a,136b], R. Di Nardo[32], K.F. Di Petrillo[59], A. Di Simone[51], R. Di Sipio[161], D. Di Valentino[31], C. Diaconu[88], M. Diamond[161], F.A. Dias[39], M.A. Diaz[34a], E.B. Diehl[92], J. Dietrich[17], S. Díez Cornell[45], A. Dimitrievska[14], J. Dingfelder[23], P. Dita[28b], S. Dita[28b], F. Dittus[32], F. Djama[88], T. Djobava[54b], J.I. Djuvsland[60a], M.A.B. do Vale[26c], D. Dobos[32], M. Dobre[28b], C. Doglioni[84], J. Dolejsi[131], Z. Dolezal[131], M. Donadelli[26d], S. Donati[126a,126b], P. Dondero[123a,123b], J. Donini[37], J. Dopke[133], A. Doria[106a], M.T. Dova[74], A.T. Doyle[56], E. Drechsler[57], M. Dris[10], Y. Du[36b], J. Duarte-Campderros[155], A. Dubreuil[52], E. Duchovni[175], G. Duckeck[102], A. Ducourthial[83], O.A. Ducu[97,p], D. Duda[109], A. Dudarev[32], A.Chr. Dudder[86], E.M. Duffield[16], L. Duflot[119], M. Dührssen[32], M. Dumancic[175], A.E. Dumitriu[28b], A.K. Duncan[56], M. Dunford[60a], H. Duran Yildiz[4a], M. Düren[55], A. Durglishvili[54b], D. Duschinger[47], B. Dutta[45], M. Dyndal[45], C. Eckardt[45], K.M. Ecker[103], R.C. Edgar[92], T. Eifert[32], G. Eigen[15], K. Einsweiler[16], T. Ekelof[168], M. El Kacimi[137c], R. El Kosseifi[88], V. Ellajosyula[88], M. Ellert[168], S. Elles[5], F. Ellinghaus[178], A.A. Elliot[172], N. Ellis[32], J. Elmsheuser[27], M. Elsing[32], D. Emeliyanov[133], Y. Enari[157], O.C. Endner[86], J.S. Ennis[173], J. Erdmann[46], A. Ereditato[18], G. Ernis[178], M. Ernst[27], S. Errede[169], E. Ertel[86], M. Escalier[119], C. Escobar[127], B. Esposito[50], O. Estrada Pastor[170], A.I. Etienvre[138], E. Etzion[155], H. Evans[64], A. Ezhilov[125], M. Ezzi[137e], F. Fabbri[22a,22b], L. Fabbri[22a,22b], G. Facini[33], R.M. Fakhrutdinov[132], S. Falciano[134a], R.J. Falla[81], J. Faltova[32], Y. Fang[35a], M. Fanti[94a,94b], A. Farbin[8], A. Farilla[136a], C. Farina[127], E.M. Farina[123a,123b], T. Farooque[93], S. Farrell[16], S.M. Farrington[173], P. Farthouat[32], F. Fassi[137e], P. Fassnacht[32], D. Fassouliotis[9], M. Faucci Giannelli[80], A. Favareto[53a,53b], W.J. Fawcett[122], L. Fayard[119], O.L. Fedin[125,q], W. Fedorko[171], S. Feigl[121], L. Feligioni[88], C. Feng[36b], E.J. Feng[32], H. Feng[92], M.J. Fenton[56], A.B. Fenyuk[132], L. Feremenga[8], P. Fernandez Martinez[170], S. Fernandez Perez[13], J. Ferrando[45], A. Ferrari[168], P. Ferrari[109], R. Ferrari[123a], D.E. Ferreira de Lima[60b], A. Ferrer[170], D. Ferrere[52], C. Ferretti[92], F. Fiedler[86], A. Filipčič[78], M. Filipuzzi[45], F. Filthaut[108], M. Fincke-Keeler[172], K.D. Finelli[152], M.C.N. Fiolhais[128a,128c,r], L. Fiorini[170], A. Fischer[2], C. Fischer[13], J. Fischer[178], W.C. Fisher[93], N. Flaschel[45], I. Fleck[143], P. Fleischmann[92], R.R.M. Fletcher[124], T. Flick[178], B.M. Flierl[102], L.R. Flores Castillo[62a], M.J. Flowerdew[103], G.T. Forcolin[87], A. Formica[138], F.A. Förster[13], A. Forti[87], A.G. Foster[19], D. Fournier[119], H. Fox[75], S. Fracchia[141], P. Francavilla[83], M. Franchini[22a,22b], S. Franchino[60a], D. Francis[32], L. Franconi[121], M. Franklin[59], M. Frate[166], M. Fraternali[123a,123b], D. Freeborn[81], S.M. Fressard-Batraneanu[32], B. Freund[97], D. Froidevaux[32], J.A. Frost[122], C. Fukunaga[158], T. Fusayasu[104], J. Fuster[170], C. Gabaldon[58], O. Gabizon[154],

A. Gabrielli[22a,22b], A. Gabrielli[16], G.P. Gach[41a], S. Gadatsch[32], S. Gadomski[80], G. Gagliardi[53a,53b], L.G. Gagnon[97], C. Galea[108], B. Galhardo[128a,128c], E.J. Gallas[122], B.J. Gallop[133], P. Gallus[130], G. Galster[39], K.K. Gan[113], S. Ganguly[37], J. Gao[36a], Y. Gao[77], Y.S. Gao[145,g], F.M. Garay Walls[49], C. García[170], J.E. García Navarro[170], M. Garcia-Sciveres[16], R.W. Gardner[33], N. Garelli[145], V. Garonne[121], A. Gascon Bravo[45], K. Gasnikova[45], C. Gatti[50], A. Gaudiello[53a,53b], G. Gaudio[123a], I.L. Gavrilenko[98], C. Gay[171], G. Gaycken[23], E.N. Gazis[10], C.N.P. Gee[133], J. Geisen[57], M. Geisen[86], M.P. Geisler[60a], K. Gellerstedt[148a,148b], C. Gemme[53a], M.H. Genest[58], C. Geng[92], S. Gentile[134a,134b], C. Gentsos[156], S. George[80], D. Gerbaudo[13], A. Gershon[155], S. Ghasemi[143], M. Ghneimat[23], B. Giacobbe[22a], S. Giagu[134a,134b], P. Giannetti[126a,126b], S.M. Gibson[80], M. Gignac[171], M. Gilchriese[16], D. Gillberg[31], G. Gilles[178], D.M. Gingrich[3,d], N. Giokaris[9,*], M.P. Giordani[167a,167c], F.M. Giorgi[22a], P.F. Giraud[138], P. Giromini[59], D. Giugni[94a], F. Giuli[122], C. Giuliani[103], M. Giulini[60b], B.K. Gjelsten[121], S. Gkaitatzis[156], I. Gkialas[9], E.L. Gkougkousis[139], L.K. Gladilin[101], C. Glasman[85], J. Glatzer[13], P.C.F. Glaysher[45], A. Glazov[45], M. Goblirsch-Kolb[25], J. Godlewski[42], S. Goldfarb[91], T. Golling[52], D. Golubkov[132], A. Gomes[128a,128b,128d], R. Gonçalo[128a], R. Goncalves Gama[26a], J. Goncalves Pinto Firmino Da Costa[138], G. Gonella[51], L. Gonella[19], A. Gongadze[68], S. González de la Hoz[170], S. Gonzalez-Sevilla[52], L. Goossens[32], P.A. Gorbounov[99], H.A. Gordon[27], I. Gorelov[107], B. Gorini[32], E. Gorini[76a,76b], A. Gorišek[78], A.T. Goshaw[48], C. Gössling[46], M.I. Gostkin[68], C.R. Goudet[119], D. Goujdami[137c], A.G. Goussiou[140], N. Govender[147b,s], E. Gozani[154], L. Graber[57], I. Grabowska-Bold[41a], P.O.J. Gradin[168], J. Gramling[166], E. Gramstad[121], S. Grancagnolo[17], V. Gratchev[125], P.M. Gravila[28f], C. Gray[56], H.M. Gray[32], Z.D. Greenwood[82,t], C. Grefe[23], K. Gregersen[81], I.M. Gregor[45], P. Grenier[145], K. Grevtsov[5], J. Griffiths[8], A.A. Grillo[139], K. Grimm[75], S. Grinstein[13,u], Ph. Gris[37], J.-F. Grivaz[119], S. Groh[86], E. Gross[175], J. Grosse-Knetter[57], G.C. Grossi[82], Z.J. Grout[81], A. Grummer[107], L. Guan[92], W. Guan[176], J. Guenther[65], F. Guescini[163a], D. Guest[166], O. Gueta[155], B. Gui[113], E. Guido[53a,53b], T. Guillemin[5], S. Guindon[2], U. Gul[56], C. Gumpert[32], J. Guo[36c], W. Guo[92], Y. Guo[36a], R. Gupta[43], S. Gupta[122], G. Gustavino[134a,134b], P. Gutierrez[115], N.G. Gutierrez Ortiz[81], C. Gutschow[81], C. Guyot[138], M.P. Guzik[41a], C. Gwenlan[122], C.B. Gwilliam[77], A. Haas[112], C. Haber[16], H.K. Hadavand[8], N. Haddad[137e], A. Hadef[88], S. Hageböck[23], M. Hagihara[164], H. Hakobyan[180,*], M. Haleem[45], J. Haley[116], G. Halladjian[93], G.D. Hallewell[88], K. Hamacher[178], P. Hamal[117], K. Hamano[172], A. Hamilton[147a], G.N. Hamity[141], P.G. Hamnett[45], L. Han[36a], S. Han[35a], K. Hanagaki[69,v], K. Hanawa[157], M. Hance[139], B. Haney[124], P. Hanke[60a], J.B. Hansen[39], J.D. Hansen[39], M.C. Hansen[23], P.H. Hansen[39], K. Hara[164], A.S. Hard[176], T. Harenberg[178], F. Hariri[119], S. Harkusha[95], R.D. Harrington[49], P.F. Harrison[173], N.M. Hartmann[102], M. Hasegawa[70], Y. Hasegawa[142], A. Hasib[49], S. Hassani[138], S. Haug[18], R. Hauser[93], L. Hauswald[47], L.B. Havener[38], M. Havranek[130], C.M. Hawkes[19], R.J. Hawkings[32], D. Hayakawa[159], D. Hayden[93], C.P. Hays[122], J.M. Hays[79], H.S. Hayward[77], S.J. Haywood[133], S.J. Head[19], T. Heck[86], V. Hedberg[84], L. Heelan[8], K.K. Heidegger[51], S. Heim[45], T. Heim[16], B. Heinemann[45,w], J.J. Heinrich[102], L. Heinrich[112], C. Heinz[55], J. Hejbal[129], L. Helary[32], A. Held[171], S. Hellman[148a,148b], C. Helsens[32], R.C.W. Henderson[75], Y. Heng[176], S. Henkelmann[171], A.M. Henriques Correia[32], S. Henrot-Versille[119], G.H. Herbert[17], H. Herde[25], V. Herget[177], Y. Hernández Jiménez[147c], G. Herten[51], R. Hertenberger[102], L. Hervas[32], T.C. Herwig[124], G.G. Hesketh[81], N.P. Hessey[163a], J.W. Hetherly[43], S. Higashino[69], E. Higón-Rodriguez[170], E. Hill[172], J.C. Hill[30], K.H. Hiller[45], S.J. Hillier[19], I. Hinchliffe[16], M. Hirose[51], D. Hirschbuehl[178], B. Hiti[78], O. Hladik[129], X. Hoad[49], J. Hobbs[150], N. Hod[163a], M.C. Hodgkinson[141], P. Hodgson[141], A. Hoecker[32], M.R. Hoeferkamp[107], F. Hoenig[102], D. Hohn[23], T.R. Holmes[33], M. Homann[46], S. Honda[164], T. Honda[69], T.M. Hong[127], B.H. Hooberman[169], W.H. Hopkins[118], Y. Horii[105], A.J. Horton[144], J-Y. Hostachy[58], S. Hou[153], A. Hoummada[137a], J. Howarth[45], J. Hoya[74], M. Hrabovsky[117], I. Hristova[17], J. Hrivnac[119], T. Hryn'ova[5], A. Hrynevich[96], P.J. Hsu[63], S.-C. Hsu[140], Q. Hu[36a], S. Hu[36c], Y. Huang[35a], Z. Hubacek[130], F. Hubaut[88], F. Huegging[23], T.B. Huffman[122], E.W. Hughes[38], G. Hughes[75], M. Huhtinen[32], P. Huo[150],

N. Huseynov[68,b], J. Huston[93], J. Huth[59], G. Iacobucci[52], G. Iakovidis[27], I. Ibragimov[143], L. Iconomidou-Fayard[119], Z. Idrissi[137e], P. Iengo[32], O. Igonkina[109,x], T. Iizawa[174], Y. Ikegami[69], M. Ikeno[69], Y. Ilchenko[11,y], D. Iliadis[156], N. Ilic[145], G. Introzzi[123a,123b], P. Ioannou[9,*], M. Iodice[136a], K. Iordanidou[38], V. Ippolito[59], M.F. Isacson[168], N. Ishijima[120], M. Ishino[157], M. Ishitsuka[159], C. Issever[122], S. Istin[20a], F. Ito[164], J.M. Iturbe Ponce[87], R. Iuppa[162a,162b], H. Iwasaki[69], J.M. Izen[44], V. Izzo[106a], S. Jabbar[3], P. Jackson[1], R.M. Jacobs[23], V. Jain[2], K.B. Jakobi[86], K. Jakobs[51], S. Jakobsen[65], T. Jakoubek[129], D.O. Jamin[116], D.K. Jana[82], R. Jansky[65], J. Janssen[23], M. Janus[57], P.A. Janus[41a], G. Jarlskog[84], N. Javadov[68,b], T. Javůrek[51], M. Javurkova[51], F. Jeanneau[138], L. Jeanty[16], J. Jejelava[54a,z], A. Jelinskas[173], P. Jenni[51,aa], C. Jeske[173], S. Jézéquel[5], H. Ji[176], J. Jia[150], H. Jiang[67], Y. Jiang[36a], Z. Jiang[145], S. Jiggins[81], J. Jimenez Pena[170], S. Jin[35a], A. Jinaru[28b], O. Jinnouchi[159], H. Jivan[147c], P. Johansson[141], K.A. Johns[7], C.A. Johnson[64], W.J. Johnson[140], K. Jon-And[148a,148b], R.W.L. Jones[75], S.D. Jones[151], S. Jones[7], T.J. Jones[77], J. Jongmanns[60a], P.M. Jorge[128a,128b], J. Jovicevic[163a], X. Ju[176], A. Juste Rozas[13,u], M.K. Köhler[175], A. Kaczmarska[42], M. Kado[119], H. Kagan[113], M. Kagan[145], S.J. Kahn[88], T. Kaji[174], E. Kajomovitz[48], C.W. Kalderon[84], A. Kaluza[86], S. Kama[43], A. Kamenshchikov[132], N. Kanaya[157], L. Kanjir[78], V.A. Kantserov[100], J. Kanzaki[69], B. Kaplan[112], L.S. Kaplan[176], D. Kar[147c], K. Karakostas[10], N. Karastathis[10], M.J. Kareem[57], E. Karentzos[10], S.N. Karpov[68], Z.M. Karpova[68], K. Karthik[112], V. Kartvelishvili[75], A.N. Karyukhin[132], K. Kasahara[164], L. Kashif[176], R.D. Kass[113], A. Kastanas[149], Y. Kataoka[157], C. Kato[157], A. Katre[52], J. Katzy[45], K. Kawade[105], K. Kawagoe[73], T. Kawamoto[157], G. Kawamura[57], E.F. Kay[77], V.F. Kazanin[111,c], R. Keeler[172], R. Kehoe[43], J.S. Keller[45], J.J. Kempster[80], H. Keoshkerian[161], O. Kepka[129], B.P. Kerševan[78], S. Kersten[178], R.A. Keyes[90], M. Khader[169], F. Khalil-zada[12], A. Khanov[116], A.G. Kharlamov[111,c], T. Kharlamova[111,c], A. Khodinov[160], T.J. Khoo[52], V. Khovanskiy[99,*], E. Khramov[68], J. Khubua[54b,ab], S. Kido[70], C.R. Kilby[80], H.Y. Kim[8], S.H. Kim[164], Y.K. Kim[33], N. Kimura[156], O.M. Kind[17], B.T. King[77], D. Kirchmeier[47], J. Kirk[133], A.E. Kiryunin[103], T. Kishimoto[157], D. Kisielewska[41a], K. Kiuchi[164], O. Kivernyk[5], E. Kladiva[146b], T. Klapdor-Kleingrothaus[51], M.H. Klein[38], M. Klein[77], U. Klein[77], K. Kleinknecht[86], P. Klimek[110], A. Klimentov[27], R. Klingenberg[46], T. Klingl[23], T. Klioutchnikova[32], E.-E. Kluge[60a], P. Kluit[109], S. Kluth[103], J. Knapik[42], E. Kneringer[65], E.B.F.G. Knoops[88], A. Knue[103], A. Kobayashi[157], D. Kobayashi[159], T. Kobayashi[157], M. Kobel[47], M. Kocian[145], P. Kodys[131], T. Koffas[31], E. Koffeman[109], N.M. Köhler[103], T. Koi[145], M. Kolb[60b], I. Koletsou[5], A.A. Komar[98,*], Y. Komori[157], T. Kondo[69], N. Kondrashova[36c], K. Köneke[51], A.C. König[108], T. Kono[69,ac], R. Konoplich[112,ad], N. Konstantinidis[81], R. Kopeliansky[64], S. Koperny[41a], A.K. Kopp[51], K. Korcyl[42], K. Kordas[156], A. Korn[81], A.A. Korol[111,c], I. Korolkov[13], E.V. Korolkova[141], O. Kortner[103], S. Kortner[103], T. Kosek[131], V.V. Kostyukhin[23], A. Kotwal[48], A. Koulouris[10], A. Kourkoumeli-Charalampidi[123a,123b], C. Kourkoumelis[9], E. Kourlitis[141], V. Kouskoura[27], A.B. Kowalewska[42], R. Kowalewski[172], T.Z. Kowalski[41a], C. Kozakai[157], W. Kozanecki[138], A.S. Kozhin[132], V.A. Kramarenko[101], G. Kramberger[78], D. Krasnopevtsev[100], M.W. Krasny[83], A. Krasznahorkay[32], D. Krauss[103], J.A. Kremer[41a], J. Kretzschmar[77], K. Kreutzfeldt[55], P. Krieger[161], K. Krizka[33], K. Kroeninger[46], H. Kroha[103], J. Kroll[129], J. Kroll[124], J. Kroseberg[23], J. Krstic[14], U. Kruchonak[68], H. Krüger[23], N. Krumnack[67], M.C. Kruse[48], T. Kubota[91], H. Kucuk[81], S. Kuday[4b], J.T. Kuechler[178], S. Kuehn[32], A. Kugel[60c], F. Kuger[177], T. Kuhl[45], V. Kukhtin[68], R. Kukla[88], Y. Kulchitsky[95], S. Kuleshov[34b], Y.P. Kulinich[169], M. Kuna[134a,134b], T. Kunigo[71], A. Kupco[129], O. Kuprash[155], H. Kurashige[70], L.L. Kurchaninov[163a], Y.A. Kurochkin[95], M.G. Kurth[35a], V. Kus[129], E.S. Kuwertz[172], M. Kuze[159], J. Kvita[117], T. Kwan[172], D. Kyriazopoulos[141], A. La Rosa[103], J.L. La Rosa Navarro[26d], L. La Rotonda[40a,40b], C. Lacasta[170], F. Lacava[134a,134b], J. Lacey[45], H. Lacker[17], D. Lacour[83], E. Ladygin[68], R. Lafaye[5], B. Laforge[83], T. Lagouri[179], S. Lai[57], S. Lammers[64], W. Lampl[7], E. Lançon[27], U. Landgraf[51], M.P.J. Landon[79], M.C. Lanfermann[52], V.S. Lang[60a], J.C. Lange[13], A.J. Lankford[166], F. Lanni[27], K. Lantzsch[23], A. Lanza[123a], A. Lapertosa[53a,53b], S. Laplace[83],

J.F. Laporte[138], T. Lari[94a], F. Lasagni Manghi[22a,22b], M. Lassnig[32], P. Laurelli[50], W. Lavrijsen[16], A.T. Law[139], P. Laycock[77], T. Lazovich[59], M. Lazzaroni[94a,94b], B. Le[91], O. Le Dortz[83], E. Le Guirriec[88], E.P. Le Quilleuc[138], M. LeBlanc[172], T. LeCompte[6], F. Ledroit-Guillon[58], C.A. Lee[27], G.R. Lee[133,*ae*], S.C. Lee[153], L. Lee[59], B. Lefebvre[90], G. Lefebvre[83], M. Lefebvre[172], F. Legger[102], C. Leggett[16], A. Lehan[77], G. Lehmann Miotto[32], X. Lei[7], W.A. Leight[45], M.A.L. Leite[26d], R. Leitner[131], D. Lellouch[175], B. Lemmer[57], K.J.C. Leney[81], T. Lenz[23], B. Lenzi[32], R. Leone[7], S. Leone[126a,126b], C. Leonidopoulos[49], G. Lerner[151], C. Leroy[97], A.A.J. Lesage[138], C.G. Lester[30], M. Levchenko[125], J. Levêque[5], D. Levin[92], L.J. Levinson[175], M. Levy[19], D. Lewis[79], B. Li[36a,*af*], C. Li[36a], H. Li[150], L. Li[36c], Q. Li[35a], S. Li[48], X. Li[36c], Y. Li[143], Z. Liang[35a], B. Liberti[135a], A. Liblong[161], K. Lie[62c], J. Liebal[23], W. Liebig[15], A. Limosani[152], S.C. Lin[153,*ag*], T.H. Lin[86], B.E. Lindquist[150], A.E. Lionti[52], E. Lipeles[124], A. Lipniacka[15], M. Lisovyi[60b], T.M. Liss[169], A. Lister[171], A.M. Litke[139], B. Liu[153,*ah*], H. Liu[92], H. Liu[27], J.K.K. Liu[122], J. Liu[36b], J.B. Liu[36a], K. Liu[88], L. Liu[169], M. Liu[36a], Y.L. Liu[36a], Y. Liu[36a], M. Livan[123a,123b], A. Lleres[58], J. Llorente Merino[35a], S.L. Lloyd[79], C.Y. Lo[62b], F. Lo Sterzo[153], E.M. Lobodzinska[45], P. Loch[7], F.K. Loebinger[87], K.M. Loew[25], A. Loginov[179,*], T. Lohse[17], K. Lohwasser[45], M. Lokajicek[129], B.A. Long[24], J.D. Long[169], R.E. Long[75], L. Longo[76a,76b], K.A. Looper[113], J.A. Lopez[34b], D. Lopez Mateos[59], I. Lopez Paz[13], A. Lopez Solis[83], J. Lorenz[102], N. Lorenzo Martinez[5], M. Losada[21], P.J. Lösel[102], X. Lou[35a], A. Lounis[119], J. Love[6], P.A. Love[75], H. Lu[62a], N. Lu[92], Y.J. Lu[63], H.J. Lubatti[140], C. Luci[134a,134b], A. Lucotte[58], C. Luedtke[51], F. Luehring[64], W. Lukas[65], L. Luminari[134a], O. Lundberg[148a,148b], B. Lund-Jensen[149], P.M. Luzi[83], D. Lynn[27], R. Lysak[129], E. Lytken[84], V. Lyubushkin[68], H. Ma[27], L.L. Ma[36b], Y. Ma[36b], G. Maccarrone[50], A. Macchiolo[103], C.M. Macdonald[141], B. Maček[78], J. Machado Miguens[124,128b], D. Madaffari[88], R. Madar[37], H.J. Maddocks[168], W.F. Mader[47], A. Madsen[45], J. Maeda[70], S. Maeland[15], T. Maeno[27], A.S. Maevskiy[101], E. Magradze[57], J. Mahlstedt[109], C. Maiani[119], C. Maidantchik[26a], A.A. Maier[103], T. Maier[102], A. Maio[128a,128b,128d], S. Majewski[118], Y. Makida[69], N. Makovec[119], B. Malaescu[83], Pa. Malecki[42], V.P. Maleev[125], F. Malek[58], U. Mallik[66], D. Malon[6], C. Malone[30], S. Maltezos[10], S. Malyukov[32], J. Mamuzic[170], G. Mancini[50], L. Mandelli[94a], I. Mandić[78], J. Maneira[128a,128b], L. Manhaes de Andrade Filho[26b], J. Manjarres Ramos[47], A. Mann[102], A. Manousos[32], B. Mansoulie[138], J.D. Mansour[35a], R. Mantifel[90], M. Mantoani[57], S. Manzoni[94a,94b], L. Mapelli[32], G. Marceca[29], L. March[52], L. Marchese[122], G. Marchiori[83], M. Marcisovsky[129], M. Marjanovic[37], D.E. Marley[92], F. Marroquim[26a], S.P. Marsden[87], Z. Marshall[16], M.U.F Martensson[168], S. Marti-Garcia[170], C.B. Martin[113], T.A. Martin[173], V.J. Martin[49], B. Martin dit Latour[15], M. Martinez[13,*u*], V.I. Martinez Outschoorn[169], S. Martin-Haugh[133], V.S. Martoiu[28b], A.C. Martyniuk[81], A. Marzin[32], L. Masetti[86], T. Mashimo[157], R. Mashinistov[98], J. Masik[87], A.L. Maslennikov[111,*c*], L. Massa[135a,135b], P. Mastrandrea[5], A. Mastroberardino[40a,40b], T. Masubuchi[157], P. Mättig[178], J. Maurer[28b], S.J. Maxfield[77], D.A. Maximov[111,*c*], R. Mazini[153], I. Maznas[156], S.M. Mazza[94a,94b], N.C. Mc Fadden[107], G. Mc Goldrick[161], S.P. Mc Kee[92], A. McCarn[92], R.L. McCarthy[150], T.G. McCarthy[103], L.I. McClymont[81], E.F. McDonald[91], J.A. Mcfayden[81], G. Mchedlidze[57], S.J. McMahon[133], P.C. McNamara[91], R.A. McPherson[172,*o*], S. Meehan[140], T.J. Megy[51], S. Mehlhase[102], A. Mehta[77], T. Meideck[58], K. Meier[60a], B. Meirose[44], D. Melini[170,*ai*], B.R. Mellado Garcia[147c], J.D. Mellenthin[57], M. Melo[146a], F. Meloni[18], S.B. Menary[87], L. Meng[77], X.T. Meng[92], A. Mengarelli[22a,22b], S. Menke[103], E. Meoni[40a,40b], S. Mergelmeyer[17], P. Mermod[52], L. Merola[106a,106b], C. Meroni[94a], F.S. Merritt[33], A. Messina[134a,134b], J. Metcalfe[6], A.S. Mete[166], C. Meyer[124], J-P. Meyer[138], J. Meyer[109], H. Meyer Zu Theenhausen[60a], F. Miano[151], R.P. Middleton[133], S. Miglioranzi[53a,53b], L. Mijović[49], G. Mikenberg[175], M. Mikestikova[129], M. Mikuž[78], M. Milesi[91], A. Milic[27], D.W. Miller[33], C. Mills[49], A. Milov[175], D.A. Milstead[148a,148b], A.A. Minaenko[132], Y. Minami[157], I.A. Minashvili[68], A.I. Mincer[112], B. Mindur[41a], M. Mineev[68], Y. Minegishi[157], Y. Ming[176], L.M. Mir[13], K.P. Mistry[124], T. Mitani[174], J. Mitrevski[102], V.A. Mitsou[170], A. Miucci[18], P.S. Miyagawa[141], A. Mizukami[69], J.U. Mjörnmark[84],

T. Mkrtchyan[180], M. Mlynarikova[131], T. Moa[148a,148b], K. Mochizuki[97], P. Mogg[51], S. Mohapatra[38], S. Molander[148a,148b], R. Moles-Valls[23], R. Monden[71], M.C. Mondragon[93], K. Mönig[45], J. Monk[39], E. Monnier[88], A. Montalbano[150], J. Montejo Berlingen[32], F. Monticelli[74], S. Monzani[94a,94b], R.W. Moore[3], N. Morange[119], D. Moreno[21], M. Moreno Llácer[57], P. Morettini[53a], S. Morgenstern[32], D. Mori[144], T. Mori[157], M. Morii[59], M. Morinaga[157], V. Morisbak[121], A.K. Morley[152], G. Mornacchi[32], J.D. Morris[79], L. Morvaj[150], P. Moschovakos[10], M. Mosidze[54b], H.J. Moss[141], J. Moss[145,aj], K. Motohashi[159], R. Mount[145], E. Mountricha[27], E.J.W. Moyse[89], S. Muanza[88], R.D. Mudd[19], F. Mueller[103], J. Mueller[127], R.S.P. Mueller[102], D. Muenstermann[75], P. Mullen[56], G.A. Mullier[18], F.J. Munoz Sanchez[87], W.J. Murray[173,133], H. Musheghyan[181], M. Muškinja[78], A.G. Myagkov[132,ak], M. Myska[130], B.P. Nachman[16], O. Nackenhorst[52], K. Nagai[122], R. Nagai[69,ac], K. Nagano[69], Y. Nagasaka[61], K. Nagata[164], M. Nagel[51], E. Nagy[88], A.M. Nairz[32], Y. Nakahama[105], K. Nakamura[69], T. Nakamura[157], I. Nakano[114], R.F. Naranjo Garcia[45], R. Narayan[11], D.I. Narrias Villar[60a], I. Naryshkin[125], T. Naumann[45], G. Navarro[21], R. Nayyar[7], H.A. Neal[92], P.Yu. Nechaeva[98], T.J. Neep[138], A. Negri[123a,123b], M. Negrini[22a], S. Nektarijevic[108], C. Nellist[119], A. Nelson[166], M.E. Nelson[122], S. Nemecek[129], P. Nemethy[112], M. Nessi[32,al], M.S. Neubauer[169], M. Neumann[178], P.R. Newman[19], T.Y. Ng[62c], T. Nguyen Manh[97], R.B. Nickerson[122], R. Nicolaidou[138], J. Nielsen[139], V. Nikolaenko[132,ak], I. Nikolic-Audit[83], K. Nikolopoulos[19], J.K. Nilsen[121], P. Nilsson[27], Y. Ninomiya[157], A. Nisati[134a], N. Nishu[35c], R. Nisius[103], T. Nobe[157], Y. Noguchi[71], M. Nomachi[120], I. Nomidis[31], M.A. Nomura[27], T. Nooney[79], M. Nordberg[32], N. Norjoharuddeen[122], O. Novgorodova[47], S. Nowak[103], M. Nozaki[69], L. Nozka[117], K. Ntekas[166], E. Nurse[81], F. Nuti[91], K. O'connor[25], D.C. O'Neil[144], A.A. O'Rourke[45], V. O'Shea[56], F.G. Oakham[31,d], H. Oberlack[103], T. Obermann[23], J. Ocariz[83], A. Ochi[70], I. Ochoa[38], J.P. Ochoa-Ricoux[34a], S. Oda[73], S. Odaka[69], H. Ogren[64], A. Oh[87], S.H. Oh[48], C.C. Ohm[16], H. Ohman[168], H. Oide[53a,53b], H. Okawa[164], Y. Okumura[157], T. Okuyama[69], A. Olariu[28b], L.F. Oleiro Seabra[128a], S.A. Olivares Pino[49], D. Oliveira Damazio[27], A. Olszewski[42], J. Olszowska[42], A. Onofre[128a,128e], K. Onogi[105], P.U.E. Onyisi[11,y], M.J. Oreglia[33], Y. Oren[155], D. Orestano[136a,136b], N. Orlando[62b], R.S. Orr[161], B. Osculati[53a,53b,*], R. Ospanov[36a], G. Otero y Garzon[29], H. Otono[73], M. Ouchrif[137d], F. Ould-Saada[121], A. Ouraou[138], K.P. Oussoren[109], Q. Ouyang[35a], M. Owen[56], R.E. Owen[19], V.E. Ozcan[20a], N. Ozturk[8], K. Pachal[144], A. Pacheco Pages[13], L. Pacheco Rodriguez[138], C. Padilla Aranda[13], S. Pagan Griso[16], M. Paganini[179], F. Paige[27], G. Palacino[64], S. Palazzo[40a,40b], S. Palestini[32], M. Palka[41b], D. Pallin[37], E.St. Panagiotopoulou[10], I. Panagoulias[10], C.E. Pandini[83], J.G. Panduro Vazquez[80], P. Pani[32], S. Panitkin[27], D. Pantea[28b], L. Paolozzi[52], Th.D. Papadopoulou[10], K. Papageorgiou[9], A. Paramonov[6], D. Paredes Hernandez[179], A.J. Parker[75], M.A. Parker[30], K.A. Parker[45], F. Parodi[53a,53b], J.A. Parsons[38], U. Parzefall[51], V.R. Pascuzzi[161], J.M. Pasner[139], E. Pasqualucci[134a], S. Passaggio[53a], Fr. Pastore[80], S. Pataraia[178], J.R. Pater[87], T. Pauly[32], B. Pearson[103], S. Pedraza Lopez[170], R. Pedro[128a,128b], S.V. Peleganchuk[111,c], O. Penc[129], C. Peng[35a], H. Peng[36a], J. Penwell[64], B.S. Peralva[26b], M.M. Perego[138], D.V. Perepelitsa[27], L. Perini[94a,94b], H. Pernegger[32], S. Perrella[106a,106b], R. Peschke[45], V.D. Peshekhonov[68,*], K. Peters[45], R.F.Y. Peters[87], B.A. Petersen[32], T.C. Petersen[39], E. Petit[58], A. Petridis[1], C. Petridou[156], P. Petroff[119], E. Petrolo[134a], M. Petrov[122], F. Petrucci[136a,136b], N.E. Pettersson[89], A. Peyaud[138], R. Pezoa[34b], F.H. Phillips[93], P.W. Phillips[133], G. Piacquadio[150], E. Pianori[173], A. Picazio[89], E. Piccaro[79], M.A. Pickering[122], R. Piegaia[29], J.E. Pilcher[33], A.D. Pilkington[87], A.W.J. Pin[87], M. Pinamonti[135a,135b], J.L. Pinfold[3], H. Pirumov[45], M. Pitt[175], L. Plazak[146a], M.-A. Pleier[27], V. Pleskot[86], E. Plotnikova[68], D. Pluth[67], P. Podberezko[111], R. Poettgen[148a,148b], R. Poggi[123a,123b], L. Poggioli[119], D. Pohl[23], G. Polesello[123a], A. Poley[45], A. Policicchio[40a,40b], R. Polifka[32], A. Polini[22a], C.S. Pollard[56], V. Polychronakos[27], K. Pommès[32], D. Ponomarenko[100], L. Pontecorvo[134a], B.G. Pope[93], G.A. Popeneciu[28d], A. Poppleton[32], S. Pospisil[130], K. Potamianos[16], I.N. Potrap[68], C.J. Potter[30], G. Poulard[32], T. Poulsen[84], J. Poveda[32], M.E. Pozo Astigarraga[32], P. Pralavorio[88], A. Pranko[16], S. Prell[67], D. Price[87], L.E. Price[6],

M. Primavera[76a], S. Prince[90], N. Proklova[100], K. Prokofiev[62c], F. Prokoshin[34b], S. Protopopescu[27], J. Proudfoot[6], M. Przybycien[41a], A. Puri[169], P. Puzo[119], J. Qian[92], G. Qin[56], Y. Qin[87], A. Quadt[57], M. Queitsch-Maitland[45], D. Quilty[56], S. Raddum[121], V. Radeka[27], V. Radescu[122], S.K. Radhakrishnan[150], P. Radloff[118], P. Rados[91], F. Ragusa[94a,94b], G. Rahal[182], J.A. Raine[87], S. Rajagopalan[27], C. Rangel-Smith[168], T. Rashid[119], M.G. Ratti[94a,94b], D.M. Rauch[45], F. Rauscher[102], S. Rave[86], I. Ravinovich[175], J.H. Rawling[87], M. Raymond[32], A.L. Read[121], N.P. Readioff[58], M. Reale[76a,76b], D.M. Rebuzzi[123a,123b], A. Redelbach[177], G. Redlinger[27], R. Reece[139], R.G. Reed[147c], K. Reeves[44], L. Rehnisch[17], J. Reichert[124], A. Reiss[86], C. Rembser[32], H. Ren[35a], M. Rescigno[134a], S. Resconi[94a], E.D. Resseguie[124], S. Rettie[171], E. Reynolds[19], O.L. Rezanova[111,c], P. Reznicek[131], R. Rezvani[97], R. Richter[103], S. Richter[81], E. Richter-Was[41b], O. Ricken[23], M. Ridel[83], P. Rieck[103], C.J. Riegel[178], J. Rieger[57], O. Rifki[115], M. Rijssenbeek[150], A. Rimoldi[123a,123b], M. Rimoldi[18], L. Rinaldi[22a], B. Ristić[52], E. Ritsch[32], I. Riu[13], F. Rizatdinova[116], E. Rizvi[79], C. Rizzi[13], R.T. Roberts[87], S.H. Robertson[90,o], A. Robichaud-Veronneau[90], D. Robinson[30], J.E.M. Robinson[45], A. Robson[56], E. Rocco[86], C. Roda[126a,126b], Y. Rodina[88,am], S. Rodriguez Bosca[170], A. Rodriguez Perez[13], D. Rodriguez Rodriguez[170], S. Roe[32], C.S. Rogan[59], O. Røhne[121], J. Roloff[59], A. Romaniouk[100], M. Romano[22a,22b], S.M. Romano Saez[37], E. Romero Adam[170], N. Rompotis[77], M. Ronzani[51], L. Roos[83], S. Rosati[134a], K. Rosbach[51], P. Rose[139], N.-A. Rosien[57], E. Rossi[106a,106b], L.P. Rossi[53a], J.H.N. Rosten[30], R. Rosten[140], M. Rotaru[28b], I. Roth[175], J. Rothberg[140], D. Rousseau[119], A. Rozanov[88], Y. Rozen[154], X. Ruan[147c], F. Rubbo[145], F. Rühr[51], A. Ruiz-Martinez[31], Z. Rurikova[51], N.A. Rusakovich[68], H.L. Russell[90], J.P. Rutherfoord[7], N. Ruthmann[32], Y.F. Ryabov[125], M. Rybar[169], G. Rybkin[119], S. Ryu[6], A. Ryzhov[132], G.F. Rzehorz[57], A.F. Saavedra[152], G. Sabato[109], S. Sacerdoti[29], H.F-W. Sadrozinski[139], R. Sadykov[68], F. Safai Tehrani[134a], P. Saha[110], M. Sahinsoy[60a], M. Saimpert[45], M. Saito[157], T. Saito[157], H. Sakamoto[157], Y. Sakurai[174], G. Salamanna[136a,136b], J.E. Salazar Loyola[34b], D. Salek[109], P.H. Sales De Bruin[168], D. Salihagic[103], A. Salnikov[145], J. Salt[170], D. Salvatore[40a,40b], F. Salvatore[151], A. Salvucci[62a,62b,62c], A. Salzburger[32], D. Sammel[51], D. Sampsonidis[156], D. Sampsonidou[156], J. Sánchez[170], V. Sanchez Martinez[170], A. Sanchez Pineda[167a,167c], H. Sandaker[121], R.L. Sandbach[79], C.O. Sander[45], M. Sandhoff[178], C. Sandoval[21], D.P.C. Sankey[133], M. Sannino[53a,53b], A. Sansoni[50], C. Santoni[37], R. Santonico[135a,135b], H. Santos[128a], I. Santoyo Castillo[151], A. Sapronov[68], J.G. Saraiva[128a,128d], B. Sarrazin[23], O. Sasaki[69], K. Sato[164], E. Sauvan[5], G. Savage[80], P. Savard[161,d], N. Savic[103], C. Sawyer[133], L. Sawyer[82,t], J. Saxon[33], C. Sbarra[22a], A. Sbrizzi[22a,22b], T. Scanlon[81], D.A. Scannicchio[166], M. Scarcella[152], V. Scarfone[40a,40b], J. Schaarschmidt[140], P. Schacht[103], B.M. Schachtner[102], D. Schaefer[32], L. Schaefer[124], R. Schaefer[45], J. Schaeffer[86], S. Schaepe[23], S. Schaetzel[60b], U. Schäfer[86], A.C. Schaffer[119], D. Schaile[102], R.D. Schamberger[150], V. Scharf[60a], V.A. Schegelsky[125], D. Scheirich[131], M. Schernau[166], C. Schiavi[53a,53b], S. Schier[139], L.K. Schildgen[23], C. Schillo[51], M. Schioppa[40a,40b], S. Schlenker[32], K.R. Schmidt-Sommerfeld[103], K. Schmieden[32], C. Schmitt[86], S. Schmitt[45], S. Schmitz[86], U. Schnoor[51], L. Schoeffel[138], A. Schoening[60b], B.D. Schoenrock[93], E. Schopf[23], M. Schott[86], J.F.P. Schouwenberg[108], J. Schovancova[181], S. Schramm[52], N. Schuh[86], A. Schulte[86], M.J. Schultens[23], H.-C. Schultz-Coulon[60a], H. Schulz[17], M. Schumacher[51], B.A. Schumm[139], Ph. Schune[138], A. Schwartzman[145], T.A. Schwarz[92], H. Schweiger[87], Ph. Schwemling[138], R. Schwienhorst[93], J. Schwindling[138], A. Sciandra[23], G. Sciolla[25], F. Scuri[126a,126b], F. Scutti[91], J. Searcy[92], P. Seema[23], S.C. Seidel[107], A. Seiden[139], J.M. Seixas[26a], G. Sekhniaidze[106a], K. Sekhon[92], S.J. Sekula[43], N. Semprini-Cesari[22a,22b], S. Senkin[37], C. Serfon[121], L. Serin[119], L. Serkin[167a,167b], M. Sessa[136a,136b], R. Seuster[172], H. Severini[115], T. Sfiligoj[78], F. Sforza[32], A. Sfyrla[52], E. Shabalina[57], N.W. Shaikh[148a,148b], L.Y. Shan[35a], R. Shang[169], J.T. Shank[24], M. Shapiro[16], P.B. Shatalov[99], K. Shaw[167a,167b], S.M. Shaw[87], A. Shcherbakova[148a,148b], C.Y. Shehu[151], Y. Shen[115], P. Sherwood[81], L. Shi[153,an], S. Shimizu[70], C.O. Shimmin[179], M. Shimojima[104], I.P.J. Shipsey[122], S. Shirabe[73], M. Shiyakova[68,ao], J. Shlomi[175], A. Shmeleva[98], D. Shoaleh Saadi[97], M.J. Shochet[33],

S. Shojaii[94a], D.R. Shope[115], S. Shrestha[113], E. Shulga[100], M.A. Shupe[7], P. Sicho[129], A.M. Sickles[169], P.E. Sidebo[149], E. Sideras Haddad[147c], O. Sidiropoulou[177], A. Sidoti[22a,22b], F. Siegert[47], Dj. Sijacki[14], J. Silva[128a,128d], S.B. Silverstein[148a], V. Simak[130], Lj. Simic[14], S. Simion[119], E. Simioni[86], B. Simmons[81], M. Simon[86], P. Sinervo[161], N.B. Sinev[118], M. Sioli[22a,22b], G. Siragusa[177], I. Siral[92], S.Yu. Sivoklokov[101], J. Sjölin[148a,148b], M.B. Skinner[75], P. Skubic[115], M. Slater[19], T. Slavicek[130], M. Slawinska[42], K. Sliwa[165], R. Slovak[131], V. Smakhtin[175], B.H. Smart[5], J. Smiesko[146a], N. Smirnov[100], S.Yu. Smirnov[100], Y. Smirnov[100], L.N. Smirnova[101,*ap*], O. Smirnova[84], J.W. Smith[57], M.N.K. Smith[38], R.W. Smith[38], M. Smizanska[75], K. Smolek[130], A.A. Snesarev[98], I.M. Snyder[118], S. Snyder[27], R. Sobie[172,*o*], F. Socher[47], A. Soffer[155], D.A. Soh[153], G. Sokhrannyi[78], C.A. Solans Sanchez[32], M. Solar[130], E.Yu. Soldatov[100], U. Soldevila[170], A.A. Solodkov[132], A. Soloshenko[68], O.V. Solovyanov[132], V. Solovyev[125], P. Sommer[51], H. Son[165], H.Y. Song[36a,*aq*], A. Sopczak[130], D. Sosa[60b], C.L. Sotiropoulou[126a,126b], R. Soualah[167a,167c], A.M. Soukharev[111,*c*], D. South[45], B.C. Sowden[80], S. Spagnolo[76a,76b], M. Spalla[126a,126b], M. Spangenberg[173], F. Spanò[80], D. Sperlich[17], F. Spettel[103], T.M. Spieker[60a], R. Spighi[22a], G. Spigo[32], L.A. Spiller[91], M. Spousta[131], R.D. St. Denis[56,*], A. Stabile[94a], R. Stamen[60a], S. Stamm[17], E. Stanecka[42], R.W. Stanek[6], C. Stanescu[136a], M.M. Stanitzki[45], S. Stapnes[121], E.A. Starchenko[132], G.H. Stark[33], J. Stark[58], S.H Stark[39], P. Staroba[129], P. Starovoitov[60a], S. Stärz[32], R. Staszewski[42], P. Steinberg[27], B. Stelzer[144], H.J. Stelzer[32], O. Stelzer-Chilton[163a], H. Stenzel[55], G.A. Stewart[56], M.C. Stockton[118], M. Stoebe[90], G. Stoicea[28b], P. Stolte[57], S. Stonjek[103], A.R. Stradling[8], A. Straessner[47], M.E. Stramaglia[18], J. Strandberg[149], S. Strandberg[148a,148b], A. Strandlie[121], M. Strauss[115], P. Strizenec[146b], R. Ströhmer[177], D.M. Strom[118], R. Stroynowski[43], A. Strubig[108], S.A. Stucci[27], B. Stugu[15], N.A. Styles[45], D. Su[145], J. Su[127], S. Suchek[60a], Y. Sugaya[120], M. Suk[130], V.V. Sulin[98], S. Sultansoy[4c], T. Sumida[71], S. Sun[59], X. Sun[3], K. Suruliz[151], C.J.E. Suster[152], M.R. Sutton[151], S. Suzuki[69], M. Svatos[129], M. Swiatlowski[33], S.P. Swift[2], I. Sykora[146a], T. Sykora[131], D. Ta[51], K. Tackmann[45], J. Taenzer[155], A. Taffard[166], R. Tafirout[163a], N. Taiblum[155], H. Takai[27], R. Takashima[72], T. Takeshita[142], Y. Takubo[69], M. Talby[88], A.A. Talyshev[111,*c*], J. Tanaka[157], M. Tanaka[159], R. Tanaka[119], S. Tanaka[69], R. Tanioka[70], B.B. Tannenwald[113], S. Tapia Araya[34b], S. Tapprogge[86], S. Tarem[154], G.F. Tartarelli[94a], P. Tas[131], M. Tasevsky[129], T. Tashiro[71], E. Tassi[40a,40b], A. Tavares Delgado[128a,128b], Y. Tayalati[137e], A.C. Taylor[107], G.N. Taylor[91], P.T.E. Taylor[91], W. Taylor[163b], P. Teixeira-Dias[80], D. Temple[144], H. Ten Kate[32], P.K. Teng[153], J.J. Teoh[120], F. Tepel[178], S. Terada[69], K. Terashi[157], J. Terron[85], S. Terzo[13], M. Testa[50], R.J. Teuscher[161,*o*], T. Theveneaux-Pelzer[88], J.P. Thomas[19], J. Thomas-Wilsker[80], P.D. Thompson[19], A.S. Thompson[56], L.A. Thomsen[179], E. Thomson[124], M.J. Tibbetts[16], R.E. Ticse Torres[88], V.O. Tikhomirov[98,*ar*], Yu.A. Tikhonov[111,*c*], S. Timoshenko[100], P. Tipton[179], S. Tisserant[88], K. Todome[159], S. Todorova-Nova[5], J. Tojo[73], S. Tokár[146a], K. Tokushuku[69], E. Tolley[59], L. Tomlinson[87], M. Tomoto[105], L. Tompkins[145,*as*], K. Toms[107], B. Tong[59], P. Tornambe[51], E. Torrence[118], H. Torres[144], E. Torró Pastor[140], J. Toth[88,*at*], F. Touchard[88], D.R. Tovey[141], C.J. Treado[112], T. Trefzger[177], F. Tresoldi[151], A. Tricoli[27], I.M. Trigger[163a], S. Trincaz-Duvoid[83], M.F. Tripiana[13], W. Trischuk[161], B. Trocmé[58], A. Trofymov[45], C. Troncon[94a], M. Trottier-McDonald[16], M. Trovatelli[172], L. Truong[167a,167c], M. Trzebinski[42], A. Trzupek[42], K.W. Tsang[62a], J.C-L. Tseng[122], P.V. Tsiareshka[95], G. Tsipolitis[10], N. Tsirintanis[9], S. Tsiskaridze[13], V. Tsiskaridze[51], E.G. Tskhadadze[54a], K.M. Tsui[62a], I.I. Tsukerman[99], V. Tsulaia[16], S. Tsuno[69], D. Tsybychev[150], Y. Tu[62b], A. Tudorache[28b], V. Tudorache[28b], T.T. Tulbure[28a], A.N. Tuna[59], S.A. Tupputi[22a,22b], S. Turchikhin[68], D. Turgeman[175], I. Turk Cakir[4b,*au*], R. Turra[94a], P.M. Tuts[38], G. Ucchielli[22a,22b], I. Ueda[69], M. Ughetto[148a,148b], F. Ukegawa[164], G. Unal[32], A. Undrus[27], G. Unel[166], F.C. Ungaro[91], Y. Unno[69], C. Unverdorben[102], J. Urban[146b], P. Urquijo[91], P. Urrejola[86], G. Usai[8], J. Usui[69], L. Vacavant[88], V. Vacek[130], B. Vachon[90], C. Valderanis[102], E. Valdes Santurio[148a,148b], S. Valentinetti[22a,22b], A. Valero[170], L. Valéry[13], S. Valkar[131], A. Vallier[5], J.A. Valls Ferrer[170], W. Van Den Wollenberg[109], H. van der Graaf[109],

P. van Gemmeren[6], J. Van Nieuwkoop[144], I. van Vulpen[109], M.C. van Woerden[109], M. Vanadia[135a,135b], W. Vandelli[32], A. Vaniachine[160], P. Vankov[109], G. Vardanyan[180], R. Vari[134a], E.W. Varnes[7], C. Varni[53a,53b], T. Varol[43], D. Varouchas[119], A. Vartapetian[8], K.E. Varvell[152], J.G. Vasquez[179], G.A. Vasquez[34b], F. Vazeille[37], T. Vazquez Schroeder[90], J. Veatch[57], V. Veeraraghavan[7], L.M. Veloce[161], F. Veloso[128a,128c], S. Veneziano[134a], A. Ventura[76a,76b], M. Venturi[172], N. Venturi[161], A. Venturini[25], V. Vercesi[123a], M. Verducci[136a,136b], W. Verkerke[109], J.C. Vermeulen[109], M.C. Vetterli[144,d], N. Viaux Maira[34b], O. Viazlo[84], I. Vichou[169,*], T. Vickey[141], O.E. Vickey Boeriu[141], G.H.A. Viehhauser[122], S. Viel[16], L. Vigani[122], M. Villa[22a,22b], M. Villaplana Perez[94a,94b], E. Vilucchi[50], M.G. Vincter[31], V.B. Vinogradov[68], A. Vishwakarma[45], C. Vittori[22a,22b], I. Vivarelli[151], S. Vlachos[10], M. Vlasak[130], M. Vogel[178], P. Vokac[130], G. Volpi[126a,126b], H. von der Schmitt[103], E. von Toerne[23], V. Vorobel[131], K. Vorobev[100], M. Vos[170], R. Voss[32], J.H. Vossebeld[77], N. Vranjes[14], M. Vranjes Milosavljevic[14], V. Vrba[130], M. Vreeswijk[109], R. Vuillermet[32], I. Vukotic[33], P. Wagner[23], W. Wagner[178], J. Wagner-Kuhr[102], H. Wahlberg[74], S. Wahrmund[47], J. Wakabayashi[105], J. Walder[75], R. Walker[102], W. Walkowiak[143], V. Wallangen[148a,148b], C. Wang[35b], C. Wang[36b,av], F. Wang[176], H. Wang[16], H. Wang[3], J. Wang[45], J. Wang[152], Q. Wang[115], R. Wang[6], S.M. Wang[153], T. Wang[38], W. Wang[153,aw], W. Wang[36a], Z. Wang[36c], C. Wanotayaroj[118], A. Warburton[90], C.P. Ward[30], D.R. Wardrope[81], A. Washbrook[49], P.M. Watkins[19], A.T. Watson[19], M.F. Watson[19], G. Watts[140], S. Watts[87], B.M. Waugh[81], A.F. Webb[11], S. Webb[86], M.S. Weber[18], S.W. Weber[177], S.A. Weber[31], J.S. Webster[6], A.R. Weidberg[122], B. Weinert[64], J. Weingarten[57], M. Weirich[86], C. Weiser[51], H. Weits[109], P.S. Wells[32], T. Wenaus[27], T. Wengler[32], S. Wenig[32], N. Wermes[23], M.D. Werner[67], P. Werner[32], M. Wessels[60a], K. Whalen[118], N.L. Whallon[140], A.M. Wharton[75], A.S. White[92], A. White[8], M.J. White[1], R. White[34b], D. Whiteson[166], F.J. Wickens[133], W. Wiedenmann[176], M. Wielers[133], C. Wiglesworth[39], L.A.M. Wiik-Fuchs[23], A. Wildauer[103], F. Wilk[87], H.G. Wilkens[32], H.H. Williams[124], S. Williams[109], C. Willis[93], S. Willocq[89], J.A. Wilson[19], I. Wingerter-Seez[5], E. Winkels[151], F. Winklmeier[118], O.J. Winston[151], B.T. Winter[23], M. Wittgen[145], M. Wobisch[82,t], T.M.H. Wolf[109], R. Wolff[88], M.W. Wolter[42], H. Wolters[128a,128c], V.W.S. Wong[171], S.D. Worm[19], B.K. Wosiek[42], J. Wotschack[32], K.W. Wozniak[42], M. Wu[33], S.L. Wu[176], X. Wu[52], Y. Wu[92], T.R. Wyatt[87], B.M. Wynne[49], S. Xella[39], Z. Xi[92], L. Xia[35c], D. Xu[35a], L. Xu[27], B. Yabsley[152], S. Yacoob[147a], D. Yamaguchi[159], Y. Yamaguchi[120], A. Yamamoto[69], S. Yamamoto[157], T. Yamanaka[157], K. Yamauchi[105], Y. Yamazaki[70], Z. Yan[24], H. Yang[36c], H. Yang[16], Y. Yang[153], Z. Yang[15], W-M. Yao[16], Y.C. Yap[83], Y. Yasu[69], E. Yatsenko[5], K.H. Yau Wong[23], J. Ye[43], S. Ye[27], I. Yeletskikh[68], E. Yigitbasi[24], E. Yildirim[86], K. Yorita[174], K. Yoshihara[124], C. Young[145], C.J.S. Young[32], D.R. Yu[16], J. Yu[8], J. Yu[67], S.P.Y. Yuen[23], I. Yusuff[30,ax], B. Zabinski[42], G. Zacharis[10], R. Zaidan[13], A.M. Zaitsev[132,ak], N. Zakharchuk[45], J. Zalieckas[15], A. Zaman[150], S. Zambito[59], D. Zanzi[91], C. Zeitnitz[178], A. Zemla[41a], J.C. Zeng[169], Q. Zeng[145], O. Zenin[132], T. Ženiš[146a], D. Zerwas[119], D. Zhang[92], F. Zhang[176], G. Zhang[36a,aq], H. Zhang[35b], J. Zhang[6], L. Zhang[51], L. Zhang[36a], M. Zhang[169], P. Zhang[35b], R. Zhang[23], R. Zhang[36a,av], X. Zhang[36b], Y. Zhang[35a], Z. Zhang[119], X. Zhao[43], Y. Zhao[36b,ay], Z. Zhao[36a], A. Zhemchugov[68], B. Zhou[92], C. Zhou[176], L. Zhou[43], M. Zhou[35a], M. Zhou[150], N. Zhou[35c], C.G. Zhu[36b], H. Zhu[35a], J. Zhu[92], Y. Zhu[36a], X. Zhuang[35a], K. Zhukov[98], A. Zibell[177], D. Zieminska[64], N.I. Zimine[68], C. Zimmermann[86], S. Zimmermann[51], Z. Zinonos[103], M. Zinser[86], M. Ziolkowski[143], L. Živković[14], G. Zobernig[176], A. Zoccoli[22a,22b], R. Zou[33], M. zur Nedden[17], L. Zwalinski[32].

[1] Department of Physics, University of Adelaide, Adelaide, Australia

[2] Physics Department, SUNY Albany, Albany NY, United States of America

[3] Department of Physics, University of Alberta, Edmonton AB, Canada

[4] (a) Department of Physics, Ankara University, Ankara; (b) Istanbul Aydin University, Istanbul; (c) Division of Physics, TOBB University of Economics and Technology, Ankara, Turkey

[5] LAPP, CNRS/IN2P3 and Université Savoie Mont Blanc, Annecy-le-Vieux, France
[6] High Energy Physics Division, Argonne National Laboratory, Argonne IL, United States of America
[7] Department of Physics, University of Arizona, Tucson AZ, United States of America
[8] Department of Physics, The University of Texas at Arlington, Arlington TX, United States of America
[9] Physics Department, National and Kapodistrian University of Athens, Athens, Greece
[10] Physics Department, National Technical University of Athens, Zografou, Greece
[11] Department of Physics, The University of Texas at Austin, Austin TX, United States of America
[12] Institute of Physics, Azerbaijan Academy of Sciences, Baku, Azerbaijan
[13] Institut de Física d'Altes Energies (IFAE), The Barcelona Institute of Science and Technology, Barcelona, Spain
[14] Institute of Physics, University of Belgrade, Belgrade, Serbia
[15] Department for Physics and Technology, University of Bergen, Bergen, Norway
[16] Physics Division, Lawrence Berkeley National Laboratory and University of California, Berkeley CA, United States of America
[17] Department of Physics, Humboldt University, Berlin, Germany
[18] Albert Einstein Center for Fundamental Physics and Laboratory for High Energy Physics, University of Bern, Bern, Switzerland
[19] School of Physics and Astronomy, University of Birmingham, Birmingham, United Kingdom
[20] [(a)] Department of Physics, Bogazici University, Istanbul; [(b)] Department of Physics Engineering, Gaziantep University, Gaziantep; [(d)] Istanbul Bilgi University, Faculty of Engineering and Natural Sciences, Istanbul; [(e)] Bahcesehir University, Faculty of Engineering and Natural Sciences, Istanbul, Turkey
[21] Centro de Investigaciones, Universidad Antonio Narino, Bogota, Colombia
[22] [(a)] INFN Sezione di Bologna; [(b)] Dipartimento di Fisica e Astronomia, Università di Bologna, Bologna, Italy
[23] Physikalisches Institut, University of Bonn, Bonn, Germany
[24] Department of Physics, Boston University, Boston MA, United States of America
[25] Department of Physics, Brandeis University, Waltham MA, United States of America
[26] [(a)] Universidade Federal do Rio De Janeiro COPPE/EE/IF, Rio de Janeiro; [(b)] Electrical Circuits Department, Federal University of Juiz de Fora (UFJF), Juiz de Fora; [(c)] Federal University of Sao Joao del Rei (UFSJ), Sao Joao del Rei; [(d)] Instituto de Fisica, Universidade de Sao Paulo, Sao Paulo, Brazil
[27] Physics Department, Brookhaven National Laboratory, Upton NY, United States of America
[28] [(a)] Transilvania University of Brasov, Brasov; [(b)] Horia Hulubei National Institute of Physics and Nuclear Engineering, Bucharest; [(c)] Department of Physics, Alexandru Ioan Cuza University of Iasi, Iasi; [(d)] National Institute for Research and Development of Isotopic and Molecular Technologies, Physics Department, Cluj Napoca; [(e)] University Politehnica Bucharest, Bucharest; [(f)] West University in Timisoara, Timisoara, Romania
[29] Departamento de Física, Universidad de Buenos Aires, Buenos Aires, Argentina
[30] Cavendish Laboratory, University of Cambridge, Cambridge, United Kingdom
[31] Department of Physics, Carleton University, Ottawa ON, Canada
[32] CERN, Geneva, Switzerland
[33] Enrico Fermi Institute, University of Chicago, Chicago IL, United States of America
[34] [(a)] Departamento de Física, Pontificia Universidad Católica de Chile, Santiago; [(b)] Departamento de Física, Universidad Técnica Federico Santa María, Valparaíso, Chile
[35] [(a)] Institute of High Energy Physics, Chinese Academy of Sciences, Beijing; [(b)] Department of Physics, Nanjing University, Jiangsu; [(c)] Physics Department, Tsinghua University, Beijing 100084, China

[36] [(a)] Department of Modern Physics and State Key Laboratory of Particle Detection and Electronics, University of Science and Technology of China, Anhui; [(b)] School of Physics, Shandong University, Shandong; [(c)] Department of Physics and Astronomy, Key Laboratory for Particle Physics, Astrophysics and Cosmology, Ministry of Education; Shanghai Key Laboratory for Particle Physics and Cosmology, Shanghai Jiao Tong University, Shanghai(also at PKU-CHEP);, China
[37] Université Clermont Auvergne, CNRS/IN2P3, LPC, Clermont-Ferrand, France
[38] Nevis Laboratory, Columbia University, Irvington NY, United States of America
[39] Niels Bohr Institute, University of Copenhagen, Kobenhavn, Denmark
[40] [(a)] INFN Gruppo Collegato di Cosenza, Laboratori Nazionali di Frascati; [(b)] Dipartimento di Fisica, Università della Calabria, Rende, Italy
[41] [(a)] AGH University of Science and Technology, Faculty of Physics and Applied Computer Science, Krakow; [(b)] Marian Smoluchowski Institute of Physics, Jagiellonian University, Krakow, Poland
[42] Institute of Nuclear Physics Polish Academy of Sciences, Krakow, Poland
[43] Physics Department, Southern Methodist University, Dallas TX, United States of America
[44] Physics Department, University of Texas at Dallas, Richardson TX, United States of America
[45] DESY, Hamburg and Zeuthen, Germany
[46] Lehrstuhl für Experimentelle Physik IV, Technische Universität Dortmund, Dortmund, Germany
[47] Institut für Kern- und Teilchenphysik, Technische Universität Dresden, Dresden, Germany
[48] Department of Physics, Duke University, Durham NC, United States of America
[49] SUPA - School of Physics and Astronomy, University of Edinburgh, Edinburgh, United Kingdom
[50] INFN e Laboratori Nazionali di Frascati, Frascati, Italy
[51] Fakultät für Mathematik und Physik, Albert-Ludwigs-Universität, Freiburg, Germany
[52] Departement de Physique Nucleaire et Corpusculaire, Université de Genève, Geneva, Switzerland
[53] [(a)] INFN Sezione di Genova; [(b)] Dipartimento di Fisica, Università di Genova, Genova, Italy
[54] [(a)] E. Andronikashvili Institute of Physics, Iv. Javakhishvili Tbilisi State University, Tbilisi; [(b)] High Energy Physics Institute, Tbilisi State University, Tbilisi, Georgia
[55] II Physikalisches Institut, Justus-Liebig-Universität Giessen, Giessen, Germany
[56] SUPA - School of Physics and Astronomy, University of Glasgow, Glasgow, United Kingdom
[57] II Physikalisches Institut, Georg-August-Universität, Göttingen, Germany
[58] Laboratoire de Physique Subatomique et de Cosmologie, Université Grenoble-Alpes, CNRS/IN2P3, Grenoble, France
[59] Laboratory for Particle Physics and Cosmology, Harvard University, Cambridge MA, United States of America
[60] [(a)] Kirchhoff-Institut für Physik, Ruprecht-Karls-Universität Heidelberg, Heidelberg; [(b)] Physikalisches Institut, Ruprecht-Karls-Universität Heidelberg, Heidelberg; [(c)] ZITI Institut für technische Informatik, Ruprecht-Karls-Universität Heidelberg, Mannheim, Germany
[61] Faculty of Applied Information Science, Hiroshima Institute of Technology, Hiroshima, Japan
[62] [(a)] Department of Physics, The Chinese University of Hong Kong, Shatin, N.T., Hong Kong; [(b)] Department of Physics, The University of Hong Kong, Hong Kong; [(c)] Department of Physics and Institute for Advanced Study, The Hong Kong University of Science and Technology, Clear Water Bay, Kowloon, Hong Kong, China
[63] Department of Physics, National Tsing Hua University, Taiwan, Taiwan
[64] Department of Physics, Indiana University, Bloomington IN, United States of America
[65] Institut für Astro- und Teilchenphysik, Leopold-Franzens-Universität, Innsbruck, Austria
[66] University of Iowa, Iowa City IA, United States of America
[67] Department of Physics and Astronomy, Iowa State University, Ames IA, United States of America
[68] Joint Institute for Nuclear Research, JINR Dubna, Dubna, Russia

[69] KEK, High Energy Accelerator Research Organization, Tsukuba, Japan
[70] Graduate School of Science, Kobe University, Kobe, Japan
[71] Faculty of Science, Kyoto University, Kyoto, Japan
[72] Kyoto University of Education, Kyoto, Japan
[73] Research Center for Advanced Particle Physics and Department of Physics, Kyushu University, Fukuoka, Japan
[74] Instituto de Física La Plata, Universidad Nacional de La Plata and CONICET, La Plata, Argentina
[75] Physics Department, Lancaster University, Lancaster, United Kingdom
[76] [(a)] INFN Sezione di Lecce; [(b)] Dipartimento di Matematica e Fisica, Università del Salento, Lecce, Italy
[77] Oliver Lodge Laboratory, University of Liverpool, Liverpool, United Kingdom
[78] Department of Experimental Particle Physics, Jožef Stefan Institute and Department of Physics, University of Ljubljana, Ljubljana, Slovenia
[79] School of Physics and Astronomy, Queen Mary University of London, London, United Kingdom
[80] Department of Physics, Royal Holloway University of London, Surrey, United Kingdom
[81] Department of Physics and Astronomy, University College London, London, United Kingdom
[82] Louisiana Tech University, Ruston LA, United States of America
[83] Laboratoire de Physique Nucléaire et de Hautes Energies, UPMC and Université Paris-Diderot and CNRS/IN2P3, Paris, France
[84] Fysiska institutionen, Lunds universitet, Lund, Sweden
[85] Departamento de Fisica Teorica C-15, Universidad Autonoma de Madrid, Madrid, Spain
[86] Institut für Physik, Universität Mainz, Mainz, Germany
[87] School of Physics and Astronomy, University of Manchester, Manchester, United Kingdom
[88] CPPM, Aix-Marseille Université and CNRS/IN2P3, Marseille, France
[89] Department of Physics, University of Massachusetts, Amherst MA, United States of America
[90] Department of Physics, McGill University, Montreal QC, Canada
[91] School of Physics, University of Melbourne, Victoria, Australia
[92] Department of Physics, The University of Michigan, Ann Arbor MI, United States of America
[93] Department of Physics and Astronomy, Michigan State University, East Lansing MI, United States of America
[94] [(a)] INFN Sezione di Milano; [(b)] Dipartimento di Fisica, Università di Milano, Milano, Italy
[95] B.I. Stepanov Institute of Physics, National Academy of Sciences of Belarus, Minsk, Republic of Belarus
[96] Research Institute for Nuclear Problems of Byelorussian State University, Minsk, Republic of Belarus
[97] Group of Particle Physics, University of Montreal, Montreal QC, Canada
[98] P.N. Lebedev Physical Institute of the Russian Academy of Sciences, Moscow, Russia
[99] Institute for Theoretical and Experimental Physics (ITEP), Moscow, Russia
[100] National Research Nuclear University MEPhI, Moscow, Russia
[101] D.V. Skobeltsyn Institute of Nuclear Physics, M.V. Lomonosov Moscow State University, Moscow, Russia
[102] Fakultät für Physik, Ludwig-Maximilians-Universität München, München, Germany
[103] Max-Planck-Institut für Physik (Werner-Heisenberg-Institut), München, Germany
[104] Nagasaki Institute of Applied Science, Nagasaki, Japan
[105] Graduate School of Science and Kobayashi-Maskawa Institute, Nagoya University, Nagoya, Japan
[106] [(a)] INFN Sezione di Napoli; [(b)] Dipartimento di Fisica, Università di Napoli, Napoli, Italy
[107] Department of Physics and Astronomy, University of New Mexico, Albuquerque NM, United States of America

[108] Institute for Mathematics, Astrophysics and Particle Physics, Radboud University Nijmegen/Nikhef, Nijmegen, Netherlands
[109] Nikhef National Institute for Subatomic Physics and University of Amsterdam, Amsterdam, Netherlands
[110] Department of Physics, Northern Illinois University, DeKalb IL, United States of America
[111] Budker Institute of Nuclear Physics, SB RAS, Novosibirsk, Russia
[112] Department of Physics, New York University, New York NY, United States of America
[113] Ohio State University, Columbus OH, United States of America
[114] Faculty of Science, Okayama University, Okayama, Japan
[115] Homer L. Dodge Department of Physics and Astronomy, University of Oklahoma, Norman OK, United States of America
[116] Department of Physics, Oklahoma State University, Stillwater OK, United States of America
[117] Palacký University, RCPTM, Olomouc, Czech Republic
[118] Center for High Energy Physics, University of Oregon, Eugene OR, United States of America
[119] LAL, Univ. Paris-Sud, CNRS/IN2P3, Université Paris-Saclay, Orsay, France
[120] Graduate School of Science, Osaka University, Osaka, Japan
[121] Department of Physics, University of Oslo, Oslo, Norway
[122] Department of Physics, Oxford University, Oxford, United Kingdom
[123] [(a)] INFN Sezione di Pavia; [(b)] Dipartimento di Fisica, Università di Pavia, Pavia, Italy
[124] Department of Physics, University of Pennsylvania, Philadelphia PA, United States of America
[125] National Research Centre "Kurchatov Institute" B.P.Konstantinov Petersburg Nuclear Physics Institute, St. Petersburg, Russia
[126] [(a)] INFN Sezione di Pisa; [(b)] Dipartimento di Fisica E. Fermi, Università di Pisa, Pisa, Italy
[127] Department of Physics and Astronomy, University of Pittsburgh, Pittsburgh PA, United States of America
[128] [(a)] Laboratório de Instrumentação e Física Experimental de Partículas - LIP, Lisboa; [(b)] Faculdade de Ciências, Universidade de Lisboa, Lisboa; [(c)] Department of Physics, University of Coimbra, Coimbra; [(d)] Centro de Física Nuclear da Universidade de Lisboa, Lisboa; [(e)] Departamento de Fisica, Universidade do Minho, Braga; [(f)] Departamento de Fisica Teorica y del Cosmos and CAFPE, Universidad de Granada, Granada; [(g)] Dep Fisica and CEFITEC of Faculdade de Ciencias e Tecnologia, Universidade Nova de Lisboa, Caparica, Portugal
[129] Institute of Physics, Academy of Sciences of the Czech Republic, Praha, Czech Republic
[130] Czech Technical University in Prague, Praha, Czech Republic
[131] Charles University, Faculty of Mathematics and Physics, Prague, Czech Republic
[132] State Research Center Institute for High Energy Physics (Protvino), NRC KI, Russia
[133] Particle Physics Department, Rutherford Appleton Laboratory, Didcot, United Kingdom
[134] [(a)] INFN Sezione di Roma; [(b)] Dipartimento di Fisica, Sapienza Università di Roma, Roma, Italy
[135] [(a)] INFN Sezione di Roma Tor Vergata; [(b)] Dipartimento di Fisica, Università di Roma Tor Vergata, Roma, Italy
[136] [(a)] INFN Sezione di Roma Tre; [(b)] Dipartimento di Matematica e Fisica, Università Roma Tre, Roma, Italy
[137] [(a)] Faculté des Sciences Ain Chock, Réseau Universitaire de Physique des Hautes Energies - Université Hassan II, Casablanca; [(b)] Centre National de l'Energie des Sciences Techniques Nucleaires, Rabat; [(c)] Faculté des Sciences Semlalia, Université Cadi Ayyad, LPHEA-Marrakech; [(d)] Faculté des Sciences, Université Mohamed Premier and LPTPM, Oujda; [(e)] Faculté des sciences, Université Mohammed V, Rabat, Morocco
[138] DSM/IRFU (Institut de Recherches sur les Lois Fondamentales de l'Univers), CEA Saclay

(Commissariat à l'Energie Atomique et aux Energies Alternatives), Gif-sur-Yvette, France
[139] Santa Cruz Institute for Particle Physics, University of California Santa Cruz, Santa Cruz CA, United States of America
[140] Department of Physics, University of Washington, Seattle WA, United States of America
[141] Department of Physics and Astronomy, University of Sheffield, Sheffield, United Kingdom
[142] Department of Physics, Shinshu University, Nagano, Japan
[143] Department Physik, Universität Siegen, Siegen, Germany
[144] Department of Physics, Simon Fraser University, Burnaby BC, Canada
[145] SLAC National Accelerator Laboratory, Stanford CA, United States of America
[146] [(a)] Faculty of Mathematics, Physics & Informatics, Comenius University, Bratislava; [(b)] Department of Subnuclear Physics, Institute of Experimental Physics of the Slovak Academy of Sciences, Kosice, Slovak Republic
[147] [(a)] Department of Physics, University of Cape Town, Cape Town; [(b)] Department of Physics, University of Johannesburg, Johannesburg; [(c)] School of Physics, University of the Witwatersrand, Johannesburg, South Africa
[148] [(a)] Department of Physics, Stockholm University; [(b)] The Oskar Klein Centre, Stockholm, Sweden
[149] Physics Department, Royal Institute of Technology, Stockholm, Sweden
[150] Departments of Physics & Astronomy and Chemistry, Stony Brook University, Stony Brook NY, United States of America
[151] Department of Physics and Astronomy, University of Sussex, Brighton, United Kingdom
[152] School of Physics, University of Sydney, Sydney, Australia
[153] Institute of Physics, Academia Sinica, Taipei, Taiwan
[154] Department of Physics, Technion: Israel Institute of Technology, Haifa, Israel
[155] Raymond and Beverly Sackler School of Physics and Astronomy, Tel Aviv University, Tel Aviv, Israel
[156] Department of Physics, Aristotle University of Thessaloniki, Thessaloniki, Greece
[157] International Center for Elementary Particle Physics and Department of Physics, The University of Tokyo, Tokyo, Japan
[158] Graduate School of Science and Technology, Tokyo Metropolitan University, Tokyo, Japan
[159] Department of Physics, Tokyo Institute of Technology, Tokyo, Japan
[160] Tomsk State University, Tomsk, Russia
[161] Department of Physics, University of Toronto, Toronto ON, Canada
[162] [(a)] INFN-TIFPA; [(b)] University of Trento, Trento, Italy
[163] [(a)] TRIUMF, Vancouver BC; [(b)] Department of Physics and Astronomy, York University, Toronto ON, Canada
[164] Faculty of Pure and Applied Sciences, and Center for Integrated Research in Fundamental Science and Engineering, University of Tsukuba, Tsukuba, Japan
[165] Department of Physics and Astronomy, Tufts University, Medford MA, United States of America
[166] Department of Physics and Astronomy, University of California Irvine, Irvine CA, United States of America
[167] [(a)] INFN Gruppo Collegato di Udine, Sezione di Trieste, Udine; [(b)] ICTP, Trieste; [(c)] Dipartimento di Chimica, Fisica e Ambiente, Università di Udine, Udine, Italy
[168] Department of Physics and Astronomy, University of Uppsala, Uppsala, Sweden
[169] Department of Physics, University of Illinois, Urbana IL, United States of America
[170] Instituto de Fisica Corpuscular (IFIC), Centro Mixto Universidad de Valencia - CSIC, Spain
[171] Department of Physics, University of British Columbia, Vancouver BC, Canada
[172] Department of Physics and Astronomy, University of Victoria, Victoria BC, Canada

[173] Department of Physics, University of Warwick, Coventry, United Kingdom
[174] Waseda University, Tokyo, Japan
[175] Department of Particle Physics, The Weizmann Institute of Science, Rehovot, Israel
[176] Department of Physics, University of Wisconsin, Madison WI, United States of America
[177] Fakultät für Physik und Astronomie, Julius-Maximilians-Universität, Würzburg, Germany
[178] Fakultät für Mathematik und Naturwissenschaften, Fachgruppe Physik, Bergische Universität Wuppertal, Wuppertal, Germany
[179] Department of Physics, Yale University, New Haven CT, United States of America
[180] Yerevan Physics Institute, Yerevan, Armenia
[181] CH-1211 Geneva 23, Switzerland
[182] Centre de Calcul de l'Institut National de Physique Nucléaire et de Physique des Particules (IN2P3), Villeurbanne, France
[a] Also at Department of Physics, King's College London, London, United Kingdom
[b] Also at Institute of Physics, Azerbaijan Academy of Sciences, Baku, Azerbaijan
[c] Also at Novosibirsk State University, Novosibirsk, Russia
[d] Also at TRIUMF, Vancouver BC, Canada
[e] Also at Department of Physics & Astronomy, University of Louisville, Louisville, KY, United States of America
[f] Also at Physics Department, An-Najah National University, Nablus, Palestine
[g] Also at Department of Physics, California State University, Fresno CA, United States of America
[h] Also at Department of Physics, University of Fribourg, Fribourg, Switzerland
[i] Also at II Physikalisches Institut, Georg-August-Universität, Göttingen, Germany
[j] Also at Departament de Fisica de la Universitat Autonoma de Barcelona, Barcelona, Spain
[k] Also at Departamento de Fisica e Astronomia, Faculdade de Ciencias, Universidade do Porto, Portugal
[l] Also at Tomsk State University, Tomsk, Russia
[m] Also at The Collaborative Innovation Center of Quantum Matter (CICQM), Beijing, China
[n] Also at Universita di Napoli Parthenope, Napoli, Italy
[o] Also at Institute of Particle Physics (IPP), Canada
[p] Also at Horia Hulubei National Institute of Physics and Nuclear Engineering, Bucharest, Romania
[q] Also at Department of Physics, St. Petersburg State Polytechnical University, St. Petersburg, Russia
[r] Also at Borough of Manhattan Community College, City University of New York, New York City, United States of America
[s] Also at Centre for High Performance Computing, CSIR Campus, Rosebank, Cape Town, South Africa
[t] Also at Louisiana Tech University, Ruston LA, United States of America
[u] Also at Institucio Catalana de Recerca i Estudis Avancats, ICREA, Barcelona, Spain
[v] Also at Graduate School of Science, Osaka University, Osaka, Japan
[w] Also at Fakultät für Mathematik und Physik, Albert-Ludwigs-Universität, Freiburg, Germany
[x] Also at Institute for Mathematics, Astrophysics and Particle Physics, Radboud University Nijmegen/Nikhef, Nijmegen, Netherlands
[y] Also at Department of Physics, The University of Texas at Austin, Austin TX, United States of America
[z] Also at Institute of Theoretical Physics, Ilia State University, Tbilisi, Georgia
[aa] Also at CERN, Geneva, Switzerland
[ab] Also at Georgian Technical University (GTU),Tbilisi, Georgia
[ac] Also at Ochadai Academic Production, Ochanomizu University, Tokyo, Japan
[ad] Also at Manhattan College, New York NY, United States of America
[ae] Also at Departamento de Física, Pontificia Universidad Católica de Chile, Santiago, Chile

[af] Also at Department of Physics, The University of Michigan, Ann Arbor MI, United States of America
[ag] Also at Academia Sinica Grid Computing, Institute of Physics, Academia Sinica, Taipei, Taiwan
[ah] Also at School of Physics, Shandong University, Shandong, China
[ai] Also at Departamento de Fisica Teorica y del Cosmos and CAFPE, Universidad de Granada, Granada, Portugal
[aj] Also at Department of Physics, California State University, Sacramento CA, United States of America
[ak] Also at Moscow Institute of Physics and Technology State University, Dolgoprudny, Russia
[al] Also at Departement de Physique Nucleaire et Corpusculaire, Université de Genève, Geneva, Switzerland
[am] Also at Institut de Física d'Altes Energies (IFAE), The Barcelona Institute of Science and Technology, Barcelona, Spain
[an] Also at School of Physics, Sun Yat-sen University, Guangzhou, China
[ao] Also at Institute for Nuclear Research and Nuclear Energy (INRNE) of the Bulgarian Academy of Sciences, Sofia, Bulgaria
[ap] Also at Faculty of Physics, M.V.Lomonosov Moscow State University, Moscow, Russia
[aq] Also at Institute of Physics, Academia Sinica, Taipei, Taiwan
[ar] Also at National Research Nuclear University MEPhI, Moscow, Russia
[as] Also at Department of Physics, Stanford University, Stanford CA, United States of America
[at] Also at Institute for Particle and Nuclear Physics, Wigner Research Centre for Physics, Budapest, Hungary
[au] Also at Giresun University, Faculty of Engineering, Turkey
[av] Also at CPPM, Aix-Marseille Université and CNRS/IN2P3, Marseille, France
[aw] Also at Department of Physics, Nanjing University, Jiangsu, China
[ax] Also at University of Malaya, Department of Physics, Kuala Lumpur, Malaysia
[ay] Also at LAL, Univ. Paris-Sud, CNRS/IN2P3, Université Paris-Saclay, Orsay, France
* Deceased